INVESTIGATING MECHANOSENSITIVE ION CHANNEL PIEZO1'S ROLE IN *IN VIVO* ULTRASONIC NEUROMODULATION

ZHU JIEJUN

PhD

The Hong Kong Polytechnic University

2022

The Hong Kong Polytechnic University

The Department of Biomedical Engineering

Investigating Mechanosensitive Ion Channel Piezo1's Role In *In Vivo* Ultrasonic Neuromodulation

ZHU JIEJUN

A thesis submitted in partial fulfilment of the requirements for the degree of Doctor of Philosophy

January 2022

CERTIFICATE OF ORIGINALITY

I hereby declare that this thesis is my own work and that, to the best of my knowledge and belief, it reproduces no material previously published or written, nor material that has been accepted for the award of any other degree or diploma, except where due acknowledgement has been made in the text.

_____ (Signed)

ZHU Jiejun
_____ (Name of student)

ACKNOWLEDGEMENTS

First and foremost, I would like to express my sincere gratitude to my supervisor Dr SUN Lei for the mentorship and support for my PhD study. His remarkable wisdom and huge passion in the field of science has led me to think out of the box and be more delighted in academic research.

I would like to specially thank my senior fellow Dr QIU Zhihai. His profound knowledge and innovative views inspired me a lot. Without his patient assistance, I would still be stuck in different obstacles by now. I would also like to thank Dr GUO Jinghui who helped me a lot assessing my progress, pointing out overlooked problems and providing valuable suggestions in my PhD project. I am also grateful to all my colleagues for their help both in research and living aspects, most notably Mr Wong Kin Fung who offered the most support on my tedious data analysis; and Dr Cao Fei who helped update the microcopy system so that imaging related studies can be taken into action. I would like to give huge thanks to my parents for their endless patience and support throughout the time.

Last but not least, I would like to specially thank ULS, UBSN and CAF who provided great help in offering different equipment and animal care.

ZHU Jiejun

ABSTRACT

Low intensity ultrasound is an emerging technology that can noninvasively modulate neurons in deep brain regions (over 10 cm through intact skull) with fine spatial (cubic millimeter) and temporal (millisecond) resolution. It thus holes great promise as a tool probing brain function and treating brain diseases. Ultrasonic activation of human cortical, sub-cortical and the related network has been widely reported, along with various clinical trials in various stages. Importantly, these studies did not find observable side effects, even with chronic stimulation. Multiple studies have also shown that ultrasonic stimulation of specific neurons or brain regions can elicit distinct behaviors in animals. These pieces of evidence demonstrate ultrasound a credible and safe method with great clinically translational potential. However, the biological mechanism underlying the neuromodulatory effects of ultrasound remains to be elucidated. This lack of clarity poses a hurdle for future ultrasound-based therapies if they are to be applied predictably and consistently, with maximal achievable efficacy and minimal side-effects.

At present, three mechanisms are most widely considered: thermo-effect, cavitation, and acoustic radiation force (ARF). Literatures have proven negligible heating effect brought by low intensity ultrasound and a frequency dependency of the neuromodulatory effect under conditions unfavoring cavitation, leaving ARF as the most conceivable physical mechanism. Mechanosensitive ion channel thus becomes a plausible candidate as the mediator since it is a pivotal component for cellular sensation of mechanical disturbance including ARF and it enables fast ultrasonic neuromodulatory effects as observed. The significantly increased sensitivity in cells overexpressing one of various such channels further imply that ultrasonic effect in the mammalian brain could be modulated by endogenous mechanosensitive ion channels. In this context, Piezo1, the most sensitive mechanotransduction ion channel that responds to force as low as 10 pN and ultrasound sonication as low as 0.1 MPa, stands out. With its broad expression of Piezo1 RNA in mouse brain as shown in the Allen Mouse Brain Atlas database and its protein level expression reported in studies, these lead to a hypothesis that Piezo1 is one of the mediators, if not the only, responsible for ultrasonic neuromodulatory effect *in vivo*.

With our previous study demonstrating Piezo1 mediates the ultrasonic neuromodulation *in vitro*, this research continues investigating the role of Piezo1 in living animals. In this study, Piezo1 is demonstrated functionally expressed and mediating the ultrasonic neuromodulation *ex vivo* and *in vivo*. It is found that the neuronal activity induced by ultrasound in P1KO (Piezo1 conditional knockout) neurons is significantly reduced comparing with the control ones in *ex vivo* brain slice experiment. Similarly, P1KO neurons displayed lower sensitivity to ultrasound stimuli *in vivo* revealed by the reduced limb movement, muscle electromyography amplitude, local neuronal calcium signaling response and c-Fos expression. Higher sensitivity to ultrasound stimuli is also found in CEA (central amygdala), one of the brain areas found highly expressing Piezo1. From the loss-of-function and gain-of-function-like investigation, followed by the exclusion of auditory confound, the prominent role Piezo1 plays in ultrasonic neuromodulation can be confirmed.

Interestingly, in this study, Piezo1 is found specially located in certain brain areas including the bed nucleus of the stria terminalis (BNST), central amygdala (CEA), Edinger-Westphal nucleus (EW), Red nucleus (RN) and paraventricular nucleus of hypothalamus (PVH) which are all stress regulating area. With the well response of CEA neurons to ultrasound stimuli, ultrasound is a promising tool for studying and treating psychiatric disease.

To conclude, Piezo1 is demonstrated a mechanism of ultrasonic neuromodulation *in vivo* and thus displayed an outstanding application probability in both neuroscience research and brain disease treatment.

Keywords: Ultrasonic brain stimulation, mechanosensitive ion channels, Piezo1, psychiatric diseases

TABLE OF CONTENT

LIST OF FIGURES

LIST OF TABLES

LIST OF ABBREVIATIONS

BDNF	Brain-derived neurotrophic factor
BNST	Bed nucleus of the stria terminalis
CA1	Cornu Ammonis 1
CEA	Central amygdala
CNO	Clozapine-N-oxide
CNS	Central nerve system
DC	Duty cycle
EEG	Electroencephalogram
EMG	Electromyography
EW	Edinger-Westphal nucleus
fMRI	Functional magnetic resonance imaging
FUS	Transcranial focused ultrasound
HIFU	High intensity focused ultrasound
I_{SPPA}	Spatial-peak, pulse-averaged intensity
I_{SPBA}	Spatial-peak, burst-averaged intensity
I_{SPTA}	Spatial-peak, temporal-averaged intensity
ISH	*in situ* hybridization

M1	Primary motor cortex
MA	Mechanically-activated
MEP	Motor evoked potential
MI	Mechanical index
MNS	Median nerve stimulation
MS	Mechanotransduction
MSC	Mechanosensitive ion channel
PRF	Pulse Repetitive Frequency
RN	Red nucleus
PVN	Paraventricular nucleus of hypothalamus
RR	Ruthenium red
S1	Somatosensory motor cortex
SEP	Somatosensory evoked potentials
TI	Thermal index
tFUS	Transcranial focused ultrasound

Chapter 1. Introduction

1.1 Ultrasound as an emerging technology for neuromodulation

Breakthrough in neuroscience can always be traced to the emerging of new technologies. Distinct from histology and molecular technology, direct modulation of neurons or neuron circuits in a healthy, free moving animal provides much more information on different neuron sets' role in the complex brain. Thereby, technologies modulating neuronal activity are widely recognized as centrally important tools for investigating brain functions and treating neurological diseases.

Generally, neuromodulation approaches rely on chemical, electrical, photonic, magnetic, or ultrasonic stimuli to influence neuronal activity, brain function, and behavior. For example, DREADDs (Designer Receptors Exclusively Activated by Designer Drugs), a group of widely adopted chemical stimulation tools activate or inhibit targeted neurons with injection of pharmacologically inert chemical clozapine-N-oxide (CNO). Based on the response of naturally-expressed GPCRs (G-protein coupled receptors) to inner ligand, followed by activation or inactivation of neurons, modified GPCRs including Gi, Gq, Gs and β-arrestin are designed to respond to CNO that leads to the same GPCR signaling pathways and further neuron activation or inhibition (Urban, D. J., & Roth, B. L., 2015; Muir J., et al, 2019). This method showed good neuron selectivity and helped answer many neuroscience questions such as learning and memory (Robinson S., et al., 2014; Yau, J. O. Y., & McNally, G. P., 2015) and mood disorders (Teissier A., et al., 2015; Urban D. J., et al., 2016). However, it suffers from poor temporal resolution, ranging from minutes to hours, in controlling neuronal activity and mice behavior (Roth, B. L., 2016; Luan, S., et al., 2014).

Electrical stimulation has made great contribution to both neuroscience research and clinical application since its appearance. One typical example in clinic is DBS (Deep brain stimulation), a marvelous treatment for Parkinson, essential tremor, spinal cord injury, and depression (Miocinovic S., et al., 2013). Yet it requires temporary or chronic implantation of electrodes, both being invasive. Meanwhile, this approach targets a certain brain area without selectivity on neuron sub-types which their roles are considered differentiated in brain diseases. Therefore, although implantation of electrodes remains a preferred choice within major clinical

environment these days, new tool is expected to overcome the drawbacks of invasiveness and non-selectivity in neuron stimulation.

To non-invasively stimulate neurons in clinics, approaches such as transcranial current stimulation (tCS) and transcranial magnetic stimulation (TMS) has been developed. They have shown their utility and clinical efficacy in treating neurological and psychological disorders. Along with lack of neuron selectivity, they also failed to provide good spatial resolution with tCS being undetectable and TMS at cm scale. They are also unable to penetrate deep brain region without unwanted affecting surrounding tissues (Polanía, R., et al., 2018). Furthermore, application of TMS is incompatible with functional magnetic resonance imaging (fMRI) which is a primary brain area mapping and directing tool (Ulmer, S., & Jansen, O. 2010; Peterchev, A. V., et al., 2012).

Optical neuron stimulation overcame major problems of other neuron stimulation approaches including neuron selectivity (electric stimulation), spatial resolution (magnetic stimulation; DREADDs) and temporal resolution (DREADDs), and thus became one of the most widely used strategy in interrogating neurons and dissecting neuronal circuit function. In brief, the light-gated ion channels Channelrhodopsins (ChRs) allow sodium or chloride ions to permeate through the membrane under stimulation of specific wavelengths of light and thus induces depolarization or hyperpolarization in neurons. Such response can be triggered within milliseconds and be specified to neuron sub-types through genetic editing method (Deisseroth, K., 2011; Boyden, E. S., et al., 2015; Häusser, M., et al., 2014). However, optical neuron stimulation still shares the same drawback of invasiveness, owing to the limited penetration of light thus the need of fiber implantation. However, even with the fiber implant, other fundamental problems for local brain stimulation exists. Such as phototoxicity that accompanies with repeated stimulation (Gorostiza, P., & Isacoff, E., 2007) or need of multiple implants when studying neural circuit dynamics on a brain-wide scale in animals. Intrinsic requirement of genetic modification adds to the list of reasons hindering optogenetic neuron stimulation from translating to clinical application.

In summary, the ideal brain stimulation technology in our expectation should avoid implantation of devices, achieving non-invasive modulation of neuronal circuits' activity with high spatial and temporal resolution.

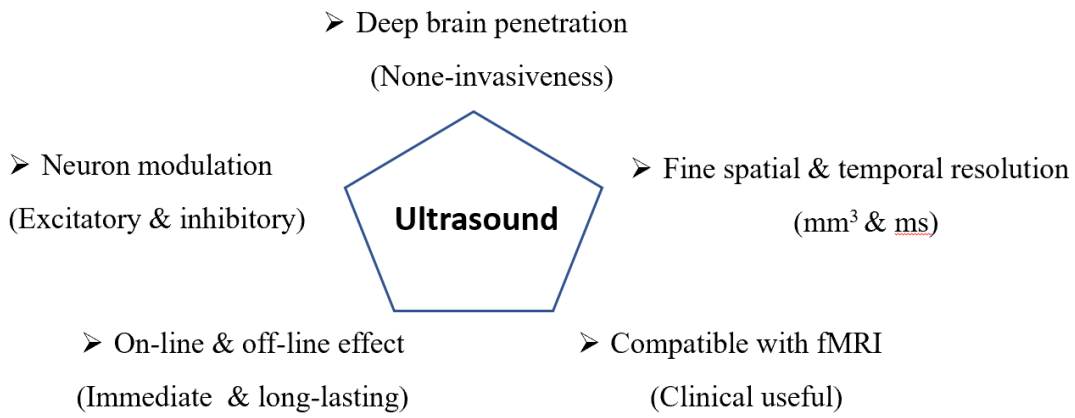

Figure 1.1 Advantages of ultrasound application in neuromodulation.

Transcranial focus ultrasound could possibly meet all these expectations (Fig1.1). It has been repetitively demonstrated targeting both cortical and deep brain regions (deeper than 10cm through intact skull) (Rezayat, E., & Toostani, I. G., 2016) with exceptional spatial resolution (at cubic millimeters scale) (Rezayat, E., & Toostani, I. G., 2016; Mehić., E., et al., 2014; Robertson, J. L., et al., 2017) and find temporal resolution (at milliseconds scale) (Yoo, S. S., et al., 2011; Legon, W., et al., 2018a) noninvasively. In addition, the size of ultrasound focal spot can be adjusted through careful piezoelectric element design and various focusing techniques. The ultrasound thus can be designed to target to a small area, a larger one or even a dynamically multiple area in a brain that meets different neuroscience research aims.

With its unprecedently physical property and the bio-effect on neurons, ultrasound has aroused much interest for the investigation and application of in neuroscience research.

The foundation of ultrasonic neuromodulation can date back to early 20th century when Harvey (1929) found sound waves can stimulate neuronal tissue. Despite more evidence demonstrated ultrasound's effects on the nervous system later on (Fry, F. J., et al., 1958; TAKAGI, S. F., et al., 1960; Lele, P. P., 1963; Gavrilov, L. R., et al., 1996), ultrasound was not recognized as a tool for non-invasive neuromodulation until early 21st century, when it was shown that ultrasound opened voltage gated Na^+ and Ca^{2+} channels in hippocampal slice cultures (Tyler, W. J., et al., 2008) along with later finding that ultrasound induced motor

responses when targeted to motor cortex in mice (Tufail, Y., et al., 2010), marking the outset of renaissance period for ultrasound brain simulations.

Followed with Tyler's study, massive research has further demonstrated ultrasound's ability altering neuron circuits and its corresponding behaviors in animals and humans (Kim, H., et al., 2012; Kim, H., et al.,2014; Younan, H., et al., 2013; King, R. L., et al., 2013; King, R. L., et al.,2014; Tufail, Y., et al., 2010; Aurup, C., et al., 2021). Its bidirectional effect on neurons, although remains mysterious, provide its potential usage in neuroscience studies. Its on-line and off-line effect are also its charming characteristic that indicates its potential application treating neurological and psychiatric disorders. In fact, Basic clinical trials have found improvement in certain behavioral outcomes, such as mood (Sanguinetti, J. L., et al., 2020; Reznik, S. J., et al., 2020) and increase in responsiveness of patients with chronic disorder of consciousness (Cain, J. A., et al., 2021).

However, with the mechanism unclear, the ultrasonic neuromodulatory outcome is sometimes hard to be predicted and even showed contradiction in some studies, which lies hidden dangers for appropriate applications in humans. Therefore, understanding the mechanism of how ultrasound modulates neurons in a brain is the key to take advantages of ultrasonic neuromodulation thoroughly without unpredicted side effects.

1.2 *In vitro* study

At cell level, electrophysiological events were found modulated by ultrasound. Action potential in Cornu Ammonis 1 (CA1) pyramidal neuron was found directly induced by ultrasound under five ultrasound pulses as short as 22.7μs (Tyler, W. J., et al.., 2008). Firing rates of action potentials (APs) in primary hippocampal neuron was also found increased upon ultrasound stimulation (Khraiche, M. L., et al., 2008). Interestingly, along with inducing neuron excitability, bidirectionally ultrasonic neuromodulation is also observed in local field potential measurement. (Bachtold, M. R., et al., 1998, Rinaldi, P. C., et al., 1991).

Subcellular responses including several ionic currents were also be reported. Voltage-gated sodium and calcium channels are the ion channels first be reported triggered by ultrasound (Tyler, W. J., et al.., 2008). Although there are disagreeing reports that sodium blocker TTX did not affect the ultrasound induced depolarization in crayfish axons, suggesting sodium channels might not play a key role (Lin, J. W., et al., 2019), the ultrasound induced sodium transient and the substantial excitation may be explained by calcium-dependent sodium channels activation since ultrasound was shown to induce calcium accumulation through mechanosensitive ion channels including Piezo1, TRPP1/2 and TRPC1 (Qiu, Z., et al., 2019; Yoo, S., et al., 2022; Oh, S. J., et al., 2020).

It might be easy to be predicted that neurotransmitter release was also found to be induced by ultrasound stimuli since it is the basic that neurons communicate after the onset of action potential. In the early article reporting voltage-gated sodium and calcium channels being triggered by ultrasound, the SNARE-mediated exocytosis and synaptic transmission in hippocampal circuits were reported (Tyler, W. J., et al.., 2008). Secretion of other neurotransmitters such as dopamine and serotine were also found induced by ultrasound stimuli *in vivo* (Min, B. K., et al., 2011). These thus indicate ultrasound a tool wiring neuron circuits, tabulating brain network and even treating neurological diseases.

Other molecular such as brain-derived neurotrophic factor (BDNF), the most prevalent neurotrophic in the central nervous system (CNS) (Nagahara, A. H., & Tuszynski, M. H., 2011; Lu, B., et al., 2013), was also reported enhanced by ultrasound *in vitro* (Yang, F. Y., et al., 2015) and *in vivo* (Lin, W. T., et al., 2015) which has indicated the ultrasound a neuronal protective effect.

Using *in vitro* methods studying ultrasonic effect on neurons shows its pros and cons. On one hand, it excludes the auditory confound (Guo, H., et al., 2018) in animal studies which has been taken into serious consideration recently. *In vitro* study also provides approaches more directly observing neurons response to ultrasound with imaging tools and different gene manipulation for different mechanism studies. On the other hand, isolates samples in an external environment are much different from that *in vivo* which may make the overall outcome of ultrasound stimulations defected. More importantly, with the nature of ultrasound, the acoustic field applied may be affected by acoustically reflective surfaces including coverslips, patch pipettes and air interfaces thus may not accurately reflect the ultrasonic neuromodulation *in vivo*.

Nevertheless, the effect of ultrasound has been widely studied in cultured cells, primary neurons, brain slices and even one isolated brain (Tyler, W. J., et al., 2008). Although the mechanism remains elusive, the accumulated knowledge provides guidance for further animal studies *in vivo*.

1.3 Transcranial animal study

Along with *in vitro* studies, massive number of studies on animals *in vivo* have been conducted. For example, stimulation targeted to motor cortex in mice (King, R. L., et al., 2013; King, R. L., et al., 2014; Tufail, Y., et al., 2010; Aurup, C., et al., 2021), rats (Kim, H., et al., 2012; Kim, H., et al., 2014; Younan, H., et al., 2013) and rabbits (Yoo, S. S., et al., 2011a) has been found inducing reproducible paw, limb, tail, or whisker movements under low levels of anesthesia. It was also reported stimulation targeting ovine sensorimotor cortex elicited electromyography signal in contralateral hindlimb (Lee, W., et al., 2016). In Kim's (King, R. L., et al., 2014) and Konofagou's lab (Kamimura, H. A., et al., 2016; Aurup, C., et al., 2021) researchers were even able to map the responding brain area in mice although not perfectly consistent with the anatomical sensorimotor cortex to our knowledge. The relatively large size of the ultrasound focal spot comparing with the rodent brain, far field of ultrasound effects, and distortions by the skull may explain this off-target phenomenon (Tufail, Y., et al., 2010; Younan, H., et al., 2013; Aurup, C., et al., 2021).

Considering this confound of ultrasound delivery, use of larger animals might be advantageous in validating region-specific ultrasound brain stimulation, since larger cranial volume may decrease acoustic reverberations and standing waves formation which are believed to deter precise targeting through small rodent skulls (Younan, H., et al., 2013; Tang, S. C., & Clement, G. T., 2009). For example, targeted to the sensorimotor cortex in a sheep is reported to elicited electromyography signal in contralateral hindlimb but bot both side limbs which is more common in mouse study (Lee, W., et al., 2016).

Besides the direction induction of neuronal activity, ultrasonic neuromodulation on the ongoing neuronal activity in animals were also reported. For instance, stimulation targeted to somatosensory thalamic nuclei in swine were found modulates trigeminal and tibia somatosensory evoked potentials (SSEPs) (Dallapiazza, R. F., et al., 2017). Similarly, in awake and behaving primates, application of unilateral single ultrasound burst over the frontal eye field (FEF) in contralateral hemisphere was reported to increase the latency of voluntary saccades away from a visual cue (Deffieux, T., et al., 2013)

Apart from involuntary responses, high-level cognition is also found affected by ultrasonic neuromodulation. For example, ultrasound stimulation on monkey's frontal eye fields

(FEF) was found biased its decision making in a two-alternative choice task (Kubanek, J., et al., 2020). Studies also showed the ability of monkeys representing and translating cue information into behavioral choices in a reward-guided decision-making tasks is affected by ultrasound stimulation on the rostral medial prefrontal cortex (Fouragnan, E. F., et al., 2019; Bongioanni, A., et al., 2021). Apart from these, stimulation of basal forebrain, though did not change the decision taken, did alter the timing of the decision in macaques (Khalighinejad, N., et al., 2020).

In addition to the immediate (on-line) effect, long-lasting (off-line) effect of ultrasound stimulation has also been observed, which could last for minutes to even days. For example, in several non-human primate studies, ultrasonic effect lasting for 30mins to 1hr has been reported in the local area, its interconnected regions (Folloni, D., et al., 2019, Verhagen, L., et al., 2019, Cain, J. A., et al., 2021b) and even in oculomotor and decision-making performance (Fouragnan, E. F., et al., 2019). Similar effect on human is also reported recently (Zeng, K., et al., 2021). Indeed, several clinical trials in various stages have been proceeding. For example, improvement of mood has been reported by stimulating frontotemporal area and right inferior frontal gyrus (Reznik, S. J., et al., 2020; Sanguinetti, J. L., et al., 2020). The acquirement and maintenance of ability to recognize different objects was also found improved in post-chronic disorder of consciousness patients after ultrasound stimulation on thalamus (Cain, J. A., et al., 2021).

With the growing ultrasonic neuron circuits modulation studies in animals, preclinical studies of ultrasound treatment for specified human disorders are also on the rise. Acute and recurrent epilepsy was found, almost ubiquitously, improved in mice and monkeys in various epilepsy models after ultrasound treatment (Min, B. K., et al., 2011a; Hakimova, H., et al., 2015; Zou, J., et al., 2020). Parkinsonian related activity represented by the mean beta power (13–30 Hz) was also reported reduced in MPTP generated Parkinson's mouse model after ultrasound stimulation on subthalamic nucleus (Wang, Z., et al., 2020). Ultrasound also showed a neuroprotective effect, along with increased BDNF expression level in rat models of vascular dementia (Huang, S. L., et al., 2017) and aluminum-induced Alzheimer's disease (Lin, W. T., et al., 2015). Depression- and anxiety-related behavior is also found be improved through the enhanced BDNF and signaling pathways with chronic ultrasound stimulation on ventromedial prefrontal cortex (vmPFC) (Legrand, M., et al., 2019, Zhang, J., et al., 2021). Stroke was also reported benefited from ultrasound stimulation, indicated by the normalized cortical oscillations and functional asymmetries towards ultrasound stimuli (Baek, H., et al., 2019). In line with these

findings, enhanced cognitive functions was also reported in mouse models of dementia after ultrasound stimulations (Eguchi, K., et al., 2018). Supported by the arousment of isoflurane anesthetized mice by target to ventral tegmental area (VTA), ultrasound showed its potential application for treating disorders of consciousness (Bian, T., et al., 2021). Anesthetized mice with traumatic brain injury required a shorter recovery time with ultrasound stimulation (Bian, T., et al., 2021). Similarly, ultrasound stimulation targeting thalamus was also reported accelerating the emergence from anesthesia in rats (Yoo, S. S., et al., 2011b).

With the rising exciting finding of ultrasonic neuromodulatory effect in animal studies, critics that ultrasonic neuromodulation is in fact, activated through auditory pathway also arouse recently (Guo, H., et al., 2018, Sato T., et al., 2018; Braun, V., et al., 2020; Qi, X., et al., 2021). Several articles reminded researchers be extra careful about the auditory confound when interpreting ultrasound induced behavior outcomes. Yet, even with the presence of auditory effect, it did not demolish the impact of direct ultrasonic neuromodulation regarding the behavior changes, such as the asymmetric limb movements induced by unilateral hemisphere stimulation of ultrasound (Lee, W., et al., 2016; Aurup, C., et al., 2021). Nevertheless, ultrasound trigged motor response has also been found in deaf mice (Mohammadjavadi, M., 2019), showing ultrasonic neuromodulation could be achieved through non-auditory pathway.

In summary, transcranial ultrasonic neuromodulation is confirmed at a wild rage of animal models, although with mechanism elusive and some outcome contradictory, these studies did enhance our understanding on the brain function connectivity and the base for neurological disorders treatment. Thus lay the foundation of its application in humans.

1.4 Human research

With the pioneering studies on animal models, it has been suggested that ultrasonic neuromodulation is a safe method to be applied on human. In fact, tremendous works have been done on humans

Similar to animal studies, immediate neural responses induced by ultrasound has been found in humans. For example, EEG potentials can be recorded when ultrasound stimulated hand region of primary somatosensory cortex (S1) (Lee, W., et al., 2015). Following study further found that stimulation of secondary somatosensory cortex (S2) or conjunction with S1 induced tactile sensations in the contralateral hand (Lee, W., et al., 2016a), demonstrating the feasibility of ultrasound stimulating multiple brain areas in a fine spatial resolution which favors its further usage on probing the role of different brain areas in mediating sensory, motor, or cognitive functions.

Recently, it was also reported human motor cortical activity can be facilitated through ultrasonic excitatory effect. Movement-related cortical potentials were found increased at both EEG sensor and source levels when concurrent transcranial focused ultrasound (tFUS) was transmitted to the primary leg motor area (Yu, K., et al., 2020). The group also found enhanced spatiotemporal EEG responses and improved discrimination ability in a sensory discrimination task conjunction with ultrasound stimulation in S1 (Liu, C., et al., 2021). Along with the local effect induced by ultrasound stimuli, activation of its network is also reported in human visual cortex area (Lee, W., et al., 2016b).

In contrast to neuron activation, several studies reported neural activity suppression by ultrasound stimulation. It is reported that delivering focused ultrasound to human S1 resulted in suppression on somatosensory evoked potentials (SEP) and cortical oscillations induced by electric median nerve stimulation (MNS), leading to an improvement of sensory discrimination in two-pin tactile finger task (Legon, W., et al., 2014). Similarly, when targeted to primary motor cortex (M1), ultrasound inhibited the amplitude of single-pulse motor evoked potentials (MEPs) resulting in enhanced motor response performance (Legon, W., et al., 2018a). Yet, the same group also reported stimulation targeting to the ventroposterolateral (VPL) nucleus of thalamus that attenuated the P14 SEP component, however decreased participants performance in sensory discrimination (Legon, W., et al., 2018b). These distinct outcomes demonstrate ultrasound

region-specific effect which might be understandable considering the complex brain connectivity.

This bidirectional of ultrasonic effect has been widely reported without an identified explanation. The above-mentioned region-specific ultrasound effects seems cannot support the wider observed bidirectional phenomenon based on the distinct outcomes when ultrasound targeted to the same area. For example, when target to S1, tactile sensations and EEG potential is found in Lee's papers which indicates an excitatory effect (Lee, W., et al., 2015, Lee, W., 2016a), while the suppression on SEP and cortical oscillations induced by MNS is reported in Legon's finding (Legon, W., et al., 2014). The similar contradictory outcome can also be found targeting to the visual cortex. The activation of visual cortex has been found in human (Lee, W., et al., 2016b), sheep (Lee, W., et al., 2016c) while suppression in VEP (visual evoked potential) in cat (Fry, F. J., et al., 1958) and rabbit (Yoo, S. S., et al., 2011a) was also reported.

Although confusing, this bidirectional phenomenon itself provides information though. Ultrasound seems to be reported activation effect when applied along and be reported suppressed effect when accompanied with other stimuli including sensory stimulation in peripheral, light stimuli in the eye and the TMS in the brain. This phenomenon can also be observed *in vitro* studies with positive ultrasound effect on action potential amplitude and the firing rate (Menz, M. D., et al., 2013; Tyler, W. J., et al.., 2008; Khraiche M. L., et al., 2008), while depression of electrical induced action potential (Rinaldi, P. C., et al., 1991) and reduced firing rate of epileptic discharges in juvenile mouse hippocampal slices upon ultrasound stimulation (Zhang, Z., et al., 2019).This seems indicates that the ultrasound leads to stimulating when neurons at a resting sate but goes inhibiting when neuron at an exciting state.

Recently, using BOLD fMRI signal as a readout, Chen's group provides more information for the bidirectional ultrasound effect that may help unveil the mechanism behind (Yang, P. F., et al., 2021). In this study, under tactile and focused ultrasound stimulation, neural activities in area 3a/b along with the tactile related downstream brain area areas 1/2, S2, MCC, VPL, and insula were found suppressed, while neural activation was found in inter-connected non-tactile zones. The authors thus proposed dependency of neuron response on brain states: inhibition (likely via small inhibitory interneurons) on tactile induced, currently activated neurons but excitation on other neurons (likely via excitatory pyramidal neurons) that in turn leads to the

activation of interconnected downstream neurons in other off-target brain regions. However, this hypothesis cannot well explain the finding that the ultrasound induced excitatory off-target area is spatially segmented from the tactile + FUS situation. It is also worth noticing that this hypothesis could be partially supported by study of Yu (Yu, K., et al., 2020), since Chen's PRF setting lays in the range of this study which ultrasound was claimed to stimulate excitatory neurons selectively. However, contradictory conclusion was made upon the inhibitory effect, that Yu stated inhibitory neurons were selectively stimulated under low PRF instead of brain state. In fact, hypothesis that ultrasound parameters are key factors responsible for the different ultrasonic neuron effect was also proposed in various studies. (More details about studies on quantifying the relationship between ultrasonic bio-effect and ultrasound parameters are presented in Chapter 1.5)

In generally, the overall trend of ultrasonic neuromodulatory effect is mostly reported excitatory in both animal and human. It may because that the animal model adopted most is the resting state of rodents. Nerveless, we cannot exclude that the ultrasound parameter may affect this bidirectional ultrasound effect. And the ultrasound induced in suppression at an excitatory circuit did not necessary to the stimulation of inhibitory neurons. Conclusions cannot be made since both these hypotheses cannot explain the finding so far. Even though these hypotheses are partially right in some circumstances, the reason why this neuron possess this different responding to ultrasound remains a big question to be answer.

Still, it can be concluded that ultrasound, being an emerging noninvasive neuromodulation method, has been demonstrated capable to modulate the central nerve system safely and reversibly through the intact skull in various scales. However, with the mechanism unclear and seemingly conflicting results being reported, there is an urgent need exploring the mechanism from both a safety and a precise controlling perspective to develop reliable clinical applications of ultrasonic neuromodulation.

1.5 Physic of ultrasound

Ultrasound is a mechanical wave with frequency over 20 kHz. As a mechanical waves, it could propagate in both longitudinal and transverse waveforms but conventionally in form of the former. Through design of different piezo transducers and driving patterns, ultrasound of varying frequency and energy can be delivered into the brain and further induce different ultrasonic bio-effect.

The ultrasonic parameters primarily include frequency (f), duty cycle (DC), pulse width, pulse interval, pulse repetition frequency (PRF), burst duration (or simply duration), burst interval (or simply interval), pressure (P), and intensity (I) (Fig 1.2 & Table 1.1).

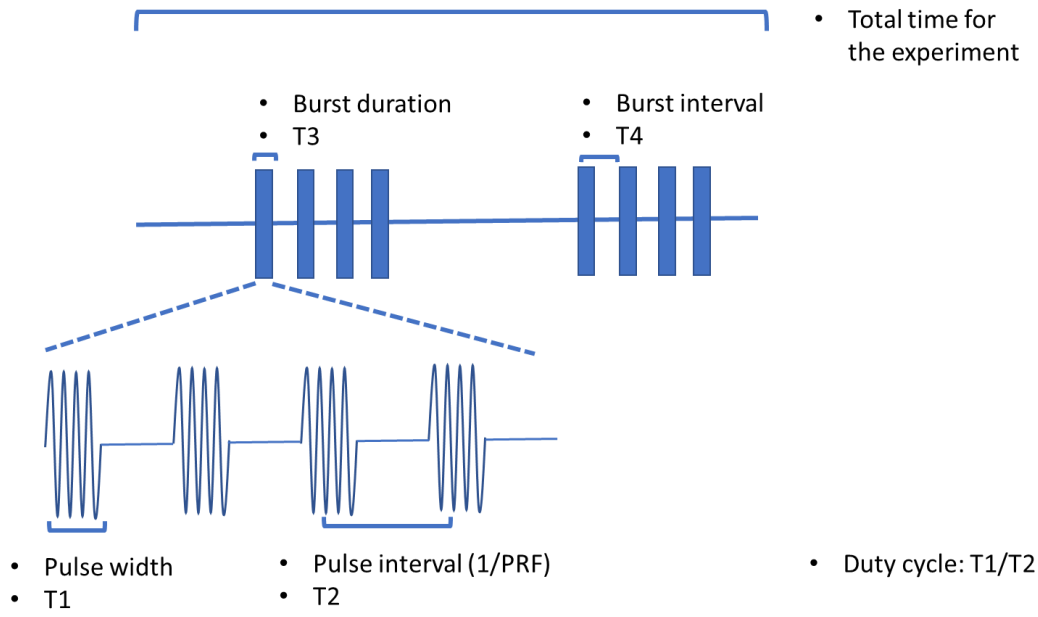

Figure 1.2 Schematic of ultrasound pulse and associated parameters typically used for ultrasonic neuromodulation

Table 1.1 List of common ultrasound parameters

Parameter	Abbreviation	Unit
Frequency	f	MHz
Duty cycle	DC	-
Pressure	P	MPa
Intensity: spatial-peak, pulse-averaged	I_{SPPA}	W/cm^2
Intensity: spatial-peak, burst-averaged	I_{SPBA}	W/cm^2
Intensity: spatial-peak, temporal-averaged	I_{SPTA}	mW/cm^2

$$\boldsymbol{I = \frac{1}{T}\int_0^T \frac{P_t^2}{\rho c}\,dt} \text{ or } \boldsymbol{\frac{max(P_t)^2}{\rho c}}$$

where T = period to be accounted for; P_t = instantaneous pressure; ρ = tissue density; c = speed of sound in tissue

Ultrasound intensity presents the amount of energy delivered to tissue per time per area (Eq. 1). Common metrics include the spatial-peak pulse-averaged intensity (ISPPA), which is the measurement of the average intensity over a single ultrasound pulse at the location of peak pressure within the ultrasound focus; and the spatial peak time averaged intensity (ISPTA), which refers to the average intensity over the complete sonication interval at the location of peak pressure within the ultrasound focus. Intensity and pressure are correlated by the propagation speed of sound in the targeted tissue and the tissue density. For example, the speed of sound in human brain tissue is approximately 1500m/s and its density is approximately 1.06g/cm3.

Frequency is the acoustic wave cycles per second, it generally depends on the alternating current driving the transducer. Generally, frequencies in the range of 1–20 MHz are adopted for diagnostic imaging, frequencies ranging from 0.7 to 3 MHz are used for therapeutic use, and 20–200 kHz are utilized in industry (Ahmadi, F., et al., 2012). The frequency determines the penetration property and spatial resolution. Theoretically, higher frequency enables a tighter and deeper focus, resulting in higher spatial resolution. However, higher frequency increases the attenuation by skull which hinders its penetration through the intact skull. Meanwhile, at this frequency，the energy is easily converted to heat which could destroy local tissue (Legon, W., et al., 2018a). To compromise the property of penetration through intact skull and thermo effect, the frequency adopted for neuromodulation should lie in an appropriate range. It has been found that, ranging from 0.25 MHz to 0.6 MHz, stimulation efficiency increases with lower frequency

(King, R. L., et al., 2013), while ranging from 0.3 MHz to 2.9 MHz, the higher the frequency, the higher the spatial peak intensity required to maintain equal efficiency (Ye, P. P., et al., 2016). Therefore, a relatively lower frequency is suggested for optimizing the neural modulatory effect.

Besides, numerous studies focused on the motor cortex in rodents (Kamimura, H. A., et al., 2016; Kim, H., et al., 2014; King, R. L., et al., 2013; King, R. L., et al., 2014; Mehić, E., et al., 2014, Ye, P. P., et al., 2016; Yoo, S. S., et al., 2011b; Younan, H., et al., 2013) provide messages on how parameters affect the ultrasonic bio-effect. One key finding is frequency dependency that intensity required to produce an EMG spike increases with ultrasound frequency from 0.25 to 0.5 MHz (Tufail, Y., et al. 2010). Similarly, lower intensity is required at frequency of 0.35 MHz compared to 0.65 MHz (Kim, H., et al. 2014). Besides, an increase in successful rate of inducing EMG spikes is observed at lower frequencies for a fixed intensity between 0.25 and 0.6 MHz (King, R. L., et al. 2013) and even a wider frequency band of 0.3 to 2.9 MHz (Ye P. P., et al., 2015). Two hypotheses were raised to explain the frequency dependency: a cavitation-based mechanism as the cavitation threshold increases with frequency, or as the result of reduced focal spot sizes with increased frequency, that summation of local activity within the volume of activated tissue dominants the overall motor outcome instead of individual activity.

DC, pulse width, pulse interval, PRF, duration, and interval are basically different time scales used for the ultrasound description. Pulse width or T1 is time of individual pulses of the ultrasound wave. The repetitions of these pulses in 1 second is defined as pulse repetition frequency (PRF), which T2 is the time for one repetition to complete (1/PRF). The duty cycle is defined as T1/T2 and generally be considered a way to reduce the risk of thermo-effect induced by ultrasound. This serial pules of ultrasound are usually the smallest unit that adopted for the bio-effect study, that the time it takes as a single stimulus is announced as duration or T3. In most cases different intervals are adopted in different studies.

It has been reported that PRF might as well be a pivot factor that affects the bio-effect. It was shown that increasing PRF in the range of 100–3000 Hz resulted in greater responses (King, R. L., et al., 2013). Similar finding was also reported that 1500 Hz PRF displayed higher calcium changes in the mouse brain slice compared to 300 Hz PRF (Manuel, T. J. et al., 2020). Regular spiking neurons in the somatosensory cortex in mice also displayed an increasing spiking rate with increasing PRF ranging from 30 Hz to 4500 Hz. All these indicate lower PRF a more effective approach when applying ultrasonic neuron stimulation.

The ultrasound parameters adopted in animals varies, with the frequency of approximately 0.25–8 MHz, mostly under 1 MHz, 100-3000 Hz PRF, 10–500 ms duration mostly, and pressure amplitudes around 0.1–0.6 MPa. Studies on cortices including M1, S1 and V1, which can be both excited and inhibited regarding different intrinsic state aroused by different experimental setup, though uncovered a certain trend, showed inconsistency in different works. Meanwhile, studies seem to provide contradictory findings over several points arising from the mechanism underlying ultrasound neuromodulatory effect. For example, Kim. H. et al. (2014) claimed that pulsed ultrasound the most effective paradigm producing motor responses in mice, while King, R. L., et al. (2013) suggested the continuous ones; the role of ISPTA in EMG response amplitude or success rate also varies with the correlation found to be negative (Tufail, Y., et al., 2010), flat with all-or-nothing responses (King, R. L., et al. 2013), or positive (Kamimura, H, A., et al., 2016, Mehić, E., et al., 2014). Such inconsistency is likely due to the different experimental setup, anatomic variations, and intrinsic states of the animals that the inhibitory and excitatory neurons contributed differently to the overall neuron networks output in studies.

1.6 Latest understanding of mechanism

Understanding the mechanisms how ultrasound modulates neurons is critical for both basic neuroscience research and clinical therapeutic applications. At present, three mechanisms are most widely considered: cavitation, thermo-effect, and ARF. In parallel, there is also opinion stating that with different parameters selected and experimental subject, these mechanisms may mingle (Darmani, G., et al., 2021).

Cavitation

Cavitation was suggested a mechanism of ultrasonic neuromodulation in some studies (Plaksin, M., et al., 2014; Ye, P. P., et al. 2015). Acoustic cavitation is generated by voids or bubbles within the tissue when acoustic wave exceeding a threshold at the tensile phase (Plesset, M. S., & Prosperetti, A., 1977) After that, the cavity oscillates resulting in physical effects such as streaming flow which finally induce bio-effects (Coussios, C. C., & Roy, R. A., 2008). Interpreted by the equation below, the likelihood for acoustic cavitation depends on the peak negative pressure and frequency, which high pressure and low frequency favors the occurrence (Leighton, T. G., 2007).

$$\boldsymbol{MI = \frac{max(P_n)}{\sqrt{f}}}$$

where P_n = peak negative pressure; f = frequency

Although it is possible such cavities forming inside the cell membrane cause capacitance changes or fracture of the cell membrane leading to neuromodulation effect, under the commonly applied ultrasound parameter, the likelihood of cavitation is proposed very low (Yoo, S., et al., 2022; Blackmore, J., et al., 2019). Especially, a finding that micron-scale tissue displacements consistent with ultrasound induced spiking activity remained unchanged to a broad acoustic frequency range (0.5–43 MHz) suggests ARF rather than cavitation is the dominant physical mechanism (Menz, M. D., et al., 2019). mechanism, it is the situation we may want to avoid for further ultrasound adoption for neuromodulation.

Thermo-effect

Ultrasound can be broadly classified into high intensity or low intensity (Ter Haar, G., 2007). Under high intensity, heating would be the dominant bio-effect. In fact, high intensity ultrasound (I_{SPTA} > 1000 W/cm^2) has been widely adopted in different neurological diseases' therapy including essential tremor (Iorio-Morin, C., et al., 2021), Parkinson's disease (Sinai, A., et al., 2021) and obsessive-compulsive disorder (Germann, J., et al., 2021). However, majority of studies adopted low-intensity ultrasound (I_{SPTA} < 500 mW/cm^2) to modulate neurons without cell damages. Under this ultrasound protocol, heat induced by ultrasound is detected minor (<0.1℃) (Dinno, M. A., et al., 1989; Dalecki, D., 2004; O'Brien Jr, W. D., 2007; Ter Haar, G., 2007; Kim, H., et al., 2014; Tyler, W. J., et al.., 2018). Further evidence that knocking out thermosensitive ion channels in mutants C. elegans showed no impact on neuronal response to ultrasound stimulation (Kubanek, J., et al., 2018), indicates presence of non-thermal mechanism.

In controversy, slightly higher temperature (0.1-0.8 ℃) induced by ultrasound has been reported by (Darrow, D. P., et al. 2019), who claimed a neuron inhibition effect based on ultrasound thermo-effect. Although some thermosensitive ion channel (e.g., potassium channels TREK1/2 and TRAAK) are found moderately sensitive to ultrasound stimulation, some hypothesize the thermo-mechanism may be delusion that increase in potassium channels conductance in turn reduces resting membrane potential and neuronal firing (Kubanek, J., et al., 2016; Prieto, M. L., et al., 2020). However, these neurons displayed both thermos-sensitivity and mechanical sensitivity, along with the coincidence of thermal rise with other mechanical factors during ultrasound exposure, the role of thermal effects in ultrasonic neuromodulation seems ambiguous.

ARF

More recently, attention has been shifted to the mechanical mechanism which states that the mechanical deformation of the cell membrane may leads channel kinetics or membrane capacitance changes and results in altered excitability.

Converting the mechanical stimulations into the electrical or biochemical signal in cells, also termed mechanotransduction, is involved in various biological processes, including cell development, pain sensation, and red blood cell volume regulation (Lee, D. A., et al., 2011; Chighizola, M., et al., 2019; Costigan, M., et al., 2009). In the field of neuroscience, however,

for a long period of time did not raise much attention. Neuroscientist focuses on the electrical and biochemical studies considering that the brain is floating in the cerebrospinal fluid and isolated from the outer mechanical cues. Nevertheless, the brain is a mechanically sensitive organ, which can sense different mechanical cues to regulate its activities. For example, the action potentials in axon are found accompanied by propagating membrane deformations (Hill, D. K., 1950; Tasaki, I., et al., 1989). The mechanical impulses were also recorded at axon terminals during action potential firing and vesicle fusion (Kim, G. H., et al., 2007). The mechanical actions of enlarged dendritic-spine on its presynaptic exocytosis has also been reported recently (Ucar, H., et al., 2021). The physical forces that influence the brain in human and rodent is also widely studied (Budday, S., et al., 2015). The ability of neuron detecting local mechanical signals that influence cell division, gene expression, cell migration, morphogenesis, cell adhesion, fluid homeostasis, ion channel gating and vesicular transport has also been reported (Tyler, W. J., 2012; Suter et al., 2011; Pfister et al., 2004). Growing evidence have demonstrated the mechanical forces integrate within the neuron system and mechanical responsive components includes the plasma membrane, ion channels, cytoskeletal proteins has also been recognized (Tyler, W. J., 2012; Mueller, J. K., & Tyler, W. J., 2014).

Physical displacement of the membrane has been found can be induced by ultrasound in synthetic bilipid membranes, and more directly in plated retinal slices (Rohr and Rooney, 1978; Prieto, M. L., et al., 2013; Menz, M. D., et al., 2019). These thus leads to a conclusion that radiation force is responsible for ultrasound excitation. Among all the components sensing this mechanical force, mechanical sensitive ion channel has drawn much attention regarding the observed milli-second timescale of ultrasound's stimulation effects (Bystritsky, A., et al., 2011, Fomenko, A., et al., 2018, Tyler, W. J., et al, 2018). Through gain-of-function or loss-of-function mutation of mechanical sensitive ion cannel in different models including single sells (Kubanek, J., et al., 2016; Qiu, Z., et al., 2019; Sorum, B., et al., 2021), simple nerve system (Kubanek, J., et al., 2018) and rodents (Qiu, Z., et al., 2020), mechanosensitive ion channel has been demonstrated response to ultrasound stimulus. For example, several two-pore-domain potassium family (K2P) channels including TREK-1, TREK-2, and TRAAK are found response to ultrasound overexpressing in the xenopus oocyte system (Kubanek, J., et al., 2016). More recently, TRAAK response to low intensity ultrasound is further be confirmed in both xenopus oocyte system and mouse brain slice. (Sorum, B., et al., 2021). Interestingly, in this study they

find thermal effects hinder instead of explaining the ultrasonic neuromodulatory effects. Piezo1, a newly found mechanosensitive ion channel is also found response to ultrasound stimulation in primary neurons (Qiu, Z., et al., 2019). Deletion of the MEC-4, a DEG/ENaC ion channel sensing touch in C. elegans, leads to its abolishment of mechanical response under ultrasound stimuli (Kubanek, J., et al., 2018). Overexpressing a mutation of mechanosensitive channel of large conductance (MscL), MscL-G22S, neurons in mouse brain exhibited higher ultrasound respondents (Qiu, Z., et al., 2020).

These thus demonstrated mechanosensitive ion channel can respond to ultrasound although with little understanding of how mechanical force alters this channel kinetics. Generally, it is assumed that various ion channels regulate ultrasonic neuromodulation through mechanical disruption of its membrane. Since channel composition is likely varies in different cell type, their ultrasonic response may various as well. While the mechanosensitive channels discussed above have also been identified thermosensitive (except for Piezo1, which is the long-sought pure mechanical sensitive ion channel) ultrasound is likely to activate these channels independent of the thermal changes.

Although mechanosensitive ion channel is indeed response to ultrasound stimulation, whether it is the reason responding for the ultrasonic neuromodulation *in vivo* requires further investigation. A mechanosensitive ion channel that endogenously expressed and functioned in central nerve system, one that is sensitive enough responding to ultrasound stimulus in an intact brain environment within the so-far studied ultrasound intensity and leading to the observed ultrasound brain stimulation outcomes may be the answer for the ultrasonic neuromodulation *in vivo*.

1.7 Piezo1 as a promising candidate for ultrasound neuromodulation

Probing the ultrasonic neuromodulation, the mechanosensitive ion channels offered a plausible explanation given the observed timescale of ultrasound's stimulation effects (Bystritsky, A., et al., 2011, Fomenko, A., et al., 2018, Tyler, W. J., et al, 2018) and several mechanosensitive ion channels including MEC-4 and MscL that demonstrate response to ultrasound stimulus (Kubanek, J., et al., 2016; Qiu, Z., et al., 2019; Qiu, Z., et al., 2020). Although these studies used the non-mammal ion channels, its responses to ultrasound did indicate mechanosensitive channels underlie physiological responses to ultrasound.

Several endogenous mechanosensitive ion channels are then taking into investigations.

Voltage-gated sodium channels and voltage-gated calcium are the first channels that reported triggered by ultrasound, followed with the SNARE-mediated exocytosis and synaptic transmission in hippocampal circuits (Tyler, W. J., et al.., 2008). Earlier work has been found that these channels possess mechanosensitive properties despite its relatively low sensitivity (Morris, C. E., & Juranka, P. F., 2007), and supporting from the findings that the ultrasound increases channel conductance when heterologous expressed in Xenopus oocytes (Kubanek, J., et al., 2016). These have aroused much interest to neuromodulation researchers and has been cited as a potential mechanism of ultrasound induced neuronal excitation (Tufail, Y., et al., 2010; Kubanek, J., et al., 2018). However, later evidence showed disagreement considering that the sodium blocker TTX did not affect the ultrasound induced depolarization in crayfish axons (Lin, W. T., et al., 2019).

Two-pore potassium channel (K2P), a family of potassium-permeable leak channels has also raised much interest due to its property of highly mechanosensitive. Subtypes TRAAK, TREK-1 and TREK-2 are widely expressed in the CNS and displayed increased conductance in response to changes in membrane tension induced by sub atmospheric pressure and laminar stress (Enyedi, P., & Czirják, G., 2010). Increased conductance of these channel subtypes is also be found when expressed in Xenopus oocytes (Kubanek, J., et al., 2016). These has led to an implication that K2P may induce hyperpolarizes in neurons and thus leading to the ultrasonic neuron inhibition. More recent study found that ultrasound activates the TRAAK with submillisecond kinetics to an extent comparable to transcranial mechanical activation. Although

not leading to hyperpolarization, the TRAAK did attenuate ultrasound induced action potentials in neuron (Sorum, B., et al., 2021).

A Subtype of acid-sensing ion channels, ASIC1a, is recently reported the molecular determinant in the mechano-signaling of low-intensity ultrasound that modulates neural activation in mouse brain. The ASIC1a is found mediated the immediate response of ERK phosphorylation and further neurogenesis under the ultrasound stimulus (Lim, J., et al., 2021). In this study, ASICs displayed an ultrasound inducible neuronal excitation, and although its immediate ultrasonic effect is demonstrated in *in vitro* experiment, it is still a possible the mediator we are seeking that response for ultrasonic neuromodulation *in vivo*.

Another mechanosensitive ion channel, a subtype of the transient receptor potential family, TRPA1, in astrocyte in mouse brain is found mediate the ultrasound induced motor response through a glia-neuron interaction way (Oh, S. J., et al., 2019).

Different experiment has suggested different candidate of mechanosensitive channels (Table 1.2) underlie the physiological responses to ultrasound. However, I propose Piezo1 as a more promising candidate base on 3 facts: its nature of high sensitivity to various forces (Coste, B., et al. 2010), especially that it is the highest sensitive one found response to force as low as10 pN; its finding that response to ultrasound as low as 0.1 MPa *in vitro* study (Prieto, M. L., et al., 2018; Qiu, Z., et al., 2019); and its expression be found in mice and rat brain (Velasco-Estevez, M., et al., 2018; Velasco-Estevez, M., et al., 2020).

Table 1.2 Mechanosensitive ion channels that expressed in mammalian brain and response to the ultrasound stimulus

Channel family	Channel	Ultrasound Response	Expressed in mammalian brain
TRP channels	TRPA1	Oh, et al., 2019	Vennekens et al., 2012
	TRPC1	Burks, et al., 2019; Yoo, S., et al., 2022	Riccio, A., et al., 2002
	TRPV1	Yang, et al., 2021	Mezey, É., et al., 2000
	TRPP1/2	Yoo, S., et al., 2022	NC
K^+ channels	K^+ channel	Lin, Z., et al., 2019	Tabarean, I. V., & Morris, C. E. (2002).
	Calcium activated K (BK)	Juffermans, L. J., et al., 2008	Niu, X., et al.,2004
	TREK1/2	Lengyel, M., et al., 2021; Kubanek, J, et al., 2016	Maingret, F., et al., 1999b

	TRAAK	Kubanek, J, et al., 2016; Sorum, B., et al., 2021	Maingret, F., et al., 1999a; Brohawn, et al., 2012
Na^+ channels	Nav 1.5	Kubanek, J, et al., 2016	Morris, C. E., & Juranka, P. F., 2007; Beyder, A., et al., 2010
Ca^{2+} channels	N-Type calcium channel	Tyler, W. J., et al., 2018 (Indication)	Calabrese, B., et al., 2002; Etzion, Y., et al.,2000
DEG/ENaC family	ASIC1a	Lim, J., et al., 2021	Wemmie, J. A., et al., 2002
Piezo family	Piezo1	Prieto, M. L., et al., 2018; QIU, Z., et al., 2019	Velasco-Estevez, M., et al., 2018; Velasco-Estevez, M., et al., 2020.
	Piezo2	Li, J., et al., 2021; Hoffman, B. U., et al., 2022	Shin, S. M., et al., 2021; Wang, J., & Hamill, O. P, 2021

The first finding that Piezo1 response to ultrasound is 2018, when ultrasound is found increased the conductance of Piezo1 in cultured mammalian neurons (Prieto, M. L., et al., 2018). Nevertheless, in this study, the ultrasound used is 43 MHz which is not generally used in animals and humans. Because of the inherent tradeoff of penetration and the optimal focal size of ultrasound, the advice acoustic frequencies are less 700 kHz in human (Sun, J., & Hynynen, K., 1998; Clement, G. T., & Hynynen, K., 2002; White, P. J., et al., 2006).

In our lab, we demonstrate that Piezo1 is indeed the medicator in ultrasonic neuromodulation *in vitro* in an optimized ultrasound circumstance. We found that ultrasound alone could activate heterologous Piezo1, initiating calcium influx in an acoustic pressure dependent manner (Fig 1.3 A). Similarly, the endogenous in primary neurons also displayed an acoustic pressure dependent neuronal activity and this effect can be eliminated by pre-treated with Piezo1 blocker GsMTx4 (Fig 1.3 B). The immediate early gene c-Fos further confirmed this finding (Fig 1.3 C). The expression of the important proteins phospho-CaMKII, phospho-CREB, and c-Fos are also found be increased with the increasement of ultrasound intensity in a cell line (Fig 1.3 D). But with the Piezo1 be knockdown, this effect is significantly reduced (Fig 1.3 E). These finding demonstrate Piezo1's role on gain-of-function mutation and loss-of-function mutation cells, testing the ultrasonic response in immediate effect through the calcium signaling and lasting effect through molecular changes *in vitro*. It thus paves the way for further study of Piezo1's role *in vivo* (Qiu, Z., et al., 2019).

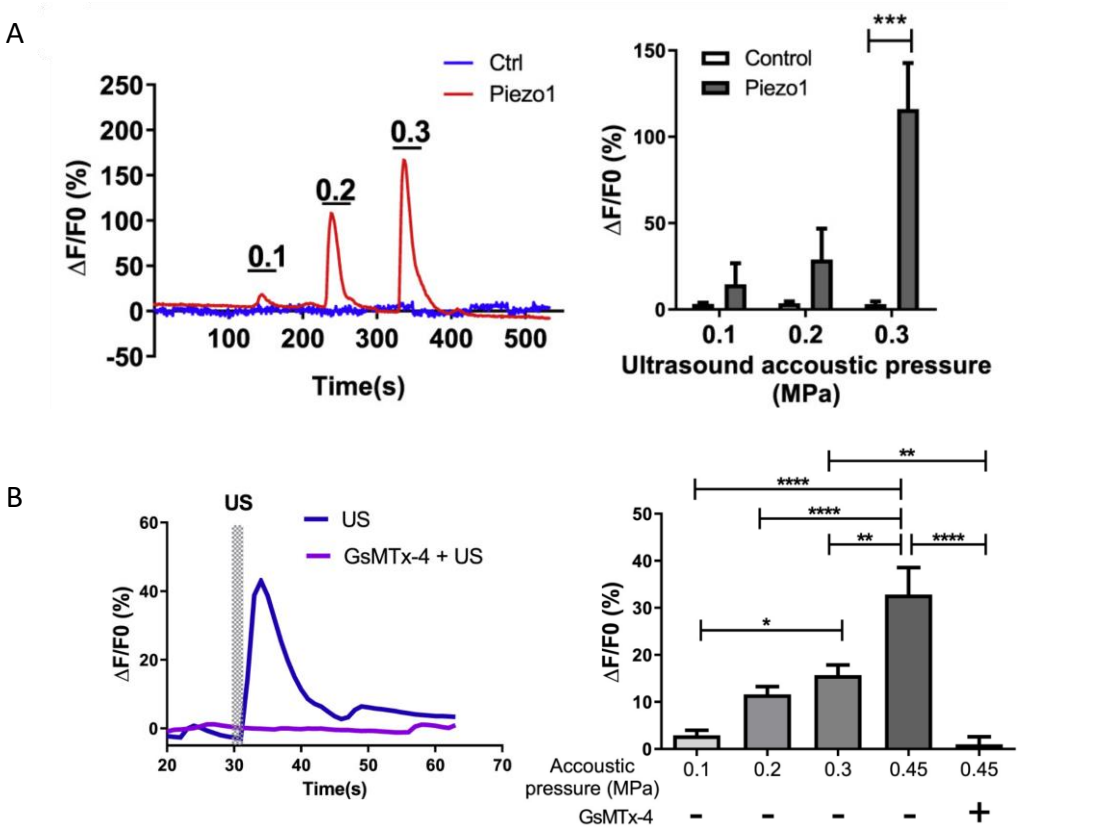
A
Ctrl
Piezo1
0.1
0.2
0.3
ΔF/F0 (%)
Time(s)
Control
Piezo1
***
Ultrasound accoustic pressure (MPa)
B
US
GsMTx-4 + US
Time(s)
Accoustic pressure (MPa)
GsMTx-4
C
Ctrl
US
US+ GsMTx-4
c-Fos/MAP2
c-Fos/MAP2/DAPI
20 μm
c-Fos+ nuclei
c-fos/DAPI (%)
Ctrl
US
+GsMTx-4 + US

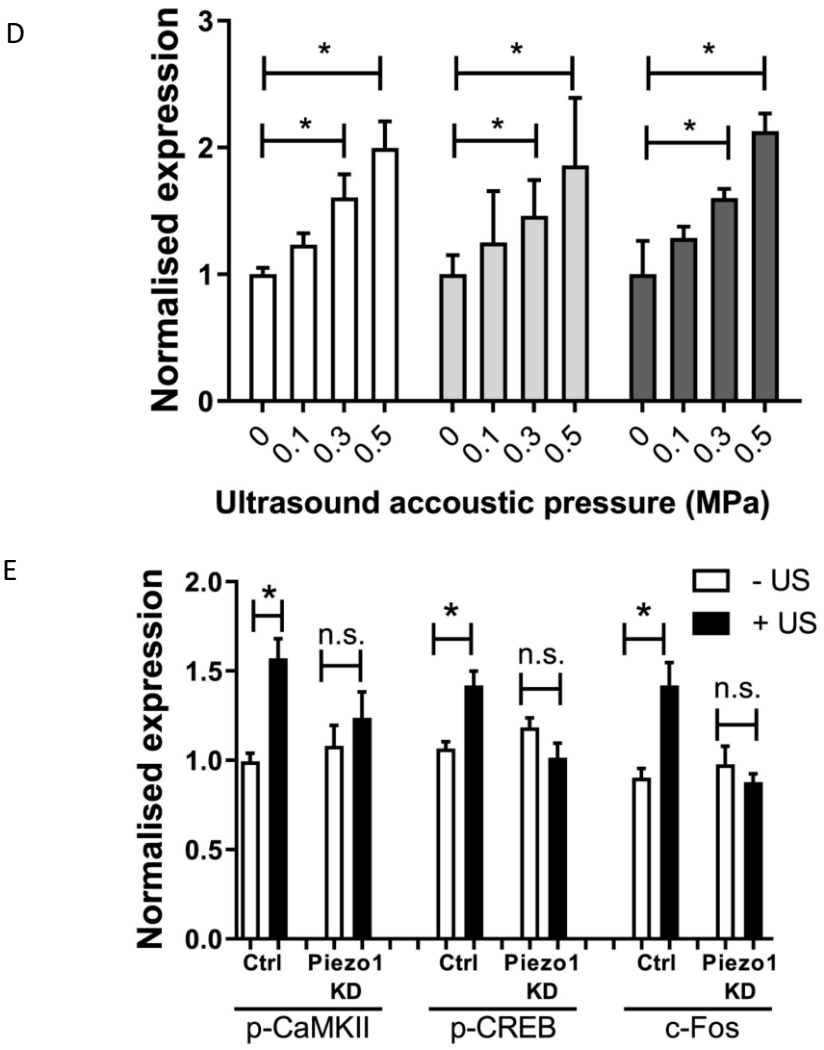

Figure 1.3 Piezo1 mediate the ultrasonic neuromodulation *in vitro* (modified from Qiu, Z., et al., 2019). A. mPiezo1 transfected HEK293T cells is activated by ultrasound. Left: a representative time course of Ca^{2+} image in Piezo1 transfected HEK293T cells and its control different intensity ultrasound stimulus; Right: Summarized calcium ΔF/F result from individual experiments. ***p < 0.0001 with two-tailed unpaired *t* test with Holm-Sidak correction. B. Calcium influx in primary neurons is activated in a Piezo1 dependent Manner. Left: a representative time course of Ca^{2+} image in primary neurons response to 4.45MPa ultrasound with or without pre-treatment of GsMTx-4. Right: Summarized calcium ΔF/F result from individual neuron treated with ultrasound 0.1-0.45 MPa. *p < 0.05, **p < 0.01, ***p < 0.001, one-way ANOVA with post-hoc Tukey test. C. c-Fos expression in primary neurons is activated in a Piezo1 dependent Manner. Left: representative of c-Fos staining in primary neuron untreated, treated with 0.3 MPa ultrasound, or with 20 μM GsMTx-4 followed by ultrasound. Right: Summarized c-Fos number in these 3 groups. *p < 0.05, **p < 0.01, one-way ANOVA with post-hoc Tukey test. D. Ultrasonic intensity dependent calcium signaling pathway induced in CLU199. *p < 0.05, unpaired two-tailed *t* test.

E Piezo1 dependent calcium signaling pathway induced by ultrasound. *p < 0.05, unpaired two-way ANOVA with post-hoc Tukey test.

Although Piezo1 is reported relatively low expressed in the central nervous systems in mice (Wang, J., & Hamill, O. P., 2021) (Fig 1.4 B), Allen mouse brain Atlas and The Human Protein Atlas data base did show a broad expression of Piezo1 RNA in both the human and mouse brain (Fig 1.4 A). Most importantly, its protein level and function in central nerve system has also been reported.

The indication of the correlation of Piezo1 and the nerves system was first recognized when Piezo1 is reported expressed along the axons and growth cones of Xenopus retinal ganglion cells (RGCs) which is a part of the CNS and determined the axon growth and regeneration (Koser, D. E., et al., 2016). The Piezo1 was later reported located in myelinated axonal pathways including the corpus callosum and cerebellar arbor vitae, particularly in neurons of the frontal cortex in the mouse and rat brain. Interestingly, the Piezo1 is found expressed in astrocyte in aging and peripheral infection mice but not the normal astrocytes or the mature oligodendrocytes (Velasco-Estevez, M., et al., 2020, Velasco-Estevez, M., et al., 2018).

Piezo1's function is also implied through several *in vitro* studies. For example, it is found direct the lineage choice of neural stem cells towards a neuronal or astrocytic phenotype in human neural stem cells. The activation of Piezo1 induced by traction forces was found directed the lineage choice of neural stem cells towards a neuronal phenotype, while the inhibition or knockdown of Piezo1 enhanced astrogenesis instead (Pathak, M. M., et al., 2014). Piezo1's role in astrocyte-neuron interactions was also be proposed based on the finding that the neuronal sensitivity to nanoroughness can be blocked by GsMTx4 which is the Piezo1 antagonist (Blumenthal, N. R., et al., 2014).

From the expression and function perspective, this evidence indicate Piezo1 is functioned in the CNS. Together with the finding that Piezo1 mediate ultrasonic neuromodulation *in vitro*, we may expect that Piezo1 as a plausible candidate for ultrasonic neuromodulation *in vivo*.

A

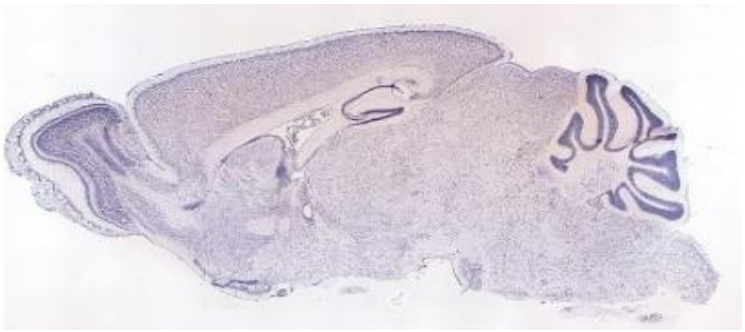

B

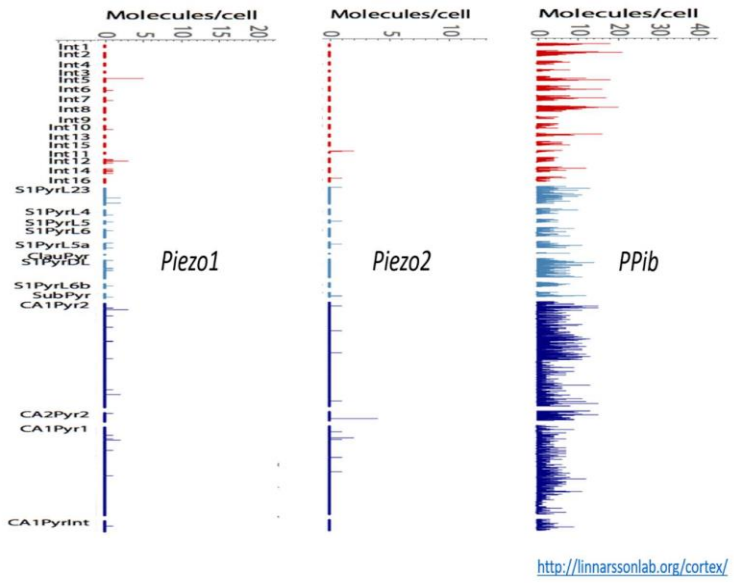

Figure 1.4 RNA data base of Piezo1 in mouse brain. A. The broad expression of Piezo1 RNA in the mouse brain by in situ hybridization in 56 days male C57BL/6J mice (https://mouse.brain-map.org). B. Quantitative single cell RNA-sequencing i(scRNA-seq) of single neurons in the S1 and the hippocampal CA1-2 regions of mice (CD-1) between 21 and 31 postnatal days and including both sexes. The vertical axis means the genetically identified interneuron and pyramidal neuron types in S1 and CA1-2 area. The horizontal axismans the single RNA transcript counts of Piezo1, Piezo2 and the housekeeper gene Ppib (Peptidylprolyl cis-trans isomerase B) (Wang, J., & Hamill, O. P., 2021).

1.8 Piezo1 protein

As pivotal mechanism of the mechanotransduction, mechanosensitive ion channels have been widely studied in organisms from bacteria to mammals (Blount, P., et al., 1999; Morris, C.E., 1990). In eukaryotic cells, mechanosensitive ion channels such as transient receptor potential (TRP) channels, voltage-gated Na^+, K^+ and Ca^{2+} channels are widely found distribution in different tissue and responsible for several genetic diseases (Lamandé, S. R., et al., 2011; Gu, Y., & Gu, C., 2014). However, these ion channels are not purely mechanosensitive. For example, the TRP channel can be activated by mechanical stimuli and chemicals, temperature, osmolality, and heat (> 27–34 °C) (Güler, A. D., et al., 2002).

Until 2010, Coste, B., et al. revealed a novel family of mechanically activated cation channels in eukaryotes, piezo families, through siRNA-based screening. The piezo which consists of Piezo1 and Piezo2, is believed to be the long-sought-after mechanosensitive ion channels in mammals and has opened a new area for the probing of mechanobiology.

During the past 10 years, studies have indicated the Piezo1 channel is mainly expressed in non-sensory tissues such as the lung, bladder, and skin; by contrast, the Piezo2 is predominantly expressed in sensory tissues including dorsal root ganglia (DRG) sensory neurons and Merkel cells (Coste, B., et al., 2020).

Piezo1 channels allow Ca^{2+} influx in response to different types of external forces, such as fluid flow (Retailleau, K., et al., 2015), pulling (Gaub, B. M., & Muller, D. J., 2017), and ultrasonic forces (Qiu, Z., et al., 2019). The pivotal role of Piezo1 channels in mechanotransduction under physiological conditions including the erythrocyte volume regulation (Cahalan, S. M., et al., 2015), cell division (Gudipaty, S. A., et al., 2017), and innate immunity (Solis, A. G., et al., 2019) is also be found. Global knockout of Piezo1 is found lethal in mice (Li, J., et al., 2014). In human, gain-of-function mutations causes congenital lymphatic dysplasia while gain-of-function mutations are associated with dehydrated hereditary xerocytosis (Alper, S. L., 2017).

Molecular structures of piezo1 protein

Piezo1 was first reported with predicted lengths of 2100–4700 aa and contain 24–36 transmembrane (TM) domains which makes Piezo the largest plasma membrane ion channel complex identified thus far. Benefit from the development of cryo-electron microscopy (cryo-EM), the mouse Piezo1 (mPiezo1) structure was resolved at as high resolution as 3.8 Å (Saotome, K., et al., 2018) and 3.97 Å (Zhao, Q., et al., 2018). mPiezo1 is now found to consist of 2547 aa and 38 TMSs. The cryo-EM studies also revealed that mPiezo1 exhibits a "nanobowl" configuration which deform lipid bilayers locally into a dome shape (Jiang, Y., et al., 2021; Zhao, Q. et al., 2018). Overall, the mPiezo1 protein has a three-bladed, propeller-shaped homotrimeric architecture (Fig 2.2 A) composing a unique 38-TM-helix topology in each subunit. Together these subunits assemble the structure of a central cap, three peripheral blade-like structures on the extracellular side, three long beams on the intracellular side that bridge the blades to the cap, and a TM region between these features (Fig 2.2 B) (Fang, X. Z., et al., 2021; Zhao, Q., et al., 2018; Saotome, K., et al., 2018; Guo, Y. R., et al., 2017; Ge, J., et al., 2015).

The first 36 TM helix formed into a highly curved blade-like clockwise structure with nine repeated transmembrane helical units (THU) which consist of four transmembrane helices (36TM = 4TM X 9THU). The large extracellular blade domains can curve the plasma membrane while the three blades are assembled into functional trimers (Syeda, R., et al., 2016). Functional studies showed that residues 1–2190 of the mechanotransduction modulus confer mechanosensitivity to trimeric channel pores (Coste, et al., 2015). The structure of the mechanotransduction modulus is essential for Piezo1 mechanical activation (Alper, S. L., 2017).

The last two TM regions (TM37 and TM38) which are designated as the inner helix (IH) and outer helix (OH), enclose a hydrophobic central pore module which is found locates in residues 2210 to 2457. Since it followed the last TM region from the C-terminus it also termed C-terminal extracellular domain (CED). These three pore moduli assemble the extracellular Cap structure. It determines the fundamental pore properties, including unitary conductance, ion selectivity, and pore blockage (Geng, J., et al., 2017; Wang, F., et al., 2017; Zhao, Q., et al., 2016).

There is a hairpin structure, also termed anchor, connecting the OH-CED-IH to c-terminal domain (CTD) plane, moves the OH-CED-IH-containing region into the neighboring subunit in a clockwise direction and remains the integrity of the channel.

On the intracellular surface, Piezo1 contains three beam-like structures supporting and bridging the blade into the central pore module via the interfaces of the C-terminal domain, the anchor-resembling domain, and the outer helix (Zhao, Q., et al., 2018). Based on this unique topological feature, a lever-like mechanotransduction mechanism was proposed (Ge, J., et al., 2015; Blount, P., et al., 1999). The curved blades act as a mechanosensor, while the beam structure, with the residues Ll1342 and Ll1345 act as a pivot. Because the pivot of the lever is located closer to the central pore than to the distal blades, the force can be amplified through this lever-like apparatus. The large conformational change in the distal blades is converted into a relatively slight opening of the central pore, allowing cation-selective permeation.

Another mechanotransduction mechanism, the membrane dome model, is also proposed based on the finding that changes in the projection area of Piezo1 from closed to open are essential for their mechano-sensitivity (Guo, Y. R., & MacKinnon, R., 2017). In short, the three-bladed, propeller-shaped trimeric architecture of Piezo1 locally deform lipid membranes into a dome-like shape (Zhao, Q., et al., 2018), and this shape acts as a potential energy source for MS gating in their closed conformation (Guo, Y. R., & MacKinnon, R., 2017; Lin, Y., et al., 2019). Lateral membrane tension flattens the Piezo dome, which increases the energy of the membrane-channel system in proportion to the expansion of the projected area of the dome. And this relative energy difference opens Piezo and leads to the cation-selective pore opening with highly sensitive.

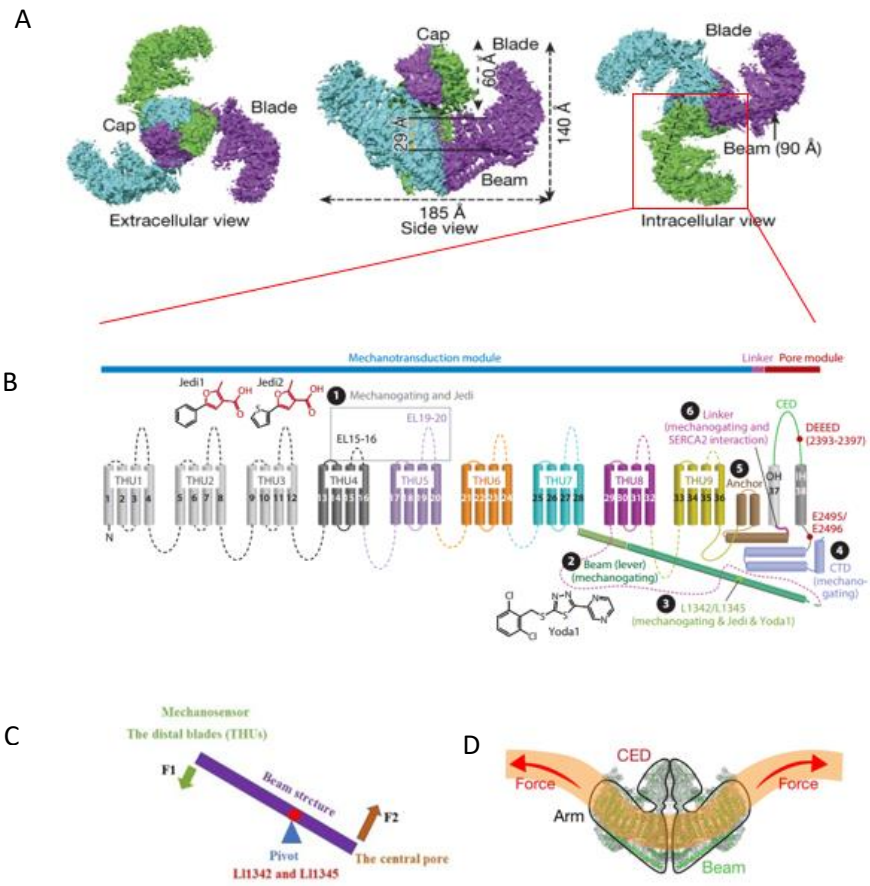

Figure 1.5 Structure of Piezo1 and its proposed mechanotransduction mechanism. A. Structure of mPiezo1 from the extracellular view, side view and intracellular view. Overall, the mPiezo1 protein displayed as a three-bladed, propeller-shaped homotrimeric architecture (Zhao, Q., et al., 2018); B. Repetitive THUs of the 38-TM topology model of piezo1. B. A 38-TM topology model in Piezo1. The first 36 TM helix formed into a highly curved blade-like clockwise structure and function as a mechanotransduction modulus. The TM37 (OH)-CED-TM38 (IH)-CTD formed the trimeric channel pores and allowed cation-selective permeation upon stimulus (Zhao, Q., et al., 2018); C. A lever-like mechano-gating model of Piezo1. The curved blades act as a mechanosensor, the residues Ll1342 and Ll1345 act as a pivot supporting the beam structure (Ge, J., et al., 2015) D. A Membrane dome model of Piezo1 (Lin, Y., et al., 2019). Changes in membrane curvature leads to a gating force applied to the Piezo1 channel.

Kinetics properties of Piezo1 protein

The kinetics of piezo1 can be defined as three states: open, closed, and inactivated. These states emerged collectedly and act as an important mechanism of piezo1 function.

The Piezo1 is proposed to be activated by the mechanism of a lever-like mechanotransduction model and membrane doming mechanism. Piezo1 can be triggered by various types of mechanical stimulation and sequentially elicit an MA current with a rapid decay, even in the presence of continued stimulation, due to rapid inactivation (Coste, B., et al., 2010). This inactivation kinetics is also displayed voltage-dependent manner. In short, it inactivates fast at rather negative membrane potentials and slow at rather positive membrane potentials.

It is implied that, the pore region which contains the OH, IH, ECD and CTD region, determines the kinetics of inactivation by the gain-of-function mutation studies (Okubo, M., et al., 2015; Wu, J., et al., 2017; Zheng, W., et al., 2019). Zoom in the cap region, 3 small subdomains in extracellular cap were shown to be individually confer Piezo channel inactivation (Lewis, A. H., & Grandl, J., 2020). These results demonstrate that the ion-conducting pore region of Piezo1 channels determines its inactivation properties.

Interestingly, a slow inactivating MS current is also be found in mouse embryonic stem cells (mESc). However, heterologous expression of Piezo1 cDNA from mES cells exhibited a fast inactivation kinetics which indicates another regulatory mechanism rather than the amino acid sequence determined inactivation kinetics of the Piezo1 channel in mES cells (Del Mármol, J. I., et al., 2018). Indeed, several modulators has been revealed regulate the Piezo1 inactivation kinetics. For instance, the SMPD3 is proposed responsible for the sustained PIEZO1 activation induced by fluid flow (Shi, J., et al. 2020). TMEM150C prolongs the duration of MA in several mechano-gated ion channels including the Piezo1 (Anderson, E. O., et al., et al., 2018). TMEM150c and Piezo1-ASIC1 Chimera are also reported enhance endogenous Piezo1 activity (Dubin, A. E., et al. 2017; Zhao, Q., et al., 2017). In addition to the positive influence of Piezo1 activity, inhibition of Piezo1 by TRPV1 is also be reported.

Moreover, Piezo1 also regulate other channels kinetics. For instant, Piezo1 opening is found upregulate the TREK/TRAAK mechanical activation and delayed its kinetics (Glogowska, E., et al., 2021). An elegant cooperation of piezo1 and RRPV1 in fluid stress is also reported. The activation of Piezo1 initiates a calcium signal that causes TRPV4 opening, which in turn

response for the sustained phase calcium elevation. Thus, deleterious effects of shear stress are initiated by Piezo1 but require TRPV4 (Swain, S. M., & Liddle, R. A., 2021).

Since the kinetics of Piezo1 is found regulate several other ion channel and other component, and in turn be regulated by these factors, we may expect that the function of Piezo1 various in different context. The outcome of the modulation this protein may be various in different tissue, animal, and the physiological state.

Pharmacological modulators of Piezo channels

Despite the relatively recent discovery of Piezo channels, the small-molecule modulators of Piezo1 have been reported. Yoda1 and Jedi1/2 are able to open Piezo1 ion channels without the mechanical stimulation. The specific inhibitors of Piezo1 are in their infancy with the RR and GsMTx4 be used the most currently.

Yoda1 is the first Piezo1 activator be identified by the high-throughput fluorescence imaging plate reader (FLIPR) screening through approximately 3.25 million compounds (Syeda, R., et al., 2015). It is be found activates both mPiezo1 and hPiezo1 with an apparent EC50 of about 17 μM and 27 μM. It is also be reported bind to the putative mechanosensory domain and acts as a molecular wedge, facilitating force-induced conformational changes, effectively lowering the channel's mechanical threshold for activation (Botello-Smith, W. M, et al., 2019).

Jedi1 and Jedi2 is a novel hydrophilic activator identified by FLIPR and GCaMP6s through around 3,000 compounds. They are be found specifically activated Piezo1 with an EC50 of about 200 μM and 158 μM, respectively. It is also be reported acts its function through the peripheral blades and utilizes a peripheral lever-like apparatus consisting of the blades and a beam to gate the central ion-conducting pore (Wang, Y., et al., 2018).

Gadolinium (Gd^{3+}) and ruthenium red (RR) are nonspecific inhibitors of the ion pore in stretch-activated ion channels including TRP channel and Piezo channels. They block the mPiezo1 channels with IC_{50} values of approximately 5 mM (Coste, B., et al., 2012).

The commonly used blocker is an amphipathic peptide toxin which inhibit the mechanosensitive channels including the Piezo1channel (Bae, C., et al., 2011; Suchyna, T. M., 2017). It reversibly blocks Piezo1 with a Kd of approximately 155 nM or 2 μM when tested under outside-out or whole-cell recording configurations, respectively (Bae, C., et al., 2011).

Consideration may be required using this drug since it might not bind Piezo1 directly, rather acting via modulating local membrane tension near the channel (Zheng, W., et al., 2019).

1.9 Conclusion and hypothesis

Ultrasound is an emerging technology that can noninvasively modulate neurons in deep brain regions area with fine spatial and temporal resolution thus provides a promising tool for both probing brain function and brain diseases. Massive evidence that demonstrates ultrasound modulate neurons has been reported in rodents (Tufail, Y., et al., 2010; Yoo, S. S., et al., 2011b; Kim, H., et al., 2012; King, R. L., et al., 2013, 2014; Ye, P. P., et al., 2016; Yu, K., et al., 2021), sheep (Lee, W., et al., 2016c) and monkeys (Deffieux, T., et al., 2013; Wattiez, N., et al., 2017) where neurons and brain circuits are directly stimulated and the related behavior such as visuomotor behavior or motor response are observed. Activation of human cortical, sub-cortical and the related network has also been widely detected (Lee, W., et al., 2015; Lee, W., et al., 2016b; Legon, W., et al., 2014; Legon, W., et al., 2018a; Legon, W., et al., 2018b). Importantly, these effects did not show observable side effects, even with chronic stimulation. Based on this, clinical trials including the mood improvement (Sanguinetti, J. L., et al., 2020; Reznik, S. J., et al., 2020), and chronic disorder of consciousness treatment (Cain, J. A., et al., 2021).

All this evidence indicate ultrasound a credible, safe, and clinical translational technics for both neuroscience research and treating brain diseases. However, with the mechanism unknown, many phenomena are hard to explain along with the bidirectional effect of the ultrasonic neuromodulation. Whether that a serial set of ultrasound parameter, the neuronal state, the neuronal subtype, or the intrinsic neuronal connectivity mattes, are all in an elusive state. The stimulation outcome of current approach is thus not easy to be predicted and even contradictory in some cases which has lied a hidden danger for appropriate applications in humans.

Therefore, understand the mechanism of how ultrasound modulate the neurons in a brain is the key to take the advantage of the ultrasonic neuromodulation thoroughly, accurately and avoiding the unpredictable side effects. Especially with the growing clinical trials for diseases treatment in various stages including neuropsychiatric disease (Tsai, S. J., 2015), depression (Reznik, S. J., et al., 2020; Sanguinetti, J. L., et al., 2020), it has become an urgent exploring the mechanism of ultrasonic neuromodulation.

Regarding the physical property of ultrasound, various mechanisms including the mechanical force, thermo-effect and cavitation are proposed in different labs. (Tyler, W. J., 2011; Tyler, W. J., et al.., 2012; Fomenko, A., et al., 2018; Kamimura, H. A., et al., 2020). The

mechanical force has stand out itself as the most promising one based on the increasing evidence from ultrasound physics perspective and biological effect found in neurons (Kim, H., et al., 2014; Tyler, W. J., et al.., 2018; Kubanek, J., et al., 2018; Menz, M. D., et al., 2019).

While there are several mechanical responsive components sensing the mechanical force, mechanosensitive ion channel has drawn much attention because of the millisecond timescale of ultrasound induced bio-effect. (Bystritsky, A., et al., 2011, Fomenko, A., et al., 2018, Tyler, W. J., et al.., 2018). The finding that multiple mechanosensitive ion channel response to ultrasound (Kubanek, J., et al., 2016; Kubanek, J., et al., 2018; Qiu, Z., et al., 2019 Qiu, Z., et al., 2020; Sorum, B., et al., 2021) further indicate the probability ultrasound neuromodulation in mammal brain may be mediated by the endogenous expression of mechanosensitive ion channel.

In this case, a mechanosensitive ion channel that endogenous expressed and functioned in central nerve system, one that is sensitive enough responding to ultrasound stimulus in an intact brain environment within the so-far studied ultrasound intensity and leading to the observed ultrasound brain stimulation outcomes may be the answer for the ultrasonic neuromodulation *in vivo.*

Piezo1 displayed a plausible mechanism for ultrasonic neuromodulation from both experimentally and theoretically perspective. Piezo1, the most sensitive mechanotransdcution ion channel, is found response to force as low as 10 pN (Coste, B., et al., 2010; Wu, J., et al., 2016) and ultrasound sonication as low as 0.1 MPa (Qiu, Z., et al., 2019). Together with the report that Piezo1 is expressed in both RNA (Allen mouse brain atlas), Protein and functional level in mouse brain (Velasco-Estevez, M., et al., 2020, Velasco-Estevez, M., et al., 2018), it is thus indicated the high possibility of Piezo1's role mediating the ultrasonic neuromodulation *in vivo*.

Chapter 2. Piezo1's role in ultrasonic neuromodulation

2.1 Material and method

Animal preparation

Mice used in this study includes C57 BL6/J (JAX# 000664) and Piezo1$^{tm2.1Apat}$ (JAX# 029231). Mice were housed under standard housing condition with 12-hour light/dark cycle food and water available ad libitum. Animal use and care were performed following the guideline of the Department of Health - Animals (Control of Experiments) of the Hong Kong S.A.R. government.

Immunohistochemically fluorescent staining

The expression of Piezo1 in mice is the foundation of this study thus the immunohistochemically fluorescent staining is firstly performed to test if it is expressed in mouse brain in protein level. Mice were deeply anesthetized by 100 mg/ml ketamine and 10 mg/ml xylazine in PBS and then perfused with PBS, followed by 4% paraformaldehyde (PFA) (cat. no. P1110, Solarbio). After dissection, brains were post-fixed overnight in 4% PFA and then rinsed in PBS. Around 30 continuous coronal brain slices with the interval of 135 μm were collected. Slices were blocked using 10% normal goat serum + 1% BSA for 90 mins and incubated in Piezo1 (ab128245, Abcam, 1:50) and MAP2 (PA1-16751, Invitrogen, 1:500) antibody solution diluted in 10% normal goat serum + 1% BSA for 3 days. Slices were then washed and incubated with goat anti-rabbit IgG (H+L) Alexa Fluor 488 (A-11008, Invitrogen, 1:1000) and goat anti-mouse IgY (H+L) Alexa Fluor 633 (A-21103, Invitrogen, 1:1000). diluted in PBS for 90 mins at room temperature. Slices were then washed, sticked to glass slides, dried, and mounted on coverslips using small drops of Prolong Diamond Antifade Mountant with DAPI and allowed to cure in the dark overnight. Coverslip edges were sealed using transparent nail enamel and imaged using a confocal laser scanning microscope (TCS SP8, Leica). The same method is also adopted confirming if Piezo1 was conditionally knockout in P1KO neurons.

Ex vivo electrophysiology

To test if the Piezo1 found in mouse brain is functional, patch clamp in acute brain slice was performed. The inward incurrent in neurons induced by Piezo1 agonist Yoda1(Cat. No. 5586, Tocris Biosciences) (20 μM) with or without the broad mechanosensitive ion channel blocker Ruthenium Red (RR, 30 μM) was measured.

Brain slice prepared (details in below) was placed on the hold chamber and perfused with oxygenated rACSF. Borosilicate glass-made patch pipettes (Vitrex, Modulohm A/S, Herlev, Denmark), were pulled with micropipette puller (P-97, Sutter Instrument Co., USA) to a resistance of 2 to 5 Mohm before being filled with KCl pipette solution (in mM): KCl 138, NaCl 10, $MgCl_2$ 1 and HEPES 10 with D-manitol compensated for 290 osm. Membrane potential was recorded with a data acquisition system (DigiData 1322A, HEKA Instruments), When the whole-cell Giga seal was formed and the capacitance of cell was measured, set holding voltage at -60 mv. Afterwards, the inward currents can be measured by voltage clamp gap free recording mode.

Calcium image in acute brain slice

To confirm the functional Piezo1's expression in mouse brain and the successfulness of Piezo1 conditional knockout (P1KO) in neurons, calcium image which reveals neuronal response to different stimulus in acute brain slice was performed.

Brain slice pre-expressed GCaMP6s proteins were prepared (details in below) and placed on the hold chamber and perfused with oxygenated rACSF. A customized calcium imaging was utilized with the excitation light of 488. The fluorescence signals were collected and captured by a sCMOS camera (ORCAFlash4.0 LT Plus C114400-42U30, Hamamatsu). To minimize phototoxic effects, the LEDs were triggered at 1 Hz and synchronized with sCMOS time-lapse imaging. The calcium signal changes were measured by ΔF/F in each neuron. The changes below 1% is excluded. Piezo1 agonist Yoda1(Cat. No. 5586, Tocris Biosciences) (20 μM) and blocker ruthenium red (RR, 30 μM) were adopted testing Piezo1's function in neurons and P1KO neurons. This same method was also adopted testing Piezo1's function in ultrasonic neuromodulation in neurons *ex vivo*.

Stereotaxic surgery

To test the Piezo1's role in ultrasonic neuromodulation *ex vivo* and *in vivo*, loss-of-function strategy built by Cre-LoxP system was adopted. With the Cre recombinase expression in neurons whose DNA is flanked with two LoxP site, the certain DNA stains can be deleted. In this study, the Cre recombinant is promoted by Syn which guided it to expressed in neurons. The mice used were Piezo1$^{tm2.1Apat}$ (JAX# 029231), whose Exons 20-23 of mouse Piezo1 gene are flanked by LoxP sites. Injection of Cre virus thus caused excision of the flanked region resulting a conditional knockout neuron in mice.

Male, 4 weeks Piezo1$^{tm2.1Apat}$ mice were deeply anesthetized by 100 mg/ml ketamine and 10 mg/ml xylazine in 0.9% NaCl and positioned in a stereotaxic injection frame (RWD Ltd, China). 400 nL of virus was delivered to 3 locations respectively by a microinjection system (Nanoliter 2010, WPI Ltd) through a craniotomy (<1 mm^2). The injection was performed unilaterally to the right motor cortex (at mm): AP: 0.0 ML: -1.0, AP: +0.5 ML: -1.0, AP: +0.5 ML: -1.5 with DV: 1. The final titer of all viruses was 5 x 10^{12} VG/ml. 3-4 weeks is required for the virus expression. Mice that injected with AAV2/9-Syn-mCherry + AAV2/9-Syn-GCaMP6s and AAV2/9-Syn-Cre-mCherry + AAV2/9-Syn-GCaMP6s are Ctrl group and P1KO group respectively, prepared for calcium image experiment.

Genotyping and tissue isolation

The successfulness of conditional knockout was determined by several methods including immunohistochemically fluorescent staining which tests its protein expression, the calcium image which tests its function and PCR analysis which tests its direct DNA excision outcome. PCR analysis was performed on the DNA extracted from brain tissue where the virus was injected. Using the following primers: P1 F: GCC TAG ATT CAC CTG GCT TC; R: GCT CTT AAC CAT TGA GCC ATC T; P1KO F: CTT GAC CTG TCC CCT TCC CCA TCA AG; R: AGG TTG CAG GGT GGC ATG GCT CTT TTT and Phire II polymerase (Thermo scientific #F-170S). PCR was run following the cycling conditions: initial denaturation 98 ℃ for 5 mins, followed by 98 ℃ for 5 s , then 10 cycles of 65 ℃ (-0.5 ℃/cycle) for 5 s, 68℃ for 20 s, followed by 30 cycles of 98 ℃ for 5 s, 60 ℃ for 5 s, 72 ℃ for 20 s, followed by a final hold of 72 ℃ for 1 min. Reactions were separated on 2% agarose gels (TAE buffer, 100V) yielding the following band sizes: WT: 188 bp, P1: 380 bp, P1KO: 230 bp.

Ultrasound setup:

Transducer placed in a handmade tube controlling the stimulation area 4 mm^2 were adjusted underneath the rACSF confocal dish. Ultrasound stimuli (0.35 MPa) were administered with the 500 µs tone of burst, 300 ms duration and 10 s intervals.

Acute brain slice preparation

The mice under the age of 6 weeks old were deciphered on the ice. The brain is extracted immediately and be moved into the ice-cold treatment ACSF (tACSF) containing (in mM): NaCl 124, KCl 3, NaH_2PO_4 1.25, $MgSO_4$ 2, $CaCl_2$ 2, $NaHCO_3$ 26, Glucose 10. Coronal brain sections of 300-400 µm thickness were cut with a vibratome (Leica, VT1000S) in ice-cold tACSF. Slices were then recovered at 35 ℃ tACSF for at least for 1 hour. The slice was then transferred to the recording ACSF (rACSF) perfusing confocal dish for the calcium image or patch clamp. The rACSF contains (in mM): 124 NaCl, 3 KCl, 1.25 NaH_2PO_4, 1 $MgSO_4$, 2 $CaCl_2$, 26 $NaHCO_3$, 10 Glucose.

The mice over the age of 8 weeks old were deeply anesthetized by intraperitoneal injection of Ketamine/Xylazine mixture (100 mg/kg and 10 mg/kg body weight) and transcranial perfused with NMDG ACSF containing (in mM): 92 NMDG, 2.5 KCl, 1.25 NaH_2PO_4, 20 $NaHCO_3$, 10 HEPES, 25 Glucose, 2 thiourea, 5 Na-ascorbate, 3 Na-pyruvate, 0.5 $CaCl_2 \cdot 4H_2O$ and 10 $MgSO_4 \cdot 7H_2O$ and 12 NAC. Titrate pH to 7.3–7.4 with concentrated hydrochloric acid. Coronal brain sections of 300-400 µm thickness were cut with a vibratome (Leica, VT1000S) in ice-cold NMDG ACSF. Slices were shortly recovered for 10-12 mins in 32 ℃ NMDG ACSF. After that, slices were recovered in HEPES ACSF containing (in mM): 92 NaCl, 2.5 KCl, 1.25 NaH_2PO_4, 30 $NaHCO_3$, 20 HEPES, 25 Glucose, 2 thiourea, 5 Na-ascorbate, 3 Na-pyruvate, 2 $CaCl_2 \cdot 4H_2O$ and 2 $MgSO_4 \cdot 7H_2O$ at room temperature for at least 1 hr. The slice was then transferred to the rACSF perfusing confocal dish for the calcium image. The rACSF contains (in mM): 126 NaCl, 1.6 KCl, 1.2 NaH_2PO_4, 1.2 $MgCl_2$, 2.4 $CaCl_2$, 18 $NaHCO_3$, 11 Glucoses.

All ACSF solutions were newly prepared and be saturated with carbogen (95% O2 /5% CO2) prior to use to ensure stable pH buffering and adequate oxygenation.

2.2 Piezo1 is functional expressed in neurons in mouse brain

To test the role of Piezo1 in ultrasonic neuromodulation in mice, its endogenous functional expression in mouse brain was first confirmed. Although Piezo1's expression in mouse brain on RNA (see https://mouse.brain-map.org/experiment/show/68443399) and protein (Velasco-Estevez, M., et al., 2018; Velasco-Estevez, M., et al., 2020) levels have previously been reported, its functional expression level lacks experimental confirmation. Here, by immunofluorescent staining, it was found that Piezo1 is broadly expressed in the mouse brain including the cortex (Fig 2.1 A, Fig 3.6 J). In light of Piezo1 studies on primary neurons harvested from cortical area (Qiu, Z., et al., 2019, Yoo, S., et al., 2022), and plentiful reports of ultrasound stimulation induced motor response on motor cortex in animals (King, R. L., et al., 2013, 2014; Ye et al., 2016; Tufail, Y., et al., 2010), cortex area was focused on this study.

Using patch clamp (Fig 2.1 B), neuron activation through Piezo1 agonist Yoda1 introduction was captured (Fig 2.1 C, bottom). Total 3 neurons were record with inward current (in pA) of 825, 50 and 0. The same neurons were then washed and incubated with broad mechanosensitive ion channel blocker Ruthenium Red (Syeda, R., et al., 2016), no inward current could be observed following Yoda1 addition (Fig 2.1 C, top). Together, functional expression of Piezo1 is suggested.

Although patch clamp offers fine electrophysiological details of individual neurons, with varying Piezo1 expression level between neurons, detecting neuronal activities collectively might as well be necessary. Calcium imaging on acute brain slice, which allows observation on multiple neurons simultaneously was thus performed (Fig 2.1 D). By expressing Ca^{2+} indicator GCaMP6s, neuronal activities can be quantified in form of fluorescence. Similar to the results from patch clamp, Yoda1 induced neuronal activity could be observed (64.07% ± 42.89%) but not on samples pre-treated with RR (1.608% ± 0.2875%) (Fig 2.1 E, F), further proving functional expression of Piezo1.

Taken together, through molecular detection and functional examination, functional expression of Piezo1 in neuron was confirmed.

A

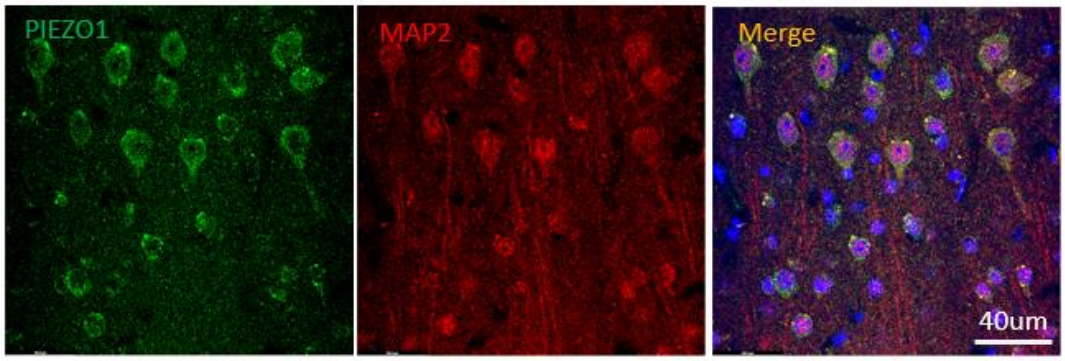
PIEZO1
MAP2
Merge
40um

B

C

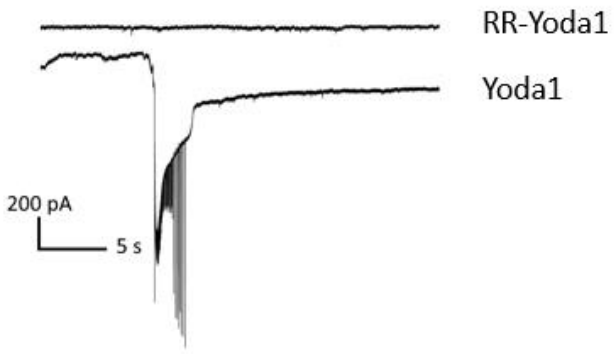
RR-Yoda1
Yoda1
200 pA
5 s

D

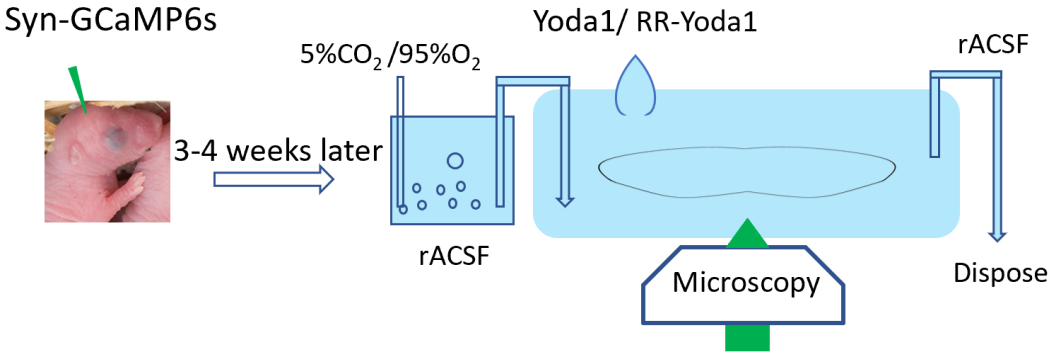
Syn-GCaMP6s
3-4 weeks later
5%CO2 /95%O2
rACSF
Yoda1/ RR-Yoda1
rACSF
Microscopy
Dispose

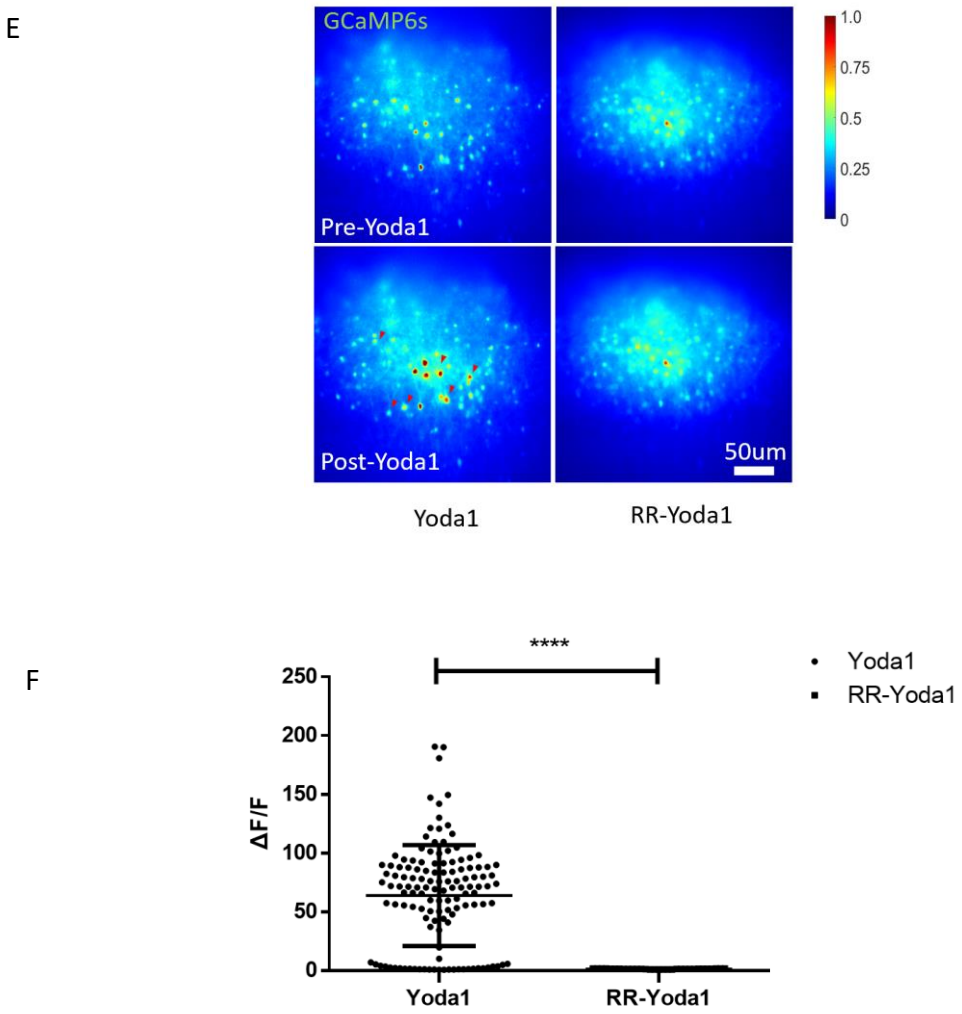

Figure 2.1 Piezo1 is functionally expressed in mouse brain. (A) Immunostaining of Piezo1 and MAP2 in mouse brain cortex. Green: Piezo1; Red: MAP2; Blue: DAPI; Scale bar: 40 μm. (B) Demonstration of patch clamp recording on cortex neuron under microscope. Brain slices were collected from neonatal mice (P3). (C) Representative patch clamp recording of inward current induced by Yoda1 on cortex neurons with or without RR pre-incubation. Yoda1 applied was 60 μM. RR incubation (30 μM, if applicable) was 10 mins. (D) Schematic of calcium imaging on acute brain slice under Yoda1 treatment, with or without RR pre-incubation. Brain slices were collected 3-4 weeks after virus (Syn-GCaMP6s) injection. Yoda1 applied was 20 μM. RR incubation (30 μM, if applicable) was 10 mins. (E) Representative calcium signaling of neurons in the acute brain slice before (upper row) and after (lower row) Yoda1 addition. Left column: Yoda1 group; Right column: RR-pretreated group; Scale bar: 50 μm. (F) Summarized ΔF/F result from individual calcium signaling experiments. Left: 130 neurons from 2 mice; Right: 31 neurons from 2 mice. Dot plots represents mean ± SD, ****$p < 0.0001$ by two-tailed t test.

2.3 Generation of Piezo1 conditional knockout models

To further test Piezo1's role in ultrasonic neuromodulation, mice with Piezo1 conditional knockout (P1KO) neurons in motor cortex was generated through Cre-LoxP system. Cre recombinase was delivered to target neurons by local injection of AAV virus with Syn promoter. By expressing Cre in the neurons in Piezo1$^{f/f}$ mice, the exon 22-23 would be deleted (Fig 2.2 A). To validate the conditional knockout, expressions of Piezo1 on DNA and protein levels were tested through genotyping and immunostaining respectively. To further confirm these results, the function of Piezo1 represented by its's response to Yoda1 was then examined through calcium imaging in acute brain slices. KCl was applied randomly in some P1KO slices after the functional testing to exclude neuronal death confound.

Genotyping results show the presence of LoxP site in all Piezo1$^{f/f}$ mice samples including P1$^{f/f}$, Ctrl and P1KO mice, while wild type (WT) mice displayed shorter band due to the lack of LoxP (Fig 2.2 C, left); since Cre recombinase was targeted to neurons, the exon 22-23 and flanking LoxP site would be retained in surrounding non-neuron cells of P1KO samples, giving rise to the band in P1KO mice as well. Regarding primer designed (P1, P3), since the sequence without knockout is too long (3080 bp) to be amplified in PCR, i.e., genotyping test, only P1KO samples detected the band at 230 bp (Fig 2.2 C, right).

Immunostaining results showed expression of Piezo1 (Green) in Ctrl (Red) mouse brain slice but unobservable of Piezo1 fluorescent signaling (Green) in P1KO (Red) mice (Fig 2.2 D), indicating successful virus transfection and the knockout of Piezo1protein at the site. Thus, the conditional knockout was determined successful in DNA and protein expression perspectives.

Function in P1KO neurons was then tested by calcium imaging on acute brain slices. Calcium influx was found induced by Yoda1 in Ctrl neurons (44.68% ± 37.71%) but much less in P1KO neurons (6.631% ± 7.465%) or RR-pretreated Ctrl neurons (6.559% ± 8.205%) (Fig 2.2 E, F), which indicates the loss of functions of Piezo1 in P1KO neurons. The neuron viability was also confirmed through KCl treatment and the response was observed (73.19% ± 40.63%) excluding confound of cell death in P1KO group.

Taken together, from molecular and functional perspective, the generation of P1KO model was confirmed successful.

A

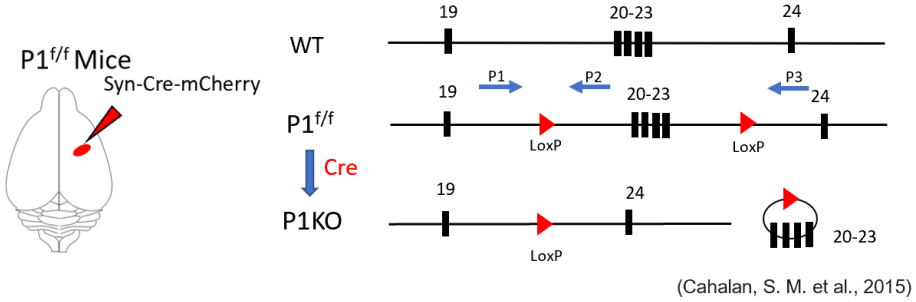

(Cahalan, S. M. et al., 2015)

B

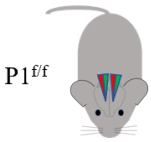

P1KO: AAV-Syn-Cre-mCherry
Ctrl: AAV-Syn-mCherry
→ Molecular test → DNA, Protein

P1KO: AAV-Syn-Cre-mCherry + AAV-Syn-GCaMP6s
Ctrl: AAV-Syn-mCherry + AAV-Syn-GCaMP6s
→ Functional examination → KO *vs*. Ctrl, Agonist *vs*. Blocker, Neuron viability

C

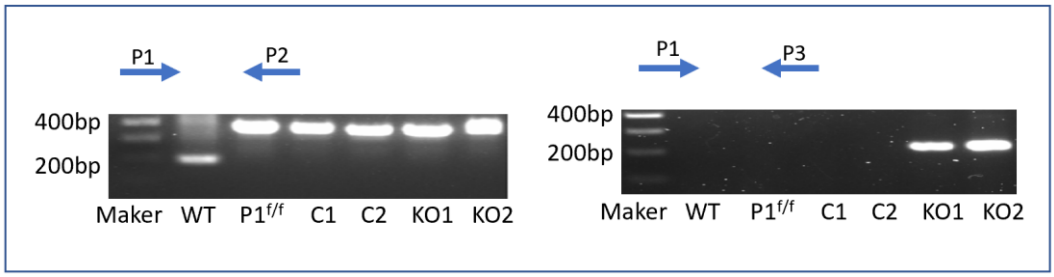

D

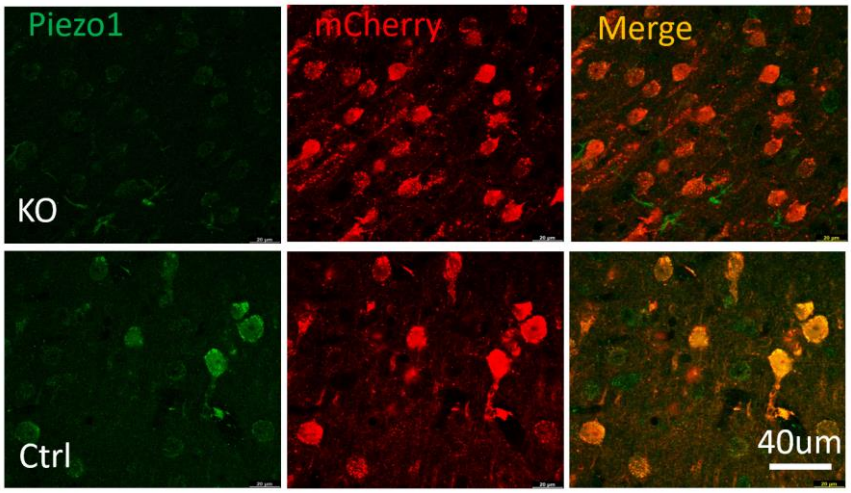
Piezo1
mCherry
Merge
KO
Ctrl
40um

E

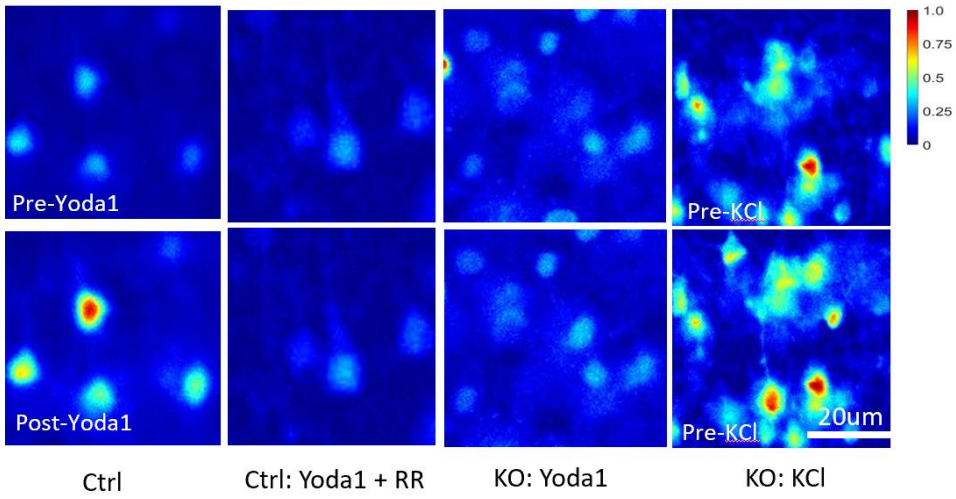
Pre-Yoda1
Post-Yoda1
Pre-KCl
Pre-KCl
20um
1.0
0.75
0.5
0.25
0
Ctrl
Ctrl: Yoda1 + RR
KO: Yoda1
KO: KCl

F

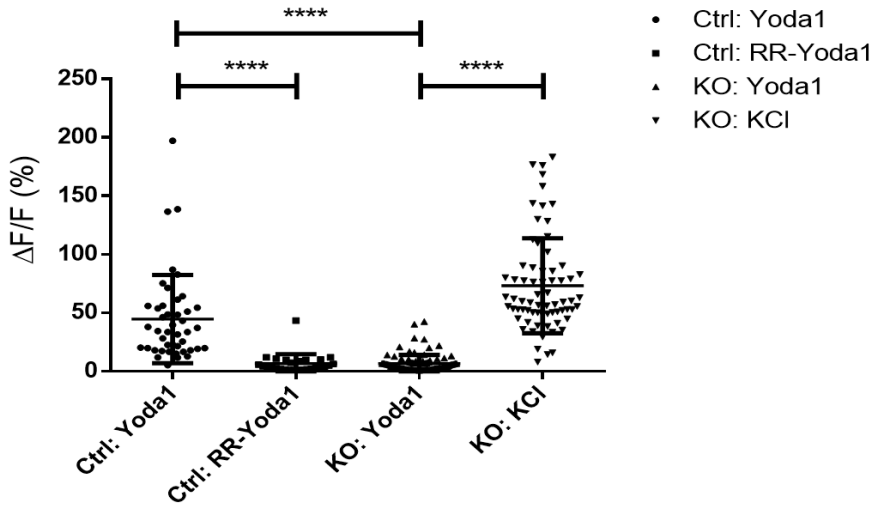
****
****
****
250
200
150
100
50
0
ΔF/F (%)
Ctrl: Yoda1
Ctrl: RR-Yoda1
KO: Yoda1
KO: KCl
Ctrl: Yoda1
Ctrl: RR-Yoda1
KO: Yoda1
KO: KCl

Figure 2.2 Piezo1 conditional knockout by Cre-LoxP system was successful. (A) Schematic of Piezo1 conditional knockout by Cre-LoxP system (modified from Cahalan., S. M., et al., 2015). $P1^{f/f}$ represents mouse line with exons 20–23 of Piezo1 flanked by LoxP sites. With the Cre recombinase recognizing the LoxP sites, exons (floxed site) would be deleted. (B) Schematic of Piezo1 conditional knockout in neurons in mouse brain by Cre-LoxP system. Mice injected with Syn-mCherry or Syn-Cre-mCherry are Ctrl and P1KO mice prepared for molecular test i.e., genotyping and immunostaining. Mice injected with Syn-mCherry + Syn-GCaMP6s or Syn-Cre-mCherry + Syn-GCaMP6s, classified as Ctrl and P1KO mice respectively, were prepared for functional experiment i.e., calcium imaging. (C) Left: genotyping results with LoxP-spanning PCR primers. The expected products are 380 bp in $Piezo1^{f/f}$ mice and 188 bp in wild type mice. Right: genotyping results with deletion-spanning PCR primers. The PCR product size after deletion was expected to be 230 bp. PCR product in mice without the deletion was not expected because the sequence is too long to be amplified (3080 bp). (D) Representative immunostaining results of Piezo1 in Ctrl and P1KO mouse brains. Green: Piezo1; Red: mCherry; Scale bar: 20 μm. (E) Representative neuron calcium signaling with Yoda1 or KCl treatment. Upper row: before Yoda1 or KCl treatment; Bottom row: after Yoda1 or KCl treatment; (from left) First column: Ctrl neurons receiving Yoda1; Second column: RR-pretreated Ctrl neurons receiving Yoda1; Third column: P1KO neurons receiving Yoda1; Last column: post-Yoda1 P1KO neurons receiving KCl. (F) Summarized ΔF/F result from individual calcium signaling experiments. (From left) First column: 44 neurons from 2 Ctrl mice; Second column: 27 neurons from 2 Ctrl mice; Third column: 99 neurons from 2 P1KO mice. Right column: 70 neurons from 2 P1KO mice. Dot plot represents the mean ± SD, ****$p < 0.0001$ by two-way ANOVA.

2.4 Piezo1 contributes to the ultrasonic neuron stimulation ex vivo

With the confirmation of Piezo1 functional expression in neurons and the success of P1KO neuron preparation, we furthered the experiments on investigating Piezo1's role in ultrasonic neuromodulation. Through co-expression of Cre-mCherry or mCherry with GCaMP6s, the calcium signaling in P1KO or Ctrl neurons was quantified (Fig 2.3 A). Acute brain slices were collected four weeks after virus injection and treated with ultrasound, in a setup using a 0.5 MHz plane transducer with three 300 ms pulses of ultrasound (US) at 0.35 MPa (low-intensity), 10 s apart (Fig 2.3 B). Consistent with the Yoda1 pattern, Ctrl neurons showed significantly stronger calcium response to sonication (61.05% ± 26.69%) than RR pre-treated ones or P1KO neurons did, and the latter twos showed similar level of response (Ctrl:RR: 1.371% ± 0.4211%, KO: 6.456% ± 6.444%; Fig 2.3 C).

Taken together, Piezo1 was found functionally expressed in neurons in the brains of mice, with expression level high enough that if Piezo1 were knocked out, neurons showed much diminished responses to ultrasound. These also imply that Piezo1 is an important component for neurons' mechano-sensitivity, as the responses from P1KO neurons were very similar to those of non-specific mechanosensitive ion channel blocker RR pre-treated Ctrl neurons. In short, Piezo1 was demonstrated indeed a significant mediator of ultrasonic neuromodulation in *ex vivo* brain slices.

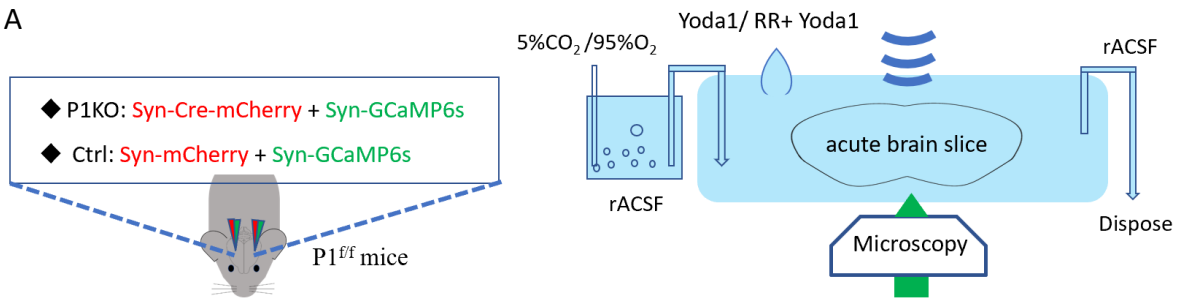

B

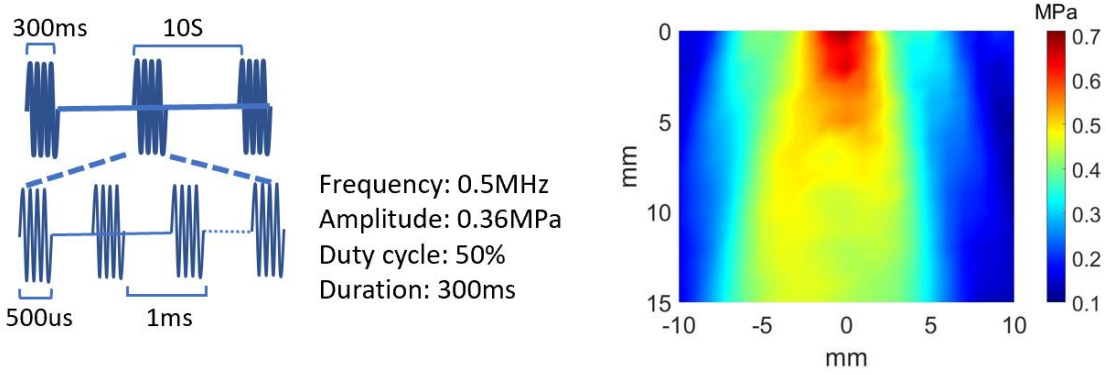
300ms
10S
500us
1ms
Frequency: 0.5MHz
Amplitude: 0.36MPa
Duty cycle: 50%
Duration: 300ms
MPa
0.7
0.6
0.5
0.4
0.3
0.2
0.1
0
5
10
15
mm
-10
-5
0
5
10
mm

C

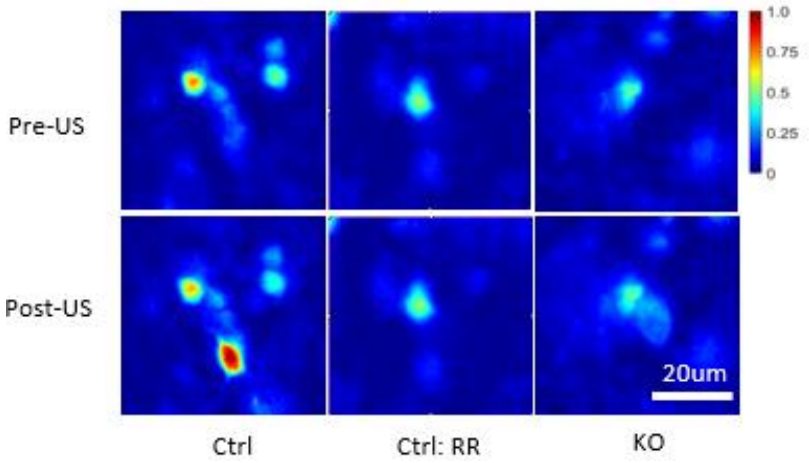
Pre-US
Post-US
1.0
0.75
0.5
0.25
0
20um
Ctrl
Ctrl: RR
KO

D

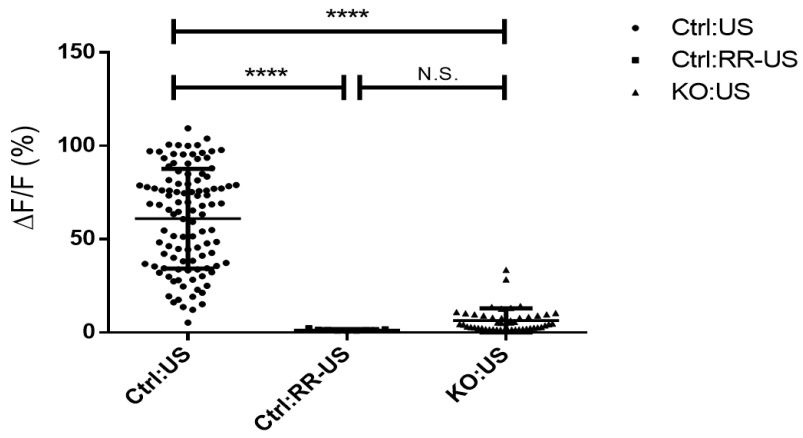
****
****
N.S.
150
100
50
0
ΔF/F (%)
Ctrl:US
Ctrl:RR-US
KO:US
Ctrl:US
Ctrl:RR-US
KO:US

Figure 2.3 Piezo1 mediates ultrasonic neuromodulation *ex vivo*. (A) Schematic of calcium imaging quantification of ultrasonic neuron response in P1KO and Ctrl mice. Left: Virus injection protocol, either Syn-mCherry + Syn-GCaMP6s or Syn-Cre-mCherry + Syn-GCaMP6s was injected in Piezo1$^{f/f}$ mice's motor cortices. 3-4 weeks later, acute brain slices were collected for calcium imaging. RR incubation (30 μM, if applicable) was 10mins. (B) Schematic of ultrasound stimulation applied. Left: parameters of the ultrasound stimuli. Frequency: 0.5 MHz, spatial-peak temporal-peak pressure: 0.35 MPa, Duty cycle: 50%, Duration: 300 ms, Interval: 10 s, 3 cycles; Right: Acoustic profile of the ultrasound field generated by the ultrasound system. For our calcium image system, the brain slices should experience approximately 0.35 MPa. (C) Representative neuron calcium signaling towards ultrasound stimulation. Upper row: before ultrasound stimulation; Bottom row: after ultrasound stimulation; Left column: Ctrl neurons; Middle column: Ctrl neurons pre-treated with RR; Right column: P1KO neurons. (D) Summarized ΔF/F result from individual calcium signaling experiments. Left column: 107 neurons from 2 Ctrl mice; Middle column: 9 neurons from 1 Ctrl mouse; Right column: 34 neurons from 2 P1KO mice. Dot plot represents the mean ± SD, ****$p < 0.0001$ by one-way ANOVA.

2.5 Discussion

In this chapter, expression of Piezo1 in mouse brain was first demonstrated, which has been previously reported locating in neurons of myelinated axonal pathways including the corpus callosum and cerebellar arbor vitae, and particularly in neurons of the frontal cortex in mouse and rat brains (Velasco‐Estevez, M., et al., 2020). On top of that, in this chapter, Piezo1 was detected in neurons broadly distributed in mouse brain including the whole cortex.

Piezo1 in CNS has been indicated, for example, directing the lineage choice of neural stem cells (Pathak, M. M, et al., 2014), and negatively correlated with the myelination in neurons (Velasco-Estevez, M., et al., 2020), however, direct evidence of function of Pieoz1 in neurons in mouse brain has not been reported. In this chapter, through the calcium response to its agonist Yoda1, Piezo1 function in neurons is confirmed, which thus provides premise studying the role of Piezo1 in ultrasonic neuromodulation.

Loss-of-function and gain-of-function mutations are two classic ways probing a protein's function. Gain-of-function mutation of Piezo1was found hard to achieve, maybe because of the protein's large size and complexity (Coste, B., et al., 2010, Coste, B., et al., 2015; Jiang et al., 2021), loss-of-function mutation was thus taken into consideration. Since global knockout of Piezo1 in mouse is embryonic lethal (Li, J., et al., 2014), conditional knockout was adopted by local expression of Cre recombinase in Piezo1$^{f/f}$ mice. The successfulness of conditional knockout of Piezo1 (P1KO) neurons generation was further confirmed with molecular tests including the DNA and protein tests, and functional test by adopting Piezo1 agonist Yoda1.

With the success of generating P1KO neurons, Piezo1's role in ultrasonic neuromodulation was then investigated. P1KO neurons were found displaying lower neuronal activity responding to ultrasound *ex vivo* which supports the hypothesis that Piezo1 mediates ultrasonic neuromodulation. This finding is consistent with our previous findings that Piezo 1 mediates ultrasonic neuromodulation *in vitro* (Qiu, Z., et al., 2019) and paves the way for further investigation of Piezo1's role *in vivo*.

Chapter 3. The role of Piezo1 in the ultrasonic neuromodulation in vivo

3.1 Material and method

Animal preparation

Mice used in this chapter were mainly Piezo1$^{tm2.1Apat}$ (JAX# 029231) for P1KO mice generation and measuring ultrasonic brain stimulation effect including behavioral, electromyography, calcium signaling and c-Fos expression *in vivo*. C57 BL6/J (JAX# 000664) were also used for immunostaining and fiber photometry experiment. Mice were housed under standard housing condition with 12-hour light/dark cycle, food and water available ad libitum. Animal use and care were performed following the guideline of the Department of Health - Animals (Control of Experiments) of the Hong Kong S.A.R. government.

Stereotaxic surgery

P1KO mice were generated through injection of Syn-Cre-mCherry virus in Piezo1$^{tm2.1Apat}$ mice in motor cortex in right hemisphere which results in Piezo1 conditional knockout in neurons in unilaterally motor cortex in mice. Ctrl mice were prepared with the same protocols but the Syn-mCherry virus. As for fiber photometry experiment, additional Syn-GCaMP6s is added all virus used.

Male, 4-6 weeks Piezo1$^{tm2.1Apat}$ mice were deeply anesthetized by 100 mg/ml ketamine and 10 mg/ml xylazine in 0.9% NaCl and positioned in a stereotaxic injection frame (RWD Ltd, China). 400 nL of virus was delivered to 3 locations respectively by a microinjection system (Nanoliter 2010, WPI Ltd) through a craniotomy (<1 mm^2). The injection was performed unilaterally to the right motor cortex (at mm): AP: 0.0, ML: -1.0; AP: +0.5 ML: -1.0; AP: +0.5 ML: -1.5, with DV: 1. For the behavioral, electromyography, and c-Fos experiment, Ctrl mice were generated by injection of AAV2/9-Syn-mCherry and P1KO mice were prepared with injection of AAV2/9-Syn-Cre-mCherry. Mice that injected with AAV2/9-Syn-mCherry + Syn-GCaMP6s and AAV2/9-Syn-Cre-mCherry + AAV2/9-Syn-GCaMP6s were Ctrl group and P1KO group respectively, prepared for calcium image experiment i.e., fiber photometry. The final titer of all viruses was 5 x 10^{12} VG/ml.

Ultrasound stimulation and behavior recording

After 4-6 weeks of viral injection. Mice were given 10-15 mins isoflurane inhaling to reach to an appropriate anesthesia plane. Mice hair was shaved, and the lithium niobate ultrasound transducer (0.5MHz, Harisonic I7-0012-P, Olympus) was coupled to the skull using ultrasound gel (Parker Aquasonic 100). Ultrasound stimuli (0.35, 0.45 MPa) were administered with the 500 μs tone of burst, 50% duty cycle, 50, 250, 500 ms and 5 s intervals, 4-6 times repetition in each duration groups. The forelimb and hindlimb movements induced by ultrasound stimuli were recorded by camera. The distance of forelimb and hindlimb movements is analyzed by an open source DeepLabCut.

EMG experiments

EMG experiments were conducted after 4-6 weeks of viral injection. Under isoflurane/ O_2 anesthesia, the mice hair was shaved, and the lithium niobate ultrasound transducer (0.5MHz, Harisonic I7-0012-P, Olympus) was coupled to the skull using ultrasound gel (Parker Aquasonic 100). Ultrasound stimuli (0.3, 0.35, 0.4, 0.45 MPa) were administered with the 500 μs tone of burst, 50% duty cycle, 500 ms duration and 15 s intervals. EMG data were collected from the left gastrocnemius muscle through fine needle electrodes connected to a Meduda (Bio-Signal Technology). Data were recorded at 1000 Hz, pre-amplified and digitized. Using MATLAB (Mathworks, USA), digitized waveforms were filtered by 50 Hz notch filter and 300 Hz high-pass filter. RMS envelope of the filtered waveforms were extracted for EMG identification and feature extraction. After smoothing the envelope, mean amplitude of ‘quiet period’ prior any ultrasound stimulation was taken as baseline. If any peak rises above 4 times the baseline within 1 s window after US stimulation onset, which the waveform remains lower than 2 times the baseline within 300 ms window prior that stimulation onset, the peak is considered a successful US induced EMG response and the amplitude is extracted.

Fiber Photometry

3 weeks after virus injection, an optical fiber (Thinker Tech Nanjing Bioscience Inc) which was placed in a ceramic ferrule and inserted to the cortex. The ceramic ferrule was supported with dental acrylic. Mice were recovered for at least 1 week before recording the data by a fiber photometry system (QAXK-FPS-DC-LED, Thinker Tech Nanjing Bioscience Inc). An optical fiber (230 mm O.D., NA 0.37; Thinker Tech Nanjing Bioscience Inc) guided the 480-nm laser between the recording system and the implanted optical fiber. The laser power was adjusted around 40 mW. Ultrasound stimuli (0.02, 0.06, 0.12 MPa) were administered with the 500 μs tone of burst, 50% duty cycle, 300 ms and 5 s intervals, 4-6 times repetition in each duration groups targeted to the cortex area. Ultrasound stimuli of 0.01, 0.02, 0.0.3 MPa were administered when targeted the CEA area. The relative change in fluorescence, $dF/F = (F-F0)/F0$, was calculated by taking F0 to be the baseline of the fluorescence signal averaged over 1 s before ultrasound in each session.

Immunohistochemical fluorescent staining

For the c-Fos detection, mice were deeply anesthetized by 100 mg/ml ketamine and 10 mg/ml xylazine in PBS. The transducer is couple to the area above the motor cortex. Ultrasound stimuli (0.5 MHz, 0.45 MPa) were administered with the 500 μs tone of burst, 50% duty cycle, 300 ms duration and 10 s intervals for 50 mins. 90 mins later, mice were perfused with PBS, followed by 4% paraformaldehyde (PFA) (cat. no. P1110, Solarbio). After dissection, brains were post-fixed overnight in 4% PFA and then rinsed in PBS. Around 30 continuous coronal brain slices with the interval of 135 μm were collected. Slices were blocked using 10% normal goat serum + 1% BSA for 90 mins and incubated in c-Fos (2250, CST, dilution 1:500), antibody solution diluted in 10% normal goat serum + 1% BSA for overnight. Slices were then washed and incubated with goat anti-rabbit IgG (H+L) Alexa Fluor 488 (A-11008, Invitrogen) diluted in PBS for 90 mins at room temperature. Slices were then washed, sticked to glass slides, dried, and mounted on coverslips using small drops of Prolong Diamond Antifade Mountant with DAPI and allowed to cure in the dark overnight. Coverslip edges were sealed using transparent nail enamel and imaged using a confocal laser scanning microscope (TCS SP8, Leica).

3.2 Piezo1 mediates the ultrasound induced motor activity in mice

Ultrasound stimulating neurons in motor cortex would induce relevant motor behaviors in rodents (King, R. L., et al., 2013; King, R. L., et al., 2014; Ye, P. P., et al., 2016; Tufail, Y., et al., 2010) has been frequently reported, providing robust, solid evidence that ultrasound stimulates motor circuits and thus, motor activity was adopted as a reporter in this study.

P1KO and Ctrl mice were first generated by expressing Cre-mCherry and m-Cherry proteins in right motor cortex in Piezo1$^{f/f}$. Ultrasound stimulation was delivered on the right hemisphere and movements of the left forelimb and hindlimb were captured by a camera (Fig 3.1 A). In both Ctrl and P1KO mice, forelimb movement was found increased with the ultrasound pulse duration under 0.35 MPa and 0.45 MPa. However, smaller range of forelimb movement in P1KO mice were found compared to Ctrl mice especially under 0.35 MPa ultrasound stimuli at 250 ms and 500 ms duration (Fig 3.1 B left); under 0.45 MPa, the difference becomes minor (Fig 3.1 B right), this may be because the ultrasound stimulation has passed a certain threshold that movement response was becoming saturated. To induce hindlimb movement, on the other hand, seems to require a higher ultrasound intensity. No hindlimb movement in all mice was induced by 0.35 MPa ultrasound (Fig 3.1 C left); hindlimb movement in mice was found only when the ultrasound reached 0.45 MPa, at 500 ms duration (Fig 3.1 C right). Although P1KO mice hindlimb movement could be triggered under this condition, the range of movement is much smaller than that of Ctrl mice. Expression of Cre in neurons was also confirmed though the co-localization of mCherry and stained NeuN, a neuron maker (Fig 3.1 D).

Together this group of data indicates that Piezo1 contributes to ultrasound induced motor response in mice. Considering the slight muscle response that might be missed by this method, especially hindlimb responses at lower ultrasound amplitude, electromyography (EMG) was performed to characterize the ultrasonic brain stimulation in P1KO and Ctrl mice.

A

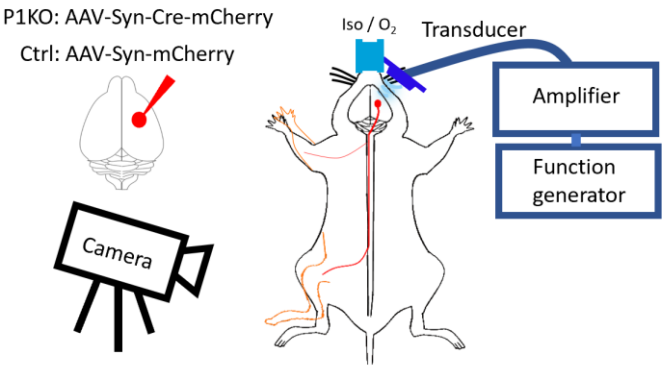
P1KO: AAV-Syn-Cre-mCherry
Ctrl: AAV-Syn-mCherry
Iso / O_2
Transducer
Amplifier
Function generator
Camera

B

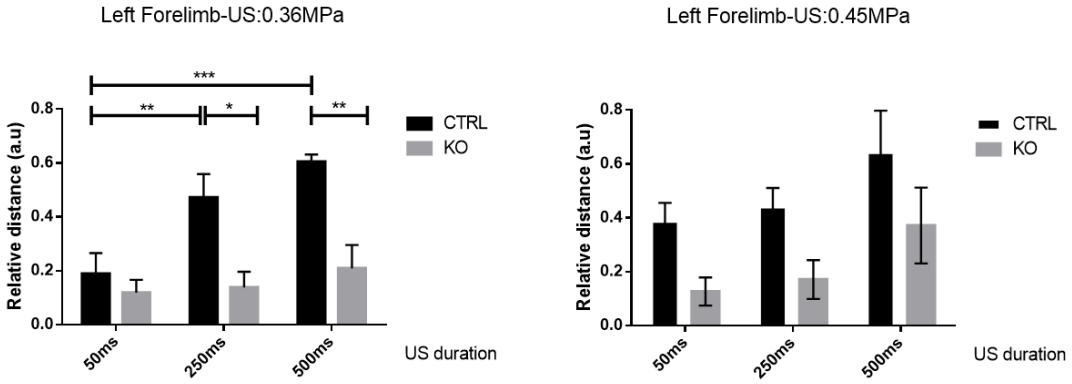
Left Forelimb-US:0.36MPa
Left Forelimb-US:0.45MPa
Relative distance (a.u)
CTRL
KO
50ms
250ms
500ms
US duration
***
**
*
**

C

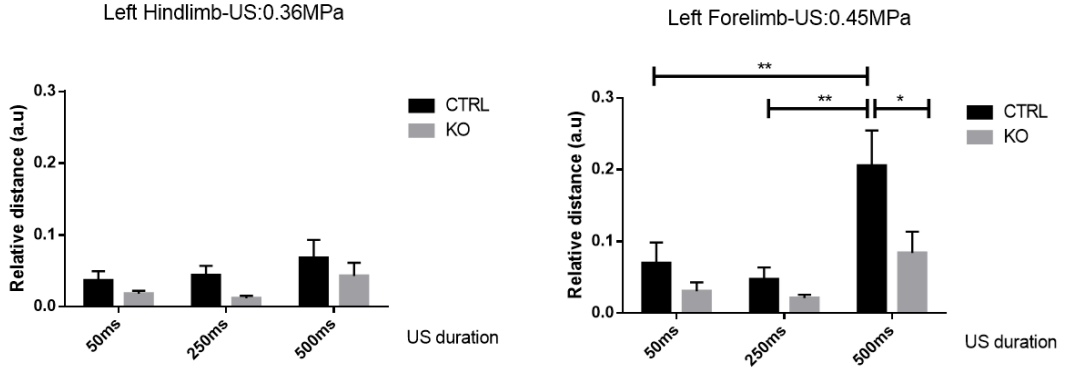
Left Hindlimb-US:0.36MPa
Left Forelimb-US:0.45MPa
Relative distance (a.u)
CTRL
KO
50ms
250ms
500ms
US duration
**
**
*

D

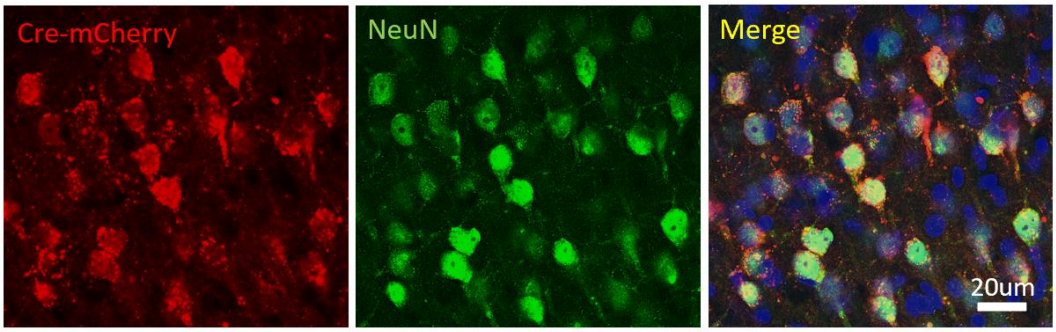

Figure 3.1 Deletion of Piezo1 in neurons in motor cortex reduce its motor response to ultrasound stimulus. (A) Schematic of capturing motor response of mice under ultrasound stimulation. P1KO and Ctrl mice were generated by virus (Syn-Cre-mCherry and Syn-mCherry respectively) injection in right motor cortex. Experiments were carried out 4 weeks after the virus injection. The mice were kept under a light anesthesia state by isoflurane. The ultrasound was applied from above the motor cortex area on the right hemisphere. The ultrasound was applied from above the motor cortex area on the right hemisphere. The ultrasound applied was: 0.5 MHz frequency, 0.35/ 0.45 MPa peak pressure, 50% duty cycle (500 μs), 50/ 250/ 500 duration, 5 s intervals, 4-6 repetitions in each experiment set. (B) Summarized forelimb movement induced by ultrasound stimulation at different ultrasound intensity and duration. n = 5 Ctrl mice and 3 P1KO mice. Bar charts represent the mean ± SEM, *p < 0.05, **p < 0.01, ***p < 0.005 by two-way ANOVA followed by Holm-Šídák's multiple comparison test. (C) Summarized hindlimb movement induced by ultrasound stimulation at different ultrasound intensity and duration. n = 5 Ctrl mice and 4 P1KO mice. Bar charts represent the mean ± SEM, *p < 0.05 by two-way ANOVA followed by Holm-Šídák's multiple comparison test. (C) Immunostaining of NeuN in cortex in P1KO mice. Red: mCherry; Green: NeuN; Blue: DAPI. Scale bar: 20 μm.

3.3 Piezo1 affect ultrasound induced electromyography in mice

To further confirm the Piezo1's role in ultrasonic neuromodulation under mouse motor response circumstance, EMG recording at the gastrocnemius was measured and quantitatively analyzed (Fig 3.2 A, B). Consistent with other studies, pressure of ultrasound required for triggering motor response and detectable EMG is around 0.35-0.7 MPa in mice.

In both Ctrl and P1KO mice, the EMG signaling was found enhanced with the ultrasound intensity increasement. Nevertheless, the signaling in P1KO mice was found smaller compared to that of Ctrl mice under every ultrasound intensity especially 0.4 and 0.45 MPa where significant difference was observed (5.20 ± 2.02 vs. 16.10 ± 8.27 at 0.4 MPa; 9.40 ± 1.33 vs. 28.64 ± 11.80 at 0.45MPa) (Fig 3.2 C, D). It thus adding support that Piezo1 contributes to ultrasound eliciting motor response in mice and therefore indicated Piezo1 an important mediator in ultrasonic neuromodulation *in vivo*.

A

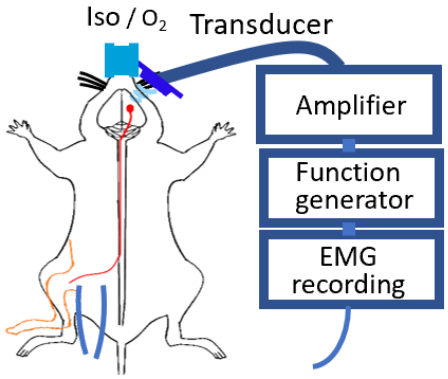

B

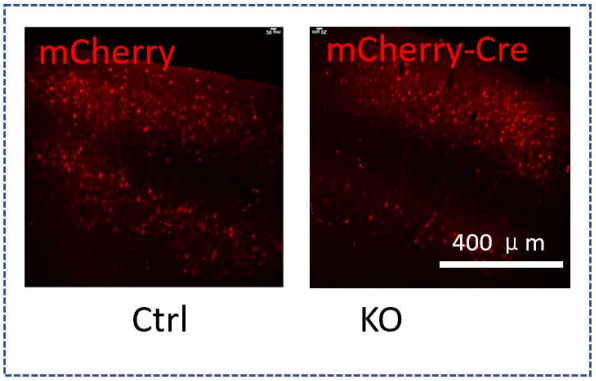

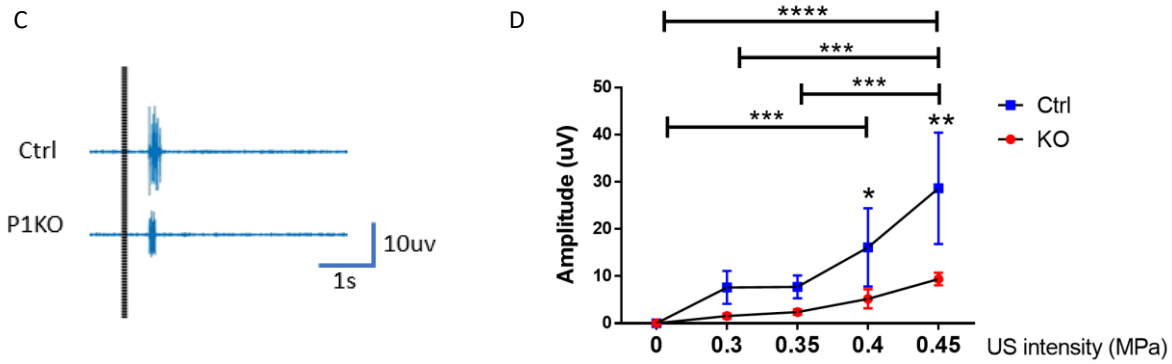

Figure 3.2 Deletion of Piezo1 reduce the ultrasound induced electromyography in mice. (A) Schematic of gastrocnemius EMG recording in the mice under ultrasound stimulation. P1KO mice generation: virus (Syn-Cre-mCherry) injection in right motor cortex; Ctrl mice generation: virus (Syn-mCherry) injection in right motor cortex. Experiments were carried out 4 weeks after the virus injection. The mice were kept under a light anesthesia state by isoflurane. The ultrasound was applied from above the motor cortex area on the right hemisphere. The ultrasound applied was: 0.5 MHz frequency, 0.3/ 0.35/ 0.4/ 0.45 MPa peak pressure, 50% duty cycle (500 µs), 500 ms duration, 15 s intervals, 4-6 repetitions in each experiment set. (B) Representative fluorescence image of mCherry (Ctrl) and Cre-mCherry (P1KO) expression in motor cortex in mice. Scale bar: 400 µm. (C) Representative recording of EMG induced by ultrasound in Ctrl (top) and P1KO (bottom) mice. (D) Summarized EMG result from 9 Ctrl and 9 P1KO mice. Line charts represent the mean ± SEM, *$p < 0.05$, **$p < 0.01$ and ***$p < 0.05$ by two-way ANOVA followed by Holm-Šídák's multiple comparisons test.

3.4 Piezo1 dependent calcium signaling induced by ultrasound in mice

To more directly measure the neuronal activity induced by ultrasound, calcium signaling was recorded by fiber photometry (Fig 3.3 A). Ultrasound at acoustic pressures between 0.02 - 0.12 MPa were used to stimulate the brains. Strong co-expression of mCherry and GCaMP6s in neurons of the targeted motor cortex can be observed (Fig 3.3 B).

Unlike the motor test, the calcium signaling was found easier to be induced by ultrasound at pressure as low as 0.06 MPa. This may be because observable motor changes require higher neuron complex corporation that higher level of neuron perturbation is needed. The ultrasound induced calcium signaling could also be an indication supporting previous finding that ultrasound could induce neuron plasticity and provide long-term effect *in vivo* (Baek, H., et al., 2018; Huang, X., et al., 2019; Folloni, D., et al., 2019; Verhagen, L., et al,.2019).

It is found that ultrasound rapidly and transiently activated neurons, as revealed by GCaMP6s fluorescence change. Such response is also found to increase with acoustic pressure under all tested values, and responses from P1KO mice were significantly lower than that from Ctrl mice. (Fig 3.3 C, D) These thus give additional evidence, from direct, immediate neuronal activity perspective, supporting the previous chapter's finding that Piezo1 mediates ultrasonic neuromodulation *in vivo*.

A

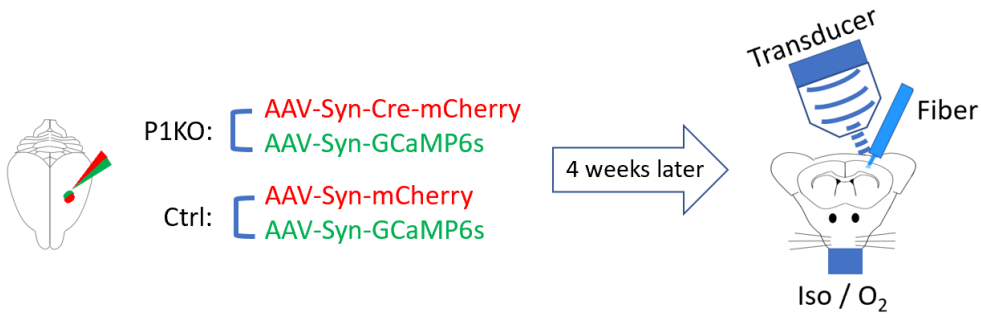

B

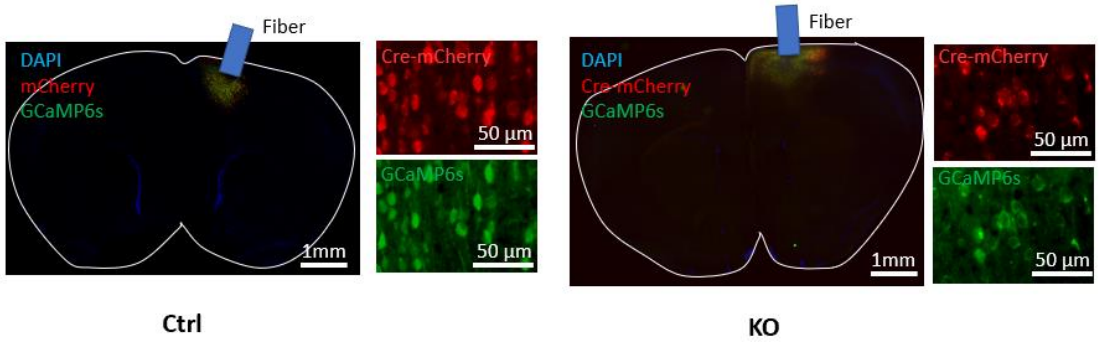
Fiber
DAPI
mCherry
GCaMP6s
1mm
Cre-mCherry
50 μm
GCaMP6s
50 μm
Ctrl
Fiber
DAPI
Cre-mCherry
GCaMP6s
1mm
Cre-mCherry
50 μm
GCaMP6s
50 μm
KO

C

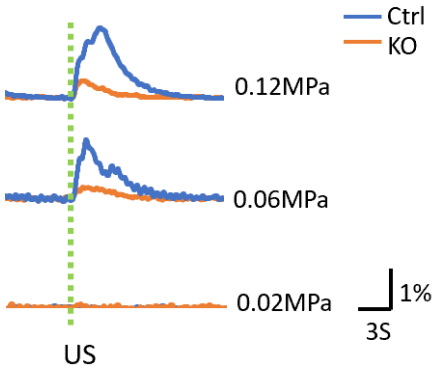
Ctrl
KO
0.12MPa
0.06MPa
0.02MPa
1%
3S
US

D

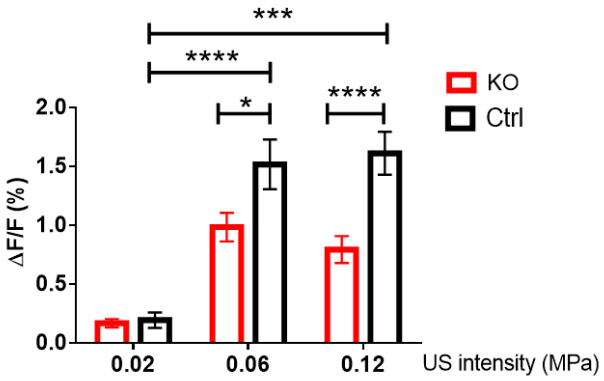
***
****
*
****
KO
Ctrl
2.0
1.5
1.0
0.5
0.0
ΔF/F (%)
0.02
0.06
0.12
US intensity (MPa)

Figure 3.3 Depletion of Piezo1 reduces ultrasound induced calcium singling in mice (A) Schematic of fiber photometry test on Ctrl and P1KO mice under ultrasound stimulus. P1KO mice generation: virus (Syn-Cre-mCherry + Syn-GCaMP6s) injection in motor cortex; Ctrl mice generation: virus (Syn-mCherry + Syn-GCaMP6s) injection in motor cortex; Experiment was carried out 4 weeks after the virus injection. The mice were kept under a deep anesthesia state by isoflurane. Ultrasound was applied adjacent to the ceramic ferrule. The ultrasound applied was: 0.5MHz frequency, 0.02/ 0.06/ 0.12 MPa peak pressure, 50% duty cycle (500 μs), 300 ms duration, 5 s intervals, 4-6 repetitions in each experiment set. (B) Representative fluorescence image of Cre-mCherry or mCherry co-expressed with GCaMP6s in motor cortex in mice. Red: mCherry; Green: GCaMP6s; Blue: DAPI; Scale bar: 1 mm or 50 μm. (C) Representative calcium signaling induced in Ctrl and P1KO mice under 0.02 (top), 0.06 (middle), and 0.12 MPa (bottom) ultrasound stimulation. (D) Summarized ΔF/F from 2 individual experiments in 3 Ctrl mice and 4 P1KO mice. Bar charts represent the mean ± SEM, *$p < 0.05$, **$p < 0.01$ and ***$p < 0.05$ by two-way ANOVA followed by Tukey–Kramer post-hoc analysis.

3.5 Immediate early gene revealed Pieoz1's role

c-Fos is one of the most studied immediate early genes whose induction has been shown to be activity-dependent in neurons (Morgan, J. I., & Curran, T., 1988). Expression of c-Fos was thus adopted as a post-stimulation measurement of neuronal activity. After 0.45 MPa ultrasound stimulation for 50 mins and 90 mins for c-Fos expression, neuronal activity in response to ultrasound was measured through immunofluorescent staining of c-Fos (Fig 3.4 A, B). Level of c-Fos expression in P1KO mouse brain slices was found much lower (4.68 ± 3.62) compared to that of Ctrl mice (53.04 ± 20.79) (Fig 3.4 C).

In short, from molecular perspective, Piezo1 is also found participating in ultrasonic neuromodulation *in vivo*.

A

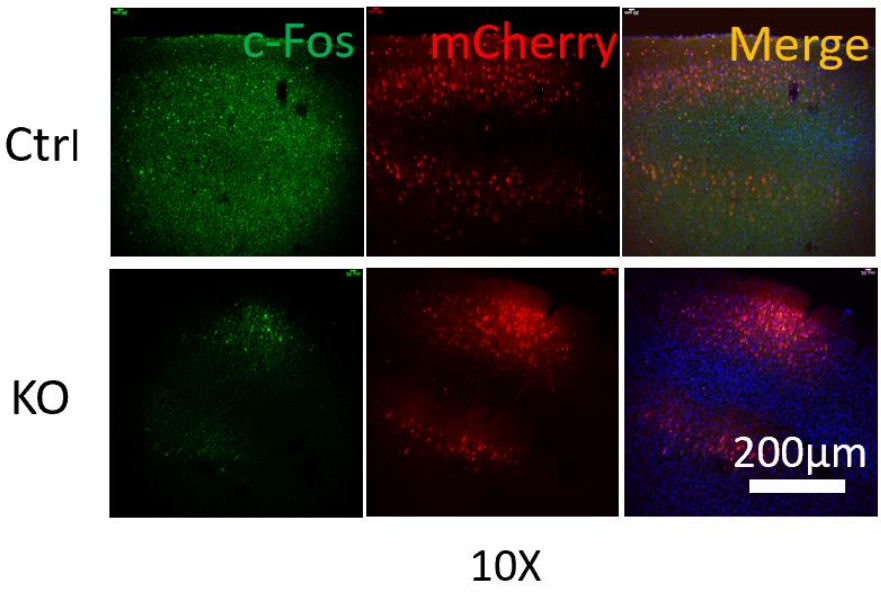

B

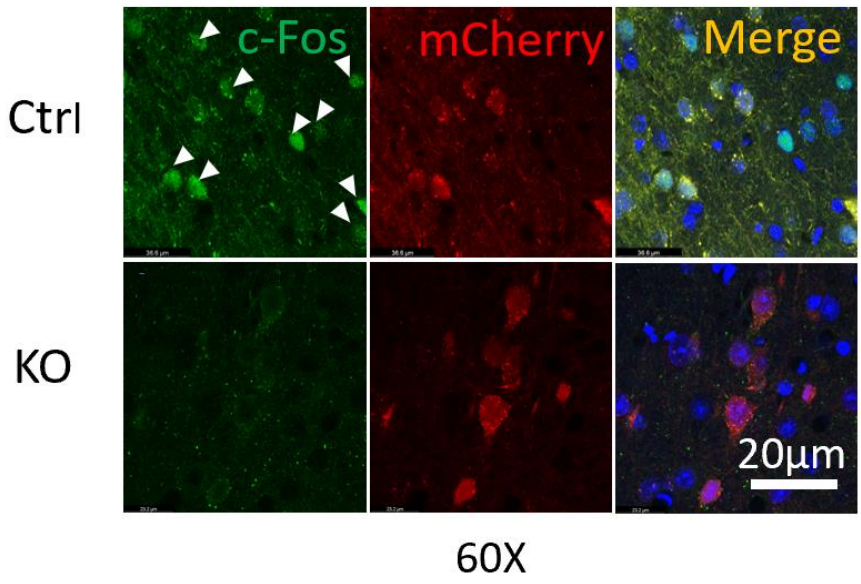

C

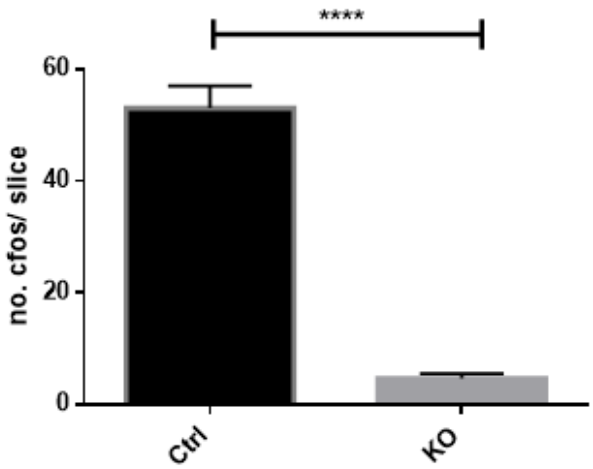

Figure 3.4 Depletion of Piezo1 reduces ultrasound induced c-Fos expression in mouse brain. (A) Immunostaining of c-Fos in cortex after ultrasound stimulation (10×). Upper row: Ctrl mice; Bottom row: Ctrl mice Green: c-Fos; Red: mCherry; Blue: DAPI; Scale bar: 200 µm. (B) Immunostaining of c-Fos in cortex in Ctrl and P1KO mice after the ultrasound stimulation. Green: c-Fos; Red: mCherry; Blue: DAPI; Scale bar: 20 µm. The ultrasound applied was: 0.5 MHz frequency, 0.45 MPa peak pressure, 50% duty cycle (500 µs), 500 ms duration, 5 s intervals, total 50 mins. (C) Summarized c-Fos expression of 27 slices from 3 Ctrl mice, 19 slices from 2 P1KO mice. Bar charts represent the mean ± SEM, ****$p < 0.0001$ by unpaired t test.

3.6 Exclusion of auditory confound

Auditory confound has recently become a debate in ultrasonic neuromodulation *in vivo* (Guo, H., et al., 2018; Sato, T., et al., 2018). Although the fact that only contralateral behavior movement and EMG signal could be observed by delivering ultrasound stimulation locally to one hemisphere serves as evidence excluding auditory confound, c-Fos expression in auditory cortex in both P1KO and Ctrl mice was checked for further confirmation. No significant difference was found in c-Fos expression between P1KO and Ctrl groups, nor between left and right hemisphere in either group. This strengthens that auditory confound was not present in this study. (Fig 3.5 A, B).

Moreover, motor response was found triggered by ultrasound in Kanamycin/Furosemide-deafened mice which further demonstrates ultrasonic stimulation of motor circuits was not dependent on the auditory pathway. This is consistent with an earlier study demonstrating that elimination of auditory pathways did not affect the ultrasound-elicited motor responses (Mohammadjavadi M., et al. 2019). Based on this, it is convinced that direct stimulation of neuronal circuits is the main reason for the ultrasound induced motor behavior in this study.

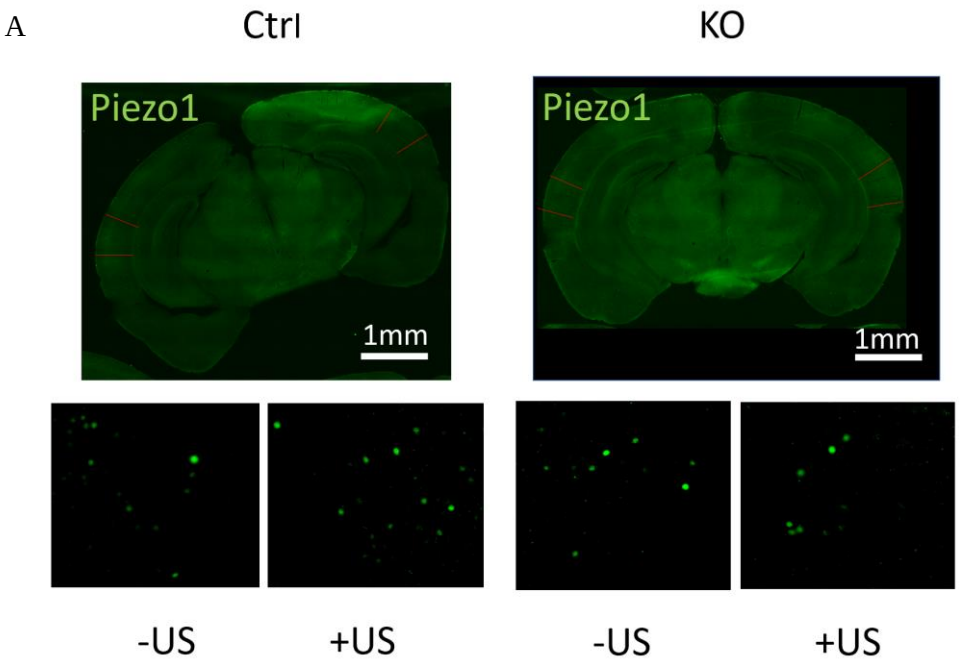

B

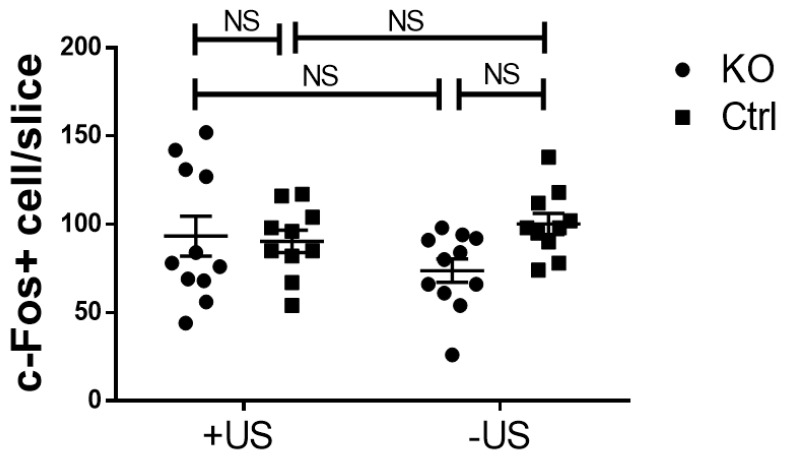

Figure 3.5 Piezo1 mediates ultrasonic neuromodulation independent from the auditory pathway. (A) Immunostaining of c-Fos in auditory cortex in left and right hemisphere after the ultrasound stimulation. Green: c-Fos. Scale bar: 1mm or 50 μm. The ultrasound applied was: 0.5 MHz frequency, 0.45 MPa peak pressure, 50% duty cycle (500 μs), 500 ms duration, 5 s intervals, total 50 mins, targeted to motor cortex. (B) Summarized c-Fos number of 19 slices from 2 P1KO mice and 27 slices from 3 Ctrl mice in both the ultrasound stimulation side and the contralateral side. Dot plots represent the mean ± SEM, $p > 0.5$ by two-way ANOVA followed by Holm-Šídák's multiple comparisons test.

3.7 Regions with high Piezo1 expression

Having found that endogenous Piezo1 is a significant mediator of ultrasonic neuromodulation in motor cortex, it was wondered whether other brain regions, possibly expressing greater levels of Piezo1, may also serve as effective targets of ultrasound. With immunofluorescent staining of WT mouse brains, several brain areas including stria terminalis (BNST), central amygdala (CEA), paraventricular nucleus of hypothalamus (PVN), Edinger-Westphal nucleus (EW) and red nucleus (RN) (Fig 3.6 J, K) were found having strong Piezo1 expressions. Out of these, CEA was chosen for further investigation due to it being a classic and well-established target of neuroscientific experiments, and its easily recognizable symmetrical anatomy feature (Fig 3.6 A). Consistent with the findings in cortex, Piezo1 was found co-stained with MAP2 which indicates its expression in neurons (Figure 3.6 B). Inward current was also recorded in 6 randomly selected neurons from this brain area, which this effect could be eliminated by pre-treatment with RR (Fig 3.6 D, E). Together, these demonstrate the function of Piezo1 in neurons in CEA area.

Neuronal activity responding to ultrasound was then investigated through fiber photometry. Interestingly, ultrasound as low as 0.03 MPa could induce the calcium influx with good synchronization (Fig 3.6 F) which indicates the higher sensitivity of neurons in CEA to ultrasound compared to neurons in cortex (both Ctrl and P1KO neurons). The higher ultrasound intensity had higher success rate and greater induced calcium influx (Fig 3.6 G, H). Time locked peaks of $\Delta F/F$ in response to ultrasound stimulation were extracted and quantified. The peak of the responses as the function of acoustic pressure were then fitted with a linear equation. It was found that the slope of the $\Delta F/F$ peak-pressure relation in CEA neurons ($k=102.7$) is steeper than that of cortex ($k=12.29$) (Fig 3.6 I). These results further confirm that Piezo1 is an important factor mediating the ultrasonic neuromodulation *in vivo*.

In summary, from the gain-of-function perspective, Piezo1 is found a prominent factor that is responsible to ultrasonic neuromodulation *in vivo*.

A

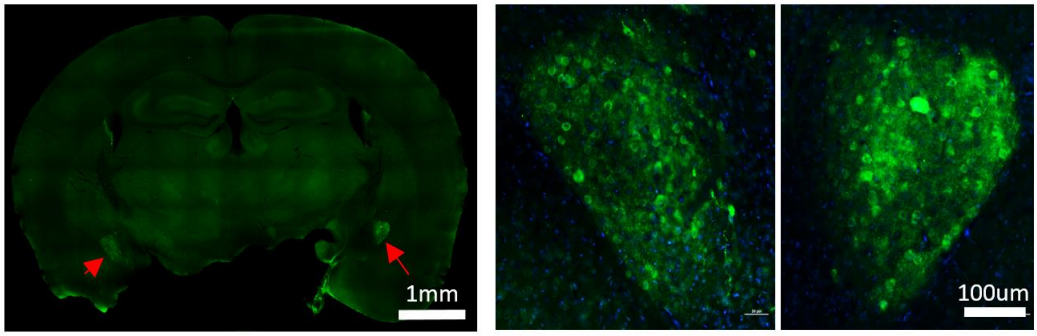
1mm
100um

B

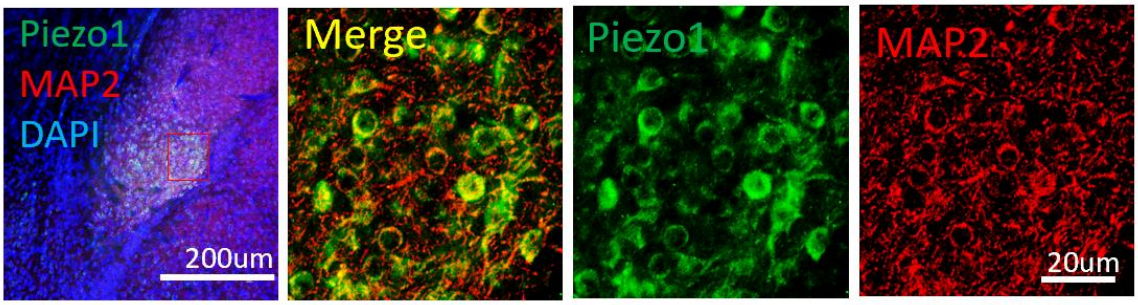
Piezo1
MAP2
DAPI
200um
Merge
Piezo1
MAP2
20um

C

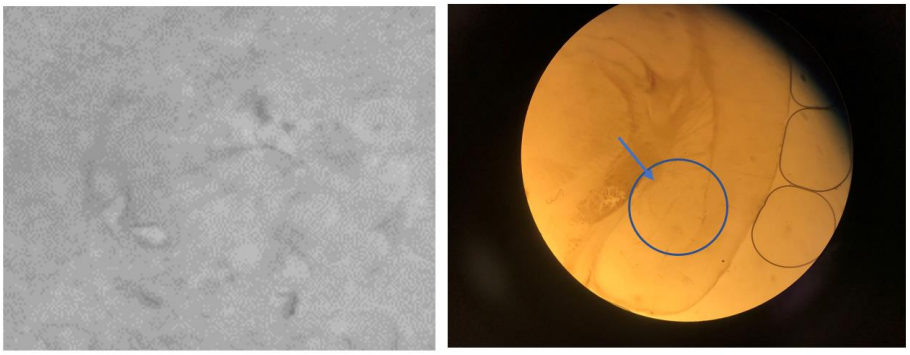

D

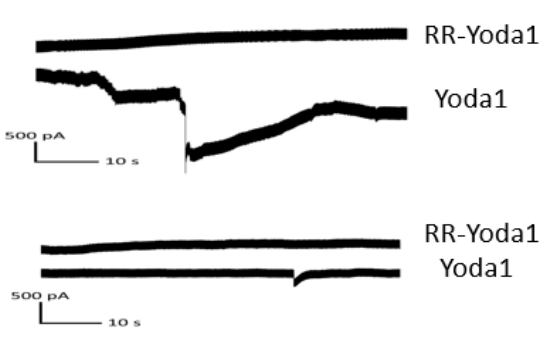
RR-Yoda1
Yoda1
500 pA
10 s
RR-Yoda1
Yoda1
500 pA
10 s

E

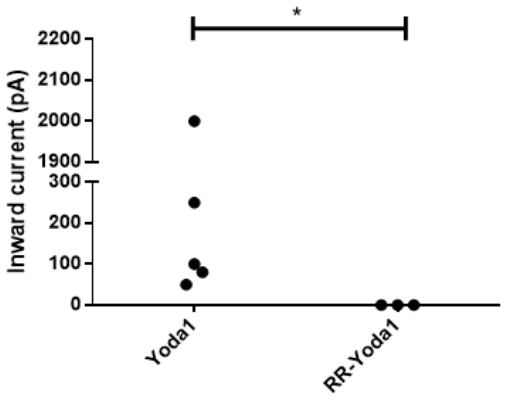
*
Inward current (pA)
2200
2100
2000
1900
300
200
100
0
Yoda1
RR-Yoda1

F

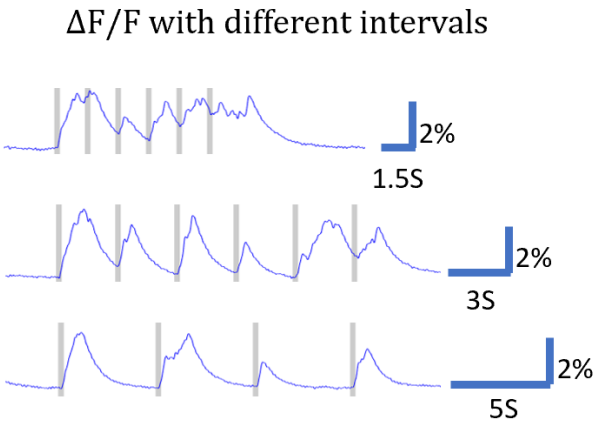
ΔF/F with different intervals
2%
1.5S
2%
3S
2%
5S

G

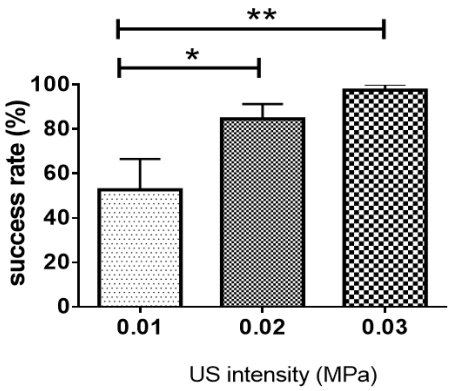
Success Rate in CEA
**
*
success rate (%)
100
80
60
40
20
0
0.01
0.02
0.03
US intensity (MPa)

H

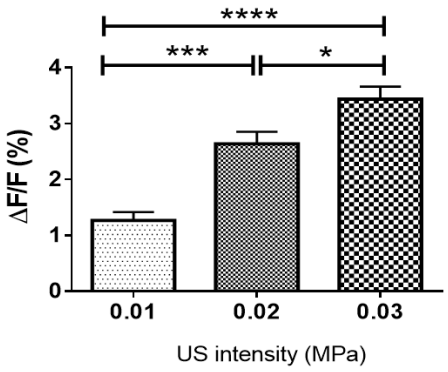
ΔF/F in CEA
****
***
*
ΔF/F (%)
4
3
2
1
0
0.01
0.02
0.03
US intensity (MPa)

I

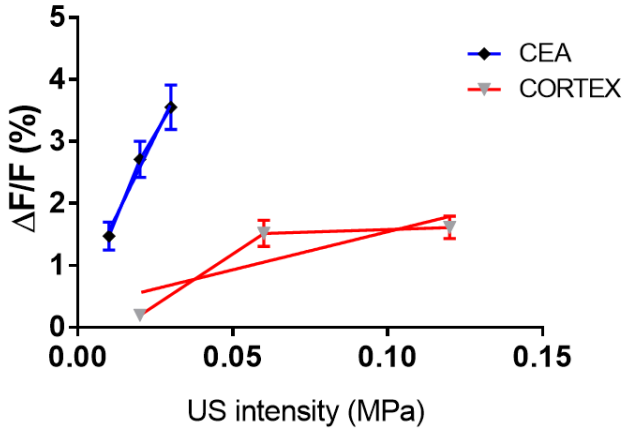
ΔF/F in CEA vs. Cortex
CEA
CORTEX
ΔF/F (%)
5
4
3
2
1
0
0.00
0.05
0.10
0.15
US intensity (MPa)

J

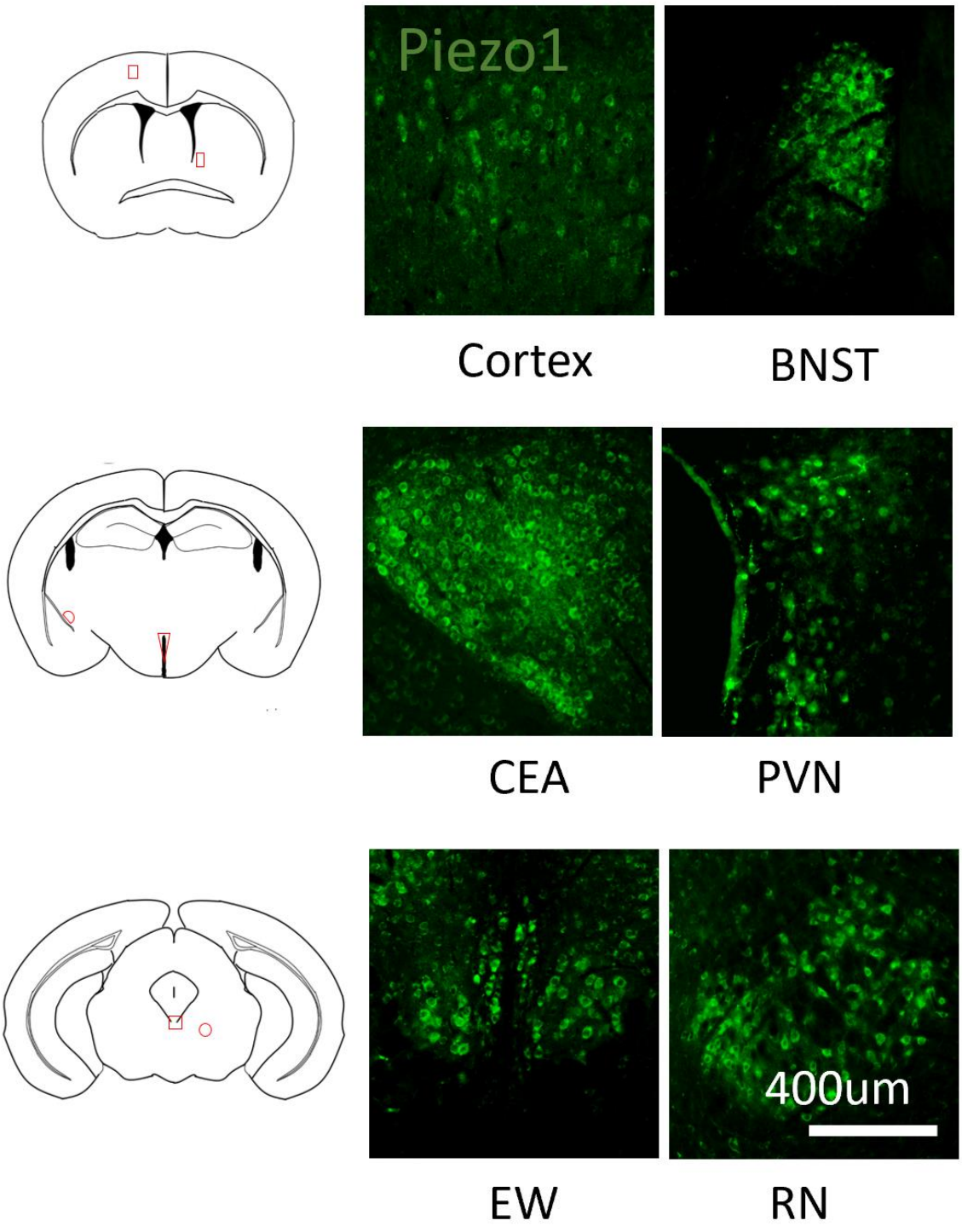

K

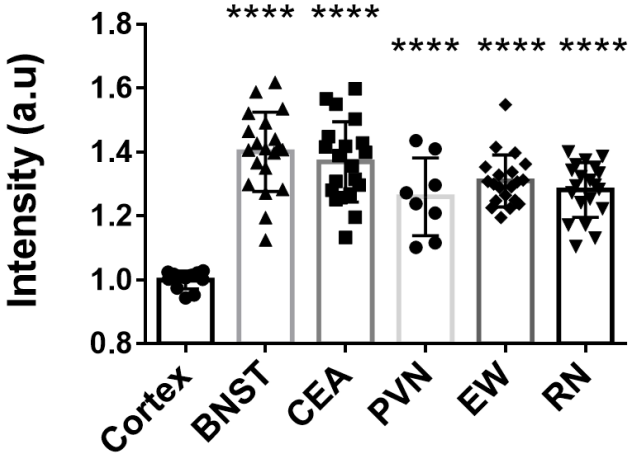

Figure 3.6 Neurons displayed greater ultrasound response in Piezo1 higher expression area. (A) Immuno-staining of Piezo1 in a whole mouse brain slice. Green: Piezo1; Arrow: CEA area; Scale bar: 1 mm or 100 μm. (B) Co-immuno-staining of Piezo1 and MAP2 in the CEA area. Green: Piezo1, Red: MAP2, Blue: DAPI. Scale bar: 200 μm or 20 μm. (C) Demonstration of a neuron in CEA being patched. Left: a neuron being patched by pipette; Right: neuron's location in CEA area. (D) Representative recording of inward current induced by Yoda1 (60 μM) with or without RR pre-treatment (30 μm) from 2 individual neurons. (E) Summarized inward current under Yoda1 with or without pre-treated with RR. Left column: 5 neurons from 2 mice; Right column: 3 neurons from 2 mice. Dot plots represent mean ± SEM, *$p < 0.05$ by Mann-Whitney test. (F) Representative calcium signaling induced by ultrasound stimulation with intervals of 1.5 s, 3 s, and 5 s in the CEA area. Gray bar: ultrasound tag. Scale bar: 2%. (G) Success rate of calcium signaling induced by 0.01/ 0.02/ 0.03 MPa ultrasound from 2 individual experiments in 4 mice. Bar charts represent mean ± SEM, *$p < 0.05$, **$p < 0.01$ by one-way ANOVA followed by Tukey–Kramer post-hoc analysis. (H) Summarized ΔF/F induced by 0.01/ 0.02/ 0.03 MPa ultrasound from 2 individual experiments in 4 mice. Bar charts represent mean ± SEM, *$p < 0.05$, ***$p < 0.005$ by one-way ANOVA followed by Tukey–Kramer post-hoc analysis. (I) Regression of calcium signal induced by ultrasound in cortex and CEA area from 4 and 3 mice respectively. CEA: $y=102.7x + 0.5278$, $p<0.0001$; Cortex: $y=12.29x + 0.3140$, $p<0.0001$. (J) Piezo1 is highly expressed in stress-processing brain areas. Left column: anatomy of brain areas location in coronal brain section view; Middle and right columns: immunostaining of Piezo1 in mouse brain, respectively the areas of cortex, BNST, CEA, PVN, EW, RN. Green: Piezo1, Scale bar: 100 μm. (K) Summarized relative light intensity of Piezo1 positive neurons to the cortex neuron. P****<0.0001 by one-way ANOVA followed with Dunnett's multiple comparisons test (each compared with cortex group).

3.8 Discussion

Consistent with the *ex vivo* study, Piezo1 is found mediating ultrasonic neuromodulation *in vivo*. Neurons in motor cortex have been found triggering the contralateral limb movement by light or ultrasound (Ayling, O. G., et al., 2009; Kamimura, H. A., et al., 2016; Aurup, C., et al., 2021). In this study, similar response was observed that left hindlimb was triggered by the right-hemisphere brain stimulation, which was harder to be induced for the P1KO mice, that higher acoustic pressure or longer ultrasound duration was required. The EMG test further confirms this finding quantitatively, demonstrating a reduced neuronal response to ultrasound without the function of Piezo1. Reduced neuronal activity indicating by the lower calcium signaling in P1KO mice further demonstrates Piezo1's participation in ultrasonic neuromodulation *in vivo*. Supporting this finding, decreased c-Fos expression after ultrasound stimulation in P1KO mouse brain slices was observed. Taken together, it is found that Piezo1 mediates ultrasound stimulated neuronal circuits activity and its corresponding behavior changes and thus is a prominent factor that mediates ultrasonic neuromodulation *in vivo*.

Importantly, this mediating effect was not dependent on the auditory pathways based on the findings that no difference in c-Fos expression in auditory cortex between P1KO and Ctrl mice and that the motor response can as well be elicited by ultrasound in deaf mice.

When studying a protein, the gain-of-function and loss-of-function mutations are widely adopted. In this study, loss-of-function was achieved through conditional knockout by Cre-LoxP system. However, gain-of-function was found hard to be achieved because of the difficulties overexpressing Piezo1. This may be due to Piezo1's extremely large size and complexity (Coste, B., et al., 2010; Coste, B., 2015; Jiang, Y., et al., 2021). The finding that the CEA neurons express higher level of Piezo1 offers an alternative to gain-of-function study. It is found that the CEA neuronal activity displayed a higher ultrasound intensity dependency compared to those of cortex where Piezo1 is found lowlier expressed. In short, neurons with higher Piezo1 expression displayed a higher ultrasound sensitivity while the low expression or KO ones, showed lower sensitivity which indicates a prominent role of Piezo1 in ultrasonic neuromodulation. Taken together, Piezo1 is demonstrated mediating ultrasonic neuromodulation *in vivo* from the gain-of-function and loss-of-function perspective.

Interestingly, Piezo1 is found specifically highly expressed in bed nucleus of the stria terminalis (BNST), central amygdala (CEA), paraventricular nucleus of hypothalamus (PVN), edinger-westphal nucleus (EW) and red nucleus (RN) in mouse brain (Fig 3.7). Having found that Piezo1 mediates ultrasonic neuromodulation *in vivo*, the lower threshold of acoustic pressure required for inducing calcium signaling in CEA may in turn demonstrate its higher expression of Piezo1.

Regarding that Piezo1 is highly expressed in stress-regulating brain area, it seems to be a possible target studying and treating psychiatric diseases. For example, amygdala is a classic emotion and motivation associated brain area (Janak, P. H., & Tye, K. M., 2015) and thus is considered a good target for various psychiatric diseases. In fact, ultrasound treatment for depression, anxiety disorders, bipolar depression and PTSD is under progression. Evidence that ultrasound treatment altered functional activity in macaques brain is also reported (Folloni, D., et al., 2019). Although whether Piezo1 participated in this treatment requires further confirmation, this study suggest such possibility and provide more targeting brain areas including BNST, PVN, EW and RN for treating related psychiatric diseases.

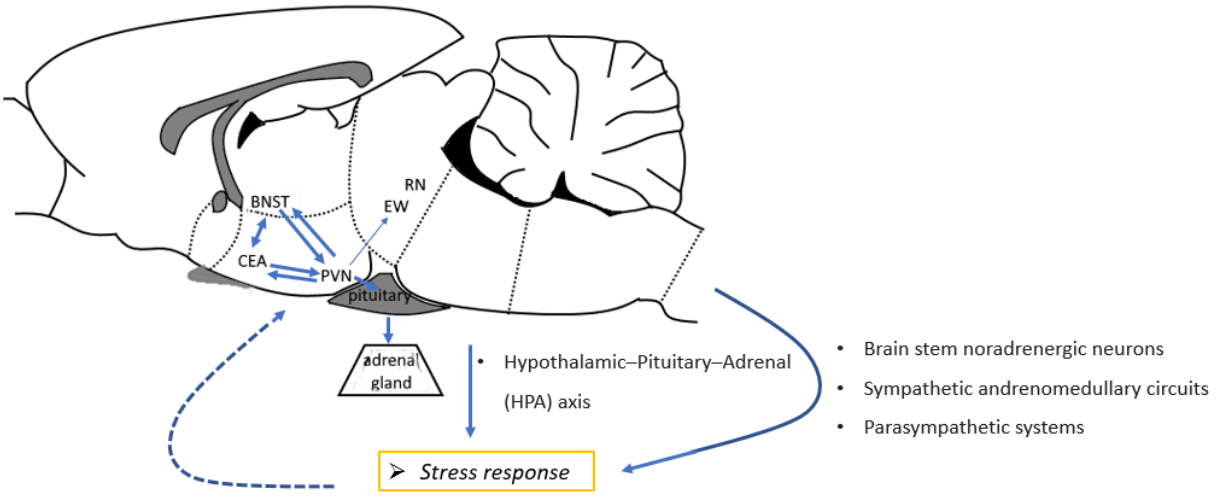

Figure 3.7 Specific distribution of Piezo1 in mouse brain. Piezo1 highly expressing brain areas interact with each other, controlling mouse's social, emotional, or motivational salience. BNST: a center of integration for limbic information and valence monitoring, has emerged as a key to psychiatric disorders. From the function perspective, it mediates the sustained fear states, and social behaviors, which include aggression, mating, offspring, and parenting (M. A., & Chen, A., 2016). From the anatomy perspective, along with its connectivity with other area and receptor subpopulations, it possesses dense connections with PVN; PVN: the node of the hypothalamic–pituitary–adrenal (HPA) axis that initiates cortisol responses and integrates stress response (Avery, S. N., et al., 2016); CeA: a brain area orchestrating various adaptive behaviors such as defensive and appetitive responses (Davis, M., & Whalen, P. J., 2001; Everitt, B. J., et al., 2003), it also has the capacity to modify the HPA axis through PVN with or without BNST (Herman, J. P., & Cullinan, W. E., 1997; Lebow, M. A., & Chen, A., 2016; de Guglielmo, G., et al., 2019); EW: The study of EW in emotion related behavior has not come into a conclusion, but evidence is increasing implying that it may underlie sex-dependent differences in stress response and may play a unique integrating stress- and reward-related processes (Kozicz, T., et al., 2011). Anatomical finding that PVN projects slightly to EW (Geerling, J., et al., 2010) may also be an indication that it participates in some psychiatric diseases' processing; RN: a large subcortical structure locating in the ventral midbrain, also be implied mediating antinociceptive responses to pain stimulation in a few studies (Basile, G.A., et al., 2021)

Chapter 4. Conclusions and perspective

In this study, Piezo1 was demonstrated a prominent factor that mediates the ultrasonic neuromodulatory effect in regulating animal motor behaviors *in vivo*. Piezo1 was first demonstrated broadly expressed in neurons in mouse brain through immunofluorescent staining. And its function in the cortex area was confirmed by the endorsement of patch clamp and calcium image. Applying Cre-LoxP system, P1KO model was generated. This thus provided a loss-of-function model for studying Piezo1's role in the ultrasonic neuromodulation. P1KO neurons displayed a lower sensitivity to ultrasound evidenced by the reduced calcium signaling responding to ultrasound in acute brain slices. Similarly, reduced neuronal activity responding to ultrasound was also found *in vivo* through ultrasonic motor response, EMG signaling, calcium changes and c-Fos expression, which were compared to that of Ctrl neurons. In contrast, neurons in CEA were found highly expressed in Piezo1 in this study, displayed a higher ultrasound sensitivity indicated by a higher acoustic pressure dependency of calcium signaling. The possible contribution of auditory pathway was also excluded through adopting normal and deafened mice. Thus, Piezo1 is demonstrated a major mediator of ultrasonic neuromodulation *in vivo*.

Since the discovery of Piezo1, it has been widely studied in various tissue in various models (Fang X. Z., et al., 2021). However, its study in brain is limited, it may because of its relatively low expression detected (Wang, J., & Hamill, O. P., 2021). Nevertheless, its expression in central nerve system has been reported in several studies. It is reported earlier that Piezo1 locates in myelinated axonal pathways including the corpus callosum and cerebellar arbor vitae, and particularly in neurons of the frontal cortex in mouse and rat brains (Velasco‐Estevez, M., et al., 2020). In this study, a wider expression of Piezo1 in neurons is found including cortex and specifically BNST, CEA, PVT, EW and RN areas. Along with its protein level expression, its function in CNS has also been implied including directing the lineage choice of neuronal stem cells (Pathak, M. M, et al., 2014), and negatively correlated with the myelination in neurons (Velasco-Estevez, M., et al., 2020). However, direct evidence of function of Pieoz1 in neurons in mouse brain has not been reported. In this study, through the calcium response to Piezo1 agonist Yoda1, function of Piezo1in neurons is confirmed. With the finding that Piezo1 mediates ultrasonic neuromodulatory effects, through P1KO and Ctrl models, the difference between

response of neurons in different brain areas (CEA vs. Cortex) in turn indicates that the Piezo1 detection through immuno-staining and calcium imaging is trustworthy.

Although the high sensitivity of Piezo1 to force may explain its ability modulating neurons despite its low expression in mouse brain (RNA be detected in single cell RNA-sequencing) (Wang, J., & Hamill, O. P., 2021), it is suspected that this effect is indeed a cooperation of Piezo1 and other components. For example, Piezo1 may act as a lead opening other ion channel based on the finding that Piezo1 is the upstream of TRPV4 when sensing fluid shear stress, where TRPV4 in turn prolongs its inactivation (Swain, S. M., & Liddle, R. A., 2021) which may enhance the entire outcome of ultrasound bio-effect. Another finding that endogenous Piezo1 interfering the TMEM150c or Piezo1-ASIC1 Chimera also indicates the pivotal function of Piezo1 in force sensing (Dubin, A. E., et al., 2017). The finding that SMPD3, TMEM150c or Piezo1-ASIC1 enhances endogenous Piezo1 activity (Shi, J., et al. 2020; Anderson, E. O., et al., et al., 2018; Dubin, A. E., et al., 2017) further indicates that Piezo1 may response to ultrasound with a magnifying effect cooperating with other factors. However, there is no direct evidence demonstrating this hypothesis yet. Further studies that focus on Piezo1 cooperation with other components under ultrasound stimulation may provide more information in mechanism investigation.

In addition to the mechanism study, Piezo1 cooperation with other components also exhibits its high potential in application perspective. For instance, the SMPD3 and TMEM150C, which are found sustaining Piezo1 activation (Shi, J., et al. 2020; Anderson, E. O., et al., 2018) may be applied for enhancing the ultrasonic neuromodulation for brain search. The finding that Piezo1 opening upregulates the TREK/TRAAK mechanical activation and delays its kinetics (Glogowska, E., et al., 2021) suggests that Piezo1 could serve as a tool for neuron inhibition under ultrasound stimulus. In short, taking the advantage of endogenous expression of Piezo1, with co-expression of its appropriate assistant protein, Piezo1 may serve as a tool both activating and inhibiting neurons under ultrasound stimulation *in vivo*. Nerveless, further investigation should be taken to confirm the feasibility.

Meanwhile, in this study, response to ultrasound in P1KO model was significantly reduced but not eliminated which may indicate parallel functioned mechanisms. For example, TRPA1 in astrocyte was previously reported mediating ultrasound induced motor response (Oh, S. J., et al., 2019). ASIC1a was found responsible for ultrasound induced neurogenesis in mice

(Lim, J., et al., 2021), although the immediate ultrasonic neuron activation in the study was demonstrated *in vitro*, with ASIC1a's expression in mouse brain, it may also play a role in ultrasonic brain stimulation. Other ion channels such as the TRP family and calcium voltage-gated channels (VGCs) which were reported expressed in the central nerves system (Árnadóttir, J., & Chalfie, M. 2010; Tyler, W. J., 2012), may also contribute to the ultrasound induced neuronal activity in P1KO mice. Nevertheless, considering Piezo1 requires much lower pressure/force to be activated than other ion channels, reducing the ultrasound stimulation power may help avoiding other ion channels' response to ultrasound stimuli which may further improve the performance in neuroscience research.

A recent work reported Piezo1 gives minor contribution in ultrasonic neuromodulation based on the finding that minor and no changes of ultrasonic response with Piezo1 blocked and knockout respectively (Yoo, S., et al., 2022). Nevertheless, Piezo1's function in their setting might be already saturated, since activation threshold for detectable calcium signaling induced by ultrasound, revealed in this study, was as low as 0.03 MPa, which is much lower than the applied ultrasound intensity in their setting. In this situation, other ion channels that require higher ultrasound intensity may take over the role mediating ultrasonic neuromodulation. It is also worth noticing, as the authors concerned, the knockout efficiency by CRISPER method might not be satisfactory, yet no tests on Piezo1's function after knockout was performed.

Interestingly, Piezo1 is found specifically highly expressed in bed nucleus of the stria terminalis (BNST), central amygdala (CEA), paraventricular nucleus of hypothalamus (PVN), edinger-westphal nucleus (EW) and red nucleus (RN) which are all corticotropin releasing factor (CRF) expressing areas that regulate stress processing in animals (Smith, S. M., & Vale, W. W., 2022; Henckens, M. J., et al., 2016). CRF is a 41 amino acid peptide which is relatively large compared to other neural transmitters. Neurons might experience a more mechanical process transporting and secreting this peptide hormone (Tyler, W. J, 2012) when processing stress in animals. However, there is no direct evidence supporting this yet. Nevertheless, with the specific expression of mechanosensitive ion channel Piezo1, ultrasound provides a way to modulate these neurons thus to study relevant neuroscience question or even treat brain diseases.

Taken together, in this study, Piezo1 is demonstrated a pivotal factor mediating ultrasonic neuromodulatory effect *in vivo* and thus displays an outstanding application potential in both neuroscience research and brain disease treatment.

Reference

· Ahmadi, F., McLoughlin, I. V., Chauhan, S., & Ter-Haar, G. (2012). Bio-effects and safety of low-intensity, low-frequency ultrasonic exposure. *Progress in biophysics and molecular biology*, 108(3), 119-138.

· Alper, S. L. (2017). Genetic diseases of PIEZO1 and PIEZO2 dysfunction. *Current topics in membranes*, *79*, 97-134.

· Anderson, E. O., Schneider, E. R., Matson, J. D., Gracheva, E. O., & Bagriantsev, S. N. (2018). TMEM150C/Tentonin3 is a regulator of mechano-gated ion channels. *Cell reports*, 23(3), 701-708.

· Árnadóttir, J., & Chalfie, M. (2010). Eukaryotic mechanosensitive channels. *Annual review of biophysics*, *39*, 111-137.

· Aurup, C., Kamimura, H. A., & Konofagou, E. E. (2021). High-Resolution Focused Ultrasound Neuromodulation Induces Limb-Specific Motor Responses in Mice in Vivo. *Ultrasound in Medicine & Biology*, *47*(4), 998-1013.

· Avery, S. N., Clauss, J. A., & Blackford, J. U. (2016). The human BNST: functional role in anxiety and addiction. *Neuropsychopharmacology*, 41(1), 126-141.

· Ayling, O. G., Harrison, T. C., Boyd, J. D., Goroshkov, A., & Murphy, T. H. (2009). Automated light-based mapping of motor cortex by photoactivation of channelrhodopsin-2 transgenic mice. *Nature methods*, *6*(3), 219-224.

· Bachtold, M. R., Rinaldi, P. C., Jones, J. P., Reines, F., & Price, L. R. (1998). Focused ultrasound modifications of neural circuit activity in a mammalian brain. *Ultrasound in medicine & biology*, 24(4), 557-565.

· Bae, C., Sachs, F., & Gottlieb, P. A. (2011). The mechanosensitive ion channel Piezo1 is inhibited by the peptide GsMTx4. *Biochemistry*, 50(29), 6295-6300.

· Baek, H., Pahk, K. J., Kim, M. J., Youn, I., & Kim, H. (2018). Modulation of cerebellar cortical plasticity using low-intensity focused ultrasound for poststroke sensorimotor function recovery. *Neurorehabilitation and neural repair*, *32*(9), 777-787.

· Baek, H., Sariev, A., Dong, S., Royer, S., & Kim, H. (2019). Cerebellar low-intensity focused ultrasound stimulation can normalize asymmetrical hemispheric delta power after mouse ischemic stroke. *Brain Stimulation: Basic, Translational, and Clinical Research in Neuromodulation*, 12(2), 487.

· Basile, G. A., Quartu, M., Bertino, S., Serra, M. P., Boi, M., Bramanti, A., ... & Cacciola, A. (2021). Red nucleus structure and function: from anatomy to clinical neurosciences. *Brain Structure and Function*, 226(1), 69-91.

· Beyder, A., Rae, J. L., Bernard, C., Strege, P. R., Sachs, F., & Farrugia, G. (2010). Mechanosensitivity of Nav1. 5, a voltage-sensitive sodium channel. *The Journal of physiology*, *588*(24), 4969-4985.

· Bian, T., Meng, W., Qiu, M., Zhong, Z., Lin, Z., Zou, J., ... & Zheng, H. (2021). Noninvasive Ultrasound Stimulation of Ventral Tegmental Area Induces Reanimation from General Anaesthesia in Mice. *Research*, *2021*.

· Blackmore, J., Shrivastava, S., Sallet, J., Butler, C. R., & Cleveland, R. O. (2019). Ultrasound neuromodulation: a review of results, mechanisms and safety. *Ultrasound in medicine & biology*, 45(7), 1509-1536.

· Blount, P., Sukharev, S. I., Moe, P. C., Martinac, B., & Kung, C. (1999). [24] Mechanosensitive channels of bacteria. *Methods in enzymology*, *294*, 458-482.

· Blumenthal, N. R., Hermanson, O., Heimrich, B., & Shastri, V. P. (2014). Stochastic nanoroughness modulates neuron–astrocyte interactions and function via mechanosensing cation channels. *Proceedings of the National Academy of Sciences*, 111(45), 16124-16129.

· Bongioanni, A., Folloni, D., Verhagen, L., Sallet, J., Klein-Flügge, M. C., & Rushworth, M. F. (2021). Activation and disruption of a neural mechanism for novel choice in monkeys. *Nature*, 591(7849), 270-274.

· Borbiro, I., Badheka, D., & Rohacs, T. (2015). Activation of TRPV1 channels inhibits mechanosensitive Piezo channel activity by depleting membrane phosphoinositides. *Science signaling*, 8(363), ra15-ra15.

· Botello-Smith, W. M., Jiang, W., Zhang, H., Ozkan, A. D., Lin, Y. C., Pham, C. N., ... & Luo, Y. (2019). A mechanism for the activation of the mechanosensitive Piezo1 channel by the small molecule Yoda1. *Nature communications*, 10(1), 1-10.

· Boyden, E. S., Zhang, F., Bamberg, E., Nagel, G., & Deisseroth, K. (2005). Millisecond-timescale, genetically targeted optical control of neural activity. *Nature neuroscience*, 8(9), 1263-1268.

· Braun, V., Blackmore, J., Cleveland, R. O., & Butler, C. R. (2020). Transcranial ultrasound stimulation in humans is associated with an auditory confound that can be effectively masked. *Brain stimulation*, 13(6), 1527-1534.

· Brohawn, S. G., Del Mármol, J., & MacKinnon, R. (2012). Crystal structure of the human K2P TRAAK, a lipid-and mechano-sensitive K+ ion channel. *Science*, *335*(6067), 436-441.

· Budday, S., Steinmann III, P., & Kuhl, E. (2015). Physical biology of human brain development. *Frontiers in cellular neuroscience*, *9*, 257.

· Bullitt, E. (1990). Expression of c-fos-like protein as a marker for neuronal activity following noxious stimulation in the rat. *Journal of Comparative Neurology*, *296*(4), 517-530.

· Burks, S. R., Lorsung, R. M., Nagle, M. E., Tu, T. W., & Frank, J. A. (2019). Focused ultrasound activates voltage-gated calcium channels through depolarizing TRPC1 sodium currents in kidney and skeletal muscle. *Theranostics*, *9*(19), 5517.

· Bystritsky, A., Korb, A. S., Douglas, P. K., Cohen, M. S., Melega, W. P., Mulgaonkar, A. P., ... & Yoo, S. S. (2011). A review of low-intensity focused ultrasound pulsation. *Brain stimulation*, 4(3), 125-136.

· Cahalan, S. M., Lukacs, V., Ranade, S. S., Chien, S., Bandell, M., & Patapoutian, A. (2015). Piezo1 links mechanical forces to red blood cell volume. *Elife*, 4, e07370.

· Cain, J. A., Spivak, N. M., Coetzee, J. P., Crone, J. S., Johnson, M. A., Lutkenhoff, E. S., ... & Monti, M. M. (2021). Ultrasonic thalamic stimulation in chronic disorders of consciousness. *Brain Stimulation: Basic, Translational, and Clinical Research in Neuromodulation*, 14(2), 301-303.

· Calabrese, B., Tabarean, I. V., Juranka, P., & Morris, C. E. (2002). Mechanosensitivity of N-type calcium

channel currents. *Biophysical journal*, *83*(5), 2560-2574.

· Chighizola, M., Dini, T., Lenardi, C., Milani, P., Podestà, A., & Schulte, C. (2019). Mechanotransduction in neuronal cell development and functioning. *Biophysical Reviews*, 11(5), 701-720.

· Clement, G. T., & Hynynen, K. (2002). A non-invasive method for focusing ultrasound through the human skull. *Physics in Medicine & Biology*, 47(8), 1219.

· Coste, B., Mathur, J., Schmidt, M., Earley, T. J., Ranade, S., Petrus, M. J., ... & Patapoutian, A. (2010). Piezo1 and Piezo2 are essential components of distinct mechanically activated cation channels. *Science*, *330*(6000), 55-60.

· Coste, B., Murthy, S. E., Mathur, J., Schmidt, M., Mechioukhi, Y., Delmas, P., & Patapoutian, A. (2015). Piezo1 ion channel pore properties are dictated by C-terminal region. *Nature communications*, *6*(1), 1-11.

· Coste, B., Xiao, B., Santos, J. S., Syeda, R., Grandl, J., Spencer, K. S., ... & Patapoutian, A. (2012). Piezo proteins are pore-forming subunits of mechanically activated channels. *Nature*, 483(7388), 176-181.

· Costigan, M., Scholz, J., & Woolf, C. J. (2009). Neuropathic pain: a maladaptive response of the nervous system to damage. *Annual review of neuroscience*, 32, 1-32.

· Coussios, C. C., & Roy, R. A. (2008). Applications of acoustics and cavitation to noninvasive therapy and drug delivery. *Annu. Rev. Fluid Mech.*, 40, 395-420.

· Dalecki, D. (2004). Mechanical bioeffects of ultrasound. *Annu. Rev. Biomed. Eng.*, *6*, 229-248.

· Dallapiazza, R. F., Timbie, K. F., Holmberg, S., Gatesman, J., Lopes, M. B., Price, R. J., ... & Elias, W. J. (2017). Noninvasive neuromodulation and thalamic mapping with low-intensity focused ultrasound. *Journal of neurosurgery*, 128(3), 875-884.

· Darmani, G., Bergmann, T. O., Pauly, K. B., Caskey, C. F., de Lecea, L., Fomenko, A., ... & Chen, R. (2021). Non-invasive transcranial ultrasound stimulation for neuromodulation. *Clinical Neurophysiology*.

· Darrow, D. P., O'Brien, P., Richner, T. J., Netoff, T. I., & Ebbini, E. S. (2019). Reversible neuroinhibition by focused ultrasound is mediated by a thermal mechanism. *Brain stimulation*, 12(6), 1439-1447.

· Davis, M., & Whalen, P. J. (2001). The amygdala: vigilance and emotion. *Molecular psychiatry*, 6(1), 13-34.

· de Guglielmo, G., Kallupi, M., Pomrenze, M. B., Crawford, E., Simpson, S., Schweitzer, P., ... & George, O. (2019). Inactivation of a CRF-dependent amygdalofugal pathway reverses addiction-like behaviors in alcohol-dependent rats. *Nature communications*, 10(1), 1-11.

· Deffieux, T., Younan, Y., Wattiez, N., Tanter, M., Pouget, P., & Aubry, J. F. (2013). Low-intensity focused ultrasound modulates monkey visuomotor behavior. *Current Biology*, *23*(23), 2430-2433.

· Deisseroth, K. (2011). Optogenetics. *Nature methods*, 8(1), 26-29.

· Del Mármol, J. I., Touhara, K. K., Croft, G., & MacKinnon, R. (2018). Piezo1 forms a slowly-inactivating mechanosensory channel in mouse embryonic stem cells. *Elife*, 7, e33149.

· Dinno, M. A., Dyson, M., Young, S. R., Mortimer, A. J., Hart, J., & Crum, L. A. (1989). The significance of membrane changes in the safe and effective use of therapeutic and diagnostic ultrasound. *Physics in Medicine & Biology*, *34*(11), 1543.

· Dubin, A. E., Murthy, S., Lewis, A. H., Brosse, L., Cahalan, S. M., Grandl, J., ... & Patapoutian, A. (2017). Endogenous Piezo1 can confound mechanically activated channel identification and characterization. *Neuron*, 94(2), 266-270.

· Eguchi, K., Shindo, T., Ito, K., Ogata, T., Kurosawa, R., Kagaya, Y., ... & Shimokawa, H. (2018). Whole-brain low-intensity pulsed ultrasound therapy markedly improves cognitive dysfunctions in mouse models of dementia-Crucial roles of endothelial nitric oxide synthase. *Brain Stimulation*, 11(5), 959-973.

· Enyedi, P., & Czirják, G. (2010). Molecular background of leak K+ currents: two-pore domain potassium channels. *Physiological reviews*, 90(2), 559-605.

· Etzion, Y., & Grossman, Y. (2000). Pressure-induced depression of Synaptic transmission in the cerebellar parallel fibre synapse involves suppression of presynaptic N-type Ca2+ channels. *European Journal of Neuroscience*, *12*(11), 4007-4016.

· Everitt, B. J., Cardinal, R. N., Parkinson, J. A., & Robbins, T. W. (2003). Appetitive behavior: impact of amygdala-dependent mechanisms of emotional learning. *Annals of the new York Academy of Sciences*, 985(1), 233-250.

· Fang, X. Z., Zhou, T., Xu, J. Q., Wang, Y. X., Sun, M. M., He, Y. J., ... & Shang, Y. (2021). Structure, kinetic properties and biological function of mechanosensitive Piezo channels. *Cell & bioscience*, 11(1), 1-20.

· Folloni, D., Verhagen, L., Mars, R. B., Fouragnan, E., Constans, C., Aubry, J. F., ... & Sallet, J. (2019). Manipulation of subcortical and deep cortical activity in the primate brain using transcranial focused ultrasound stimulation. *Neuron*, *101*(6), 1109-1116.

· Fomenko, A., Neudorfer, C., Dallapiazza, R. F., Kalia, S. K., & Lozano, A. M. (2018). Low-intensity ultrasound neuromodulation: An overview of mechanisms and emerging human applications. *Brain stimulation*, *11*(6), 1209-1217.

· Fouragnan, E. F., Chau, B. K., Folloni, D., Kolling, N., Verhagen, L., Klein-Flügge, M., ... & Rushworth, M. F. (2019). The macaque anterior cingulate cortex translates counterfactual choice value into actual behavioral change. *Nature neuroscience*, *22*(5), 797-808.

· Franze, K., Janmey, P. A., & Guck, J. (2013). Mechanics in neuronal development and repair. *Annual review of biomedical engineering*, 15, 227-251.

· Fry, F. J., Ades, H. W., & Fry, W. J. (1958). Production of reversible changes in the central nervous system by ultrasound. Science, 127(3289), 83-84.

· Gaub, B. M., & Muller, D. J. (2017). Mechanical stimulation of Piezo1 receptors depends on extracellular matrix proteins and directionality of force. *Nano letters*, 17(3), 2064-2072.

· Gavrilov, L. R., Tsirulnikov, E. M., & Davies, I. A. I. (1996). Application of focused ultrasound for the stimulation of neural structures. *Ultrasound in medicine & biology*, 22(2), 179-192.

· Ge, J., Li, W., Zhao, Q., Li, N., Chen, M., Zhi, P., ... & Yang, M. (2015). Architecture of the mammalian mechanosensitive Piezo1 channel. *Nature*, *527*(7576), 64-69.

· Geerling, J. C., Shin, J. W., Chimenti, P. C., & Loewy, A. D. (2010). Paraventricular hypothalamic nucleus: axonal projections to the brainstem. *Journal of Comparative Neurology*, 518(9), 1460-1499.

· Geng, J., Zhao, Q., Zhang, T., & Xiao, B. (2017). In touch with the mechanosensitive piezo channels: structure, ion permeation, and mechanotransduction. *Current topics in membranes*, 79, 159-195.

· Germann, J., Elias, G. J., Neudorfer, C., Boutet, A., Chow, C. T., Wong, E. H., ... & Lozano, A. M. (2021). Potential optimization of focused ultrasound capsulotomy for obsessive compulsive disorder. *Brain*, 144(11), 3529-3540.

· Glogowska, E., Arhatte, M., Chatelain, F. C., Lesage, F., Xu, A., Grashoff, C., ... & Honoré, E. (2021). Piezo1 and Piezo2 foster mechanical gating of K2P channels. *Cell reports*, 37(9), 110070.

· Gorostiza, P., & Isacoff, E. (2007). Optical switches and triggers for the manipulation of ion channels and pores. Molecular BioSystems, 3(10), 686-704.

· Govorunova, E. G., Sineshchekov, O. A., Janz, R., Liu, X., & Spudich, J. L. (2015). Natural lightgated anion channels: A family of microbial rhodopsins for advanced optogenetics. *Science*, 349(6248), 647-650.

· Grimm, C., Kraft, R., Sauerbruch, S., Schultz, G., & Harteneck, C. (2003). Molecular and functional characterization of the melastatin-related cation channel TRPM3. *Journal of Biological Chemistry*, *278*(24), 21493-21501.

· Gu, Y., & Gu, C. (2014). Physiological and pathological functions of mechanosensitive ion channels. *Molecular neurobiology*, 50(2), 339-347.

· Gudipaty, S. A., Lindblom, J., Loftus, P. D., Redd, M. J., Edes, K., Davey, C. F., ... & Rosenblatt, J. (2017). Mechanical stretch triggers rapid epithelial cell division through Piezo1. *Nature*, 543(7643), 118-121.

· Güler, A. D., Lee, H., Iida, T., Shimizu, I., Tominaga, M., & Caterina, M. (2002). Heat-evoked activation of the ion channel, TRPV4. *Journal of Neuroscience*, 22(15), 6408-6414.

· Guo, H., Hamilton II, M., Offutt, S. J., Gloeckner, C. D., Li, T., Kim, Y., ... & Lim, H. H. (2018). Ultrasound produces extensive brain activation via a cochlear pathway. *Neuron*, *98*(5), 1020-1030.

· Guo, Y. R., & MacKinnon, R. (2017). Structure-based membrane dome mechanism for Piezo mechanosensitivity. *Elife*, 6, e33660.

· Hakimova, H., Kim, S., Chu, K., Lee, S. K., Jeong, B., & Jeon, D. (2015). Ultrasound stimulation inhibits recurrent seizures and improves behavioral outcome in an experimental model of mesial temporal lobe epilepsy. *Epilepsy & Behavior*, 49, 26-32.

· Häusser, M. (2014). Optogenetics: the age of light. *Nature methods*, 11(10), 1012.

· Henckens, M. J., Deussing, J. M., & Chen, A. (2016). Region-specific roles of the corticotropin-releasing factor–urocortin system in stress. *Nature Reviews Neuroscience*, 17(10), 636-651.

· Herman, J. P., & Cullinan, W. E. (1997). Neurocircuitry of stress: central control of the hypothalamo–pituitary–adrenocortical axis. *Trends in neurosciences*, 20(2), 78-84.

· Hill, D. K. (1950). The volume change resulting from stimulation of a giant nerve fibre. *The Journal of physiology*, 111(3-4), 304.

· Hoffman, B. U., Baba, Y., Lee, S. A., Tong, C. K., Konofagou, E. E., & Lumpkin, E. A. (2022). Focused ultrasound excites action potentials in mammalian peripheral neurons in part through the mechanically gated ion channel PIEZO2. *Proceedings of the National Academy of Sciences*, 119(21), e2115821119.

· Hu, J. H., & Ulrich, W. D. (1976). Effects of low-intensity ultrasound on the central nervous system of primates. *Aviation, space, and environmental medicine*, 47(6), 640-643.

· Huang, S. L., Chang, C. W., Lee, Y. H., & Yang, F. Y. (2017). Protective effect of low-intensity pulsed ultrasound on memory impairment and brain damage in a rat model of vascular dementia. *Radiology*, 282(1), 113-122.

· Huang, X., Lin, Z., Wang, K., Liu, X., Zhou, W., Meng, L., ... & Zheng, H. (2019). Transcranial low-intensity pulsed ultrasound modulates structural and functional synaptic plasticity in rat hippocampus. *IEEE transactions on ultrasonics, ferroelectrics, and frequency control*, *66*(5), 930-938.

· Iorio-Morin, C., Yamamoto, K., Sarica, C., Zemmar, A., Levesque, M., Brisebois, S., ... & Lozano, A. M. (2021). Bilateral Focused Ultrasound Thalamotomy for Essential Tremor (BEST-FUS Phase 2 Trial). *Movement Disorders*, 36(11), 2653-2662.

· Janak, P. H., & Tye, K. M. (2015). From circuits to behaviour in the amygdala. *Nature*, 517(7534), 284-292.

· Jiang, Y., Yang, X., Jiang, J., & Xiao, B. (2021). Structural designs and mechanogating mechanisms of the mechanosensitive piezo channels. *Trends in Biochemical Sciences*.

· Juffermans, L. J., Kamp, O., Dijkmans, P. A., Visser, C. A., & Musters, R. J. (2008). Low-intensity ultrasound-exposed microbubbles provoke local hyperpolarization of the cell membrane via activation of BKCa channels. *Ultrasound in medicine & biology*, *34*(3), 502-508.

· Kamimura, H. A., Conti, A., Toschi, N., & Konofagou, E. E. (2020). Ultrasound neuromodulation: Mechanisms and the potential of multimodal stimulation for neuronal function assessment. *Frontiers in physics*, 8, 150.

· Kamimura, H. A., Wang, S., Chen, H., Wang, Q., Aurup, C., Acosta, C., ... & Konofagou, E. E. (2016). Focused ultrasound neuromodulation of cortical and subcortical brain structures using 1.9 MHz. *Medical physics*, *43*(10), 5730-5735.

· Khalighinejad, N., Bongioanni, A., Verhagen, L., Folloni, D., Attali, D., Aubry, J. F., ... & Rushworth, M. F. (2020). A basal forebrain-cingulate circuit in macaques decides it is time to act. *Neuron*, 105(2), 370-384.

· Khraiche, M. L., Phillips, W. B., Jackson, N., & Muthuswamy, J. (2008, August). Ultrasound induced increase in excitability of single neurons. In 2008 30th Annual International Conference of the IEEE Engineering in Medicine and Biology Society (pp. 4246-4249). *IEEE*.

· Kim, G. H., Kosterin, P., Obaid, A. L., & Salzberg, B. M. (2007). A mechanical spike accompanies the action potential in mammalian nerve terminals. *Biophysical journal*, 92(9), 3122-3129.

· Kim, H., Chiu, A., Lee, S. D., Fischer, K., & Yoo, S. S. (2014). Focused ultrasound-mediated non-invasive brain stimulation: examination of sonication parameters. *Brain stimulation*, *7*(5), 748-756.

· Kim, H., Park, M. Y., Lee, S. D., Lee, W., Chiu, A., & Yoo, S. S. (2015). Suppression of EEG visual-evoked potentials in rats via neuromodulatory focused ultrasound. *Neuroreport*, 26(4), 211.

· Kim, H., Taghados, S. J., Fischer, K., Maeng, L. S., Park, S., & Yoo, S. S. (2012). Noninvasive transcranial stimulation of rat abducens nerve by focused ultrasound. *Ultrasound in medicine & biology*, *38*(9), 1568-1575.

· King, R. L., Brown, J. R., & Pauly, K. B. (2014). Localization of ultrasound-induced in vivo neurostimulation in the mouse model. *Ultrasound in medicine & biology*, *40*(7), 1512-1522.

· King, R. L., Brown, J. R., Newsome, W. T., & Pauly, K. B. (2013). Effective parameters for ultrasound-induced in vivo neurostimulation. *Ultrasound in medicine & biology*, *39*(2), 312-331.

· Koser, D. E., Thompson, A. J., Foster, S. K., Dwivedy, A., Pillai, E. K., Sheridan, G. K., ... & Franze, K. (2016). Mechanosensing is critical for axon growth in the developing brain. *Nature neuroscience*, 19(12), 1592-1598.

· Kozicz, T., Bittencourt, J. C., May, P. J., Reiner, A., Gamlin, P. D., Palkovits, M., ... & Ryabinin, A. E. (2011). The Edinger-Westphal nucleus: A historical, structural, and functional perspective on a dichotomous terminology. *Journal of Comparative Neurology*, 519(8), 1413-1434.

· Kubanek, J., Brown, J., Ye, P., Pauly, K. B., Moore, T., & Newsome, W. (2020). Remote, brain region–specific control of choice behavior with ultrasonic waves. Science advances, 6(21), eaaz4193.

· Kubanek, J., Shi, J., Marsh, J., Chen, D., Deng, C., & Cui, J. (2016). Ultrasound modulates ion channel currents. *Scientific reports*, *6*(1), 1-14.

· Kubanek, J., Shukla, P., Das, A., Baccus, S. A., & Goodman, M. B. (2018). Ultrasound elicits behavioral responses through mechanical effects on neurons and ion channels in a simple nervous system. *Journal of Neuroscience*, *38*(12), 3081-3091.

· Lamandé, S. R., Yuan, Y., Gresshoff, I. L., Rowley, L., Belluoccio, D., Kaluarachchi, K., ... & Bateman, J. F. (2011). Mutations in TRPV4 cause an inherited arthropathy of hands and feet. *Nature genetics*, 43(11), 1142-1146.

· Lebow, M. A., & Chen, A. (2016). Overshadowed by the amygdala: the bed nucleus of the stria terminalis emerges as key to psychiatric disorders. *Molecular psychiatry*, 21(4), 450-463.

· Lee, D. A., Knight, M. M., Campbell, J. J., & Bader, D. L. (2011). Stem cell mechanobiology. *Journal of cellular biochemistry*, 112(1), 1-9.

· Lee, W., Chung, Y. A., Jung, Y., Song, I. U., & Yoo, S. S. (2016a). Simultaneous acoustic stimulation of human primary and secondary somatosensory cortices using transcranial focused ultrasound. *BMC neuroscience*, 17(1), 1-11.

· Lee, W., Kim, H. C., Jung, Y., Chung, Y. A., Song, I. U., Lee, J. H., & Yoo, S. S. (2016b). Transcranial focused ultrasound stimulation of human primary visual cortex. *Scientific reports*, *6*(1), 1-12.

· Lee, W., Kim, H., Jung, Y., Song, I. U., Chung, Y. A., & Yoo, S. S. (2015). Image-guided transcranial focused ultrasound stimulates human primary somatosensory cortex. *Scientific reports*, *5*(1), 1-10.

· Lee, W., Lee, S. D., Park, M. Y., Foley, L., Purcell-Estabrook, E., Kim, H., ... & Yoo, S. S. (2016c). Image-guided focused ultrasound-mediated regional brain stimulation in sheep. *Ultrasound in medicine & biology*, *42*(2), 459-470.

· Legon, W., Ai, L., Bansal, P., & Mueller, J. K. (2018b). Neuromodulation with single-element transcranial focused ultrasound in human thalamus. *Human brain mapping*, *39*(5), 1995-2006.

· Legon, W., Bansal, P., Tyshynsky, R., Ai, L., & Mueller, J. K. (2018a). Transcranial focused ultrasound

neuromodulation of the human primary motor cortex. *Scientific reports, 8*(1), 1-14.

· Legon, W., Sato, T. F., Opitz, A., Mueller, J., Barbour, A., Williams, A., & Tyler, W. J. (2014). Transcranial focused ultrasound modulates the activity of primary somatosensory cortex in humans. *Nature neuroscience, 17*(2), 322-329.

· Legrand, M., Galineau, L., Novell, A., Planchez, B., Brizard, B., Leman, S., ... & Bouakaz, A. (2019). Efficacy of chronic ultrasound neurostimulation on behaviors and distributed brain metabolism in depressive-like mice. *BioRxiv,* 813006.

· Leighton, T. G. (2007). What is ultrasound?. *Progress in biophysics and molecular biology*, *93*(1-3), 3-83.

· Lele, P. P. (1963). Effects of focused ultrasonic radiation on peripheral nerve, with observations on local heating. *Experimental Neurology*, 8(1), 47-83.

· Lengyel, M., Enyedi, P., & Czirják, G. (2021). Negative Influence by the Force: Mechanically Induced Hyperpolarization via K2P Background Potassium Channels. *International Journal of Molecular Sciences*, *22*(16), 9062.

· Lewis, A. H., & Grandl, J. (2020). Inactivation kinetics and mechanical gating of Piezo1 ion channels depend on subdomains within the cap. *Cell reports*, 30(3), 870-880.

· Li, J., Hou, B., Tumova, S., Muraki, K., Bruns, A., Ludlow, M. J., ... & Beech, D. J. (2014). Piezo1 integration of vascular architecture with physiological force. *Nature*, *515*(7526), 279-282.

· Li, J., Liu, S., Song, C., Hu, Q., Zhao, Z., Deng, T., ... & Xiong, W. (2021). PIEZO2 mediates ultrasonic hearing via cochlear outer hair cells in mice. *Proceedings of the National Academy of Sciences*, 118(28).

· Lim, J., Tai, H. H., Liao, W. H., Chu, Y. C., Hao, C. M., Huang, Y. C., ... & Wang, J. L. (2021). ASIC1a is required for neuronal activation via low-intensity ultrasound stimulation in mouse brain. *Elife*, *10*.

· Lin, J. W., Yu, F., Müller, W. S., Ehnholm, G., & Okada, Y. (2019). Focused ultrasound transiently increases membrane conductance in isolated crayfish axon. *Journal of Neurophysiology*, 121(2), 480-489.

· Lin, W. T., Chen, R. C., Lu, W. W., Liu, S. H., & Yang, F. Y. (2015). Protective effects of low-intensity pulsed ultrasound on aluminum-induced cerebral damage in Alzheimer's disease rat model. *Scientific reports*, 5(1), 1-7.

· Lin, W., Laitko, U., Juranka, P. F., & Morris, C. E. (2007). Dual stretch responses of mHCN2 pacemaker channels: accelerated activation, accelerated deactivation. *Biophysical journal*, *92*(5), 1559-1572.

· Lin, Y. C., Guo, Y. R., Miyagi, A., Levring, J., MacKinnon, R., & Scheuring, S. (2019). Force-induced conformational changes in PIEZO1. *Nature*, 573(7773), 230-234.

· Lin, Z., Huang, X., Zhou, W., Zhang, W., Liu, Y., Bian, T., ... & Guo, Y. (2019). Ultrasound stimulation modulates voltage-gated potassium currents associated with action potential shape in hippocampal CA1 pyramidal neurons. *Frontiers in pharmacology*, *10*, 544.

· Liu, C., Yu, K., Niu, X., & He, B. (2021). Transcranial focused ultrasound enhances sensory discrimination capability through somatosensory cortical excitation. *Ultrasound in Medicine & Biology*, 47(5), 1356-1366.

· Lu, B., Nagappan, G., Guan, X., Nathan, P. J., & Wren, P. (2013). BDNF-based synaptic repair as a disease-modifying strategy for neurodegenerative diseases. *Nature Reviews Neuroscience*, 14(6), 401-416.

· Luan, S., Williams, I., Nikolic, K., & Constandinou, T. G. (2014). Neuromodulation: present and emerging methods. *Frontiers in neuroengineering*, 7, 27.

· Maingret, F., Fosset, M., Lesage, F., Lazdunski, M., & Honoré, E. (1999). TRAAK is a mammalian neuronal mechano-gated K+ channel. *Journal of Biological Chemistry*, *274*(3), 1381-1387.

· Maingret, F., Patel, A. J., Lesage, F., Lazdunski, M., & Honoré, E. (1999). Mechano-or acid stimulation, two interactive modes of activation of the TREK-1 potassium channel. *Journal of Biological Chemistry*, *274*(38), 26691-26696.

· Manuel, T. J., Kusunose, J., Zhan, X., Lv, X., Kang, E., Yang, A., ... & Caskey, C. F. (2020). Ultrasound neuromodulation depends on pulse repetition frequency and can modulate inhibitory effects of TTX. *Scientific reports*, 10(1), 1-10.

· Mehić, E., Xu, J. M., Caler, C. J., Coulson, N. K., Moritz, C. T., & Mourad, P. D. (2014). Increased anatomical specificity of neuromodulation via modulated focused ultrasound. *PloS one*, 9(2), e86939.

· Menz, M. D., Ye, P., Firouzi, K., Nikoozadeh, A., Pauly, K. B., Khuri-Yakub, P., & Baccus, S. A. (2019). Radiation force as a physical mechanism for ultrasonic neurostimulation of the ex vivo retina. *Journal of Neuroscience*, *39*(32), 6251-6264.

· Mezey, É., Tóth, Z. E., Cortright, D. N., Arzubi, M. K., Krause, J. E., Elde, R., ... & Szallasi, A. (2000). Distribution of mRNA for vanilloid receptor subtype 1 (VR1), and VR1-like immunoreactivity, in the central nervous system of the rat and human. *Proceedings of the National Academy of Sciences*, 97(7), 3655-3660.

· Min, B. K., Bystritsky, A., Jung, K. I., Fischer, K., Zhang, Y., Maeng, L. S., ... & Yoo, S. S. (2011). Focused ultrasound-mediated suppression of chemically-induced acute epileptic EEG activity. *BMC neuroscience*, 12(1), 1-12.

· Miocinovic, S., Somayajula, S., Chitnis, S., & Vitek, J. L. (2013). History, applications, and mechanisms of deep brain stimulation. *JAMA neurology*, 70(2), 163-171

· Mohammadjavadi, M., Ye, P. P., Xia, A., Brown, J., Popelka, G., & Pauly, K. B. (2019). Elimination of peripheral auditory pathway activation does not affect motor responses from ultrasound neuromodulation. *Brain stimulation*, *12*(4), 901-910.

· Morgan, J. I., & Curran, T. (1988). Calcium as a modulator of the immediate-early gene cascade in neurons. *Cell calcium*, 9(5-6), 303-311.

· Morris, C. E. (1990). Mechanosensitive ion channels. *The Journal of membrane biology*, 113(2), 93-107.

· Morris, C. E., & Juranka, P. F. (2007). Nav channel mechanosensitivity: activation and inactivation accelerate reversibly with stretch. *Biophysical journal*, *93*(3), 822-833.

· Mueller, J. K., & Tyler, W. J. (2014). A quantitative overview of biophysical forces impinging on neural function. *Physical biology*, *11*(5), 051001.

· Muir, J., Lopez, J., & Bagot, R. C. (2019). Wiring the depressed brain: optogenetic and chemogenetic circuit interrogation in animal models of depression. *Neuropsychopharmacology*, 44(6), 1013-1026.

· Nagahara, A. H., & Tuszynski, M. H. (2011). Potential therapeutic uses of BDNF in neurological and psychiatric disorders. *Nature reviews Drug discovery*, 10(3), 209-219.

· Niu, X., Qian, X., & Magleby, K. L. (2004). Linker-gating ring complex as passive spring and Ca2+-dependent machine for a voltage-and Ca2+-activated potassium channel. *Neuron*, *42*(5), 745-756.

· O'Brien Jr, W. D. (2007). Ultrasound–biophysics mechanisms. *Progress in biophysics and molecular biology*, *93*(1-3), 212-255.

· Oh, S. J., Lee, J. M., Kim, H. B., Lee, J., Han, S., Bae, J. Y., ... & Lee, C. J. (2019). Ultrasonic neuromodulation via astrocytic TRPA1. *Current Biology*, *29*(20), 3386-3401.

· Okubo, M., Fujita, A., Saito, Y., Komaki, H., Ishiyama, A., Takeshita, E., ... & Sasaki, M. (2015). A family of distal arthrogryposis type 5 due to a novel PIEZO2 mutation. *American journal of medical genetics* Part A, 167(5), 1100-1106.

· Paoletti, P., & Ascher, P. (1994). Mechanosensitivity of NMDA receptors in cultured mouse central neurons. *Neuron*, *13*(3), 645-655.

· Pathak, M. M., Nourse, J. L., Tran, T., Hwe, J., Arulmoli, J., Dai Trang, T. L., ... & Tombola, F. (2014). Stretch-activated ion channel Piezo1 directs lineage choice in human neural stem cells. *Proceedings of the National Academy of Sciences,* 111(45), 16148-16153.

· Peterchev, A. V., Wagner, T. A., Miranda, P. C., Nitsche, M. A., Paulus, W., Lisanby, S. H., ... & Bikson, M. (2012). Fundamentals of transcranial electric and magnetic stimulation dose: definition, selection, and reporting practices. *Brain stimulation*, 5(4), 435-453.

· Pfister, B. J., Iwata, A., Meaney, D. F., & Smith, D. H. (2004). Extreme stretch growth of integrated axons. *Journal of Neuroscience*, 24(36), 7978-7983.

· Plaksin, M., Shoham, S., & Kimmel, E. (2014). Intramembrane cavitation as a predictive bio-piezoelectric mechanism for ultrasonic brain stimulation. *Physical review X*, 4(1), 011004.

· Plesset, M. S., & Prosperetti, A. (1977). Bubble dynamics and cavitation. *Annual review of fluid mechanics*, 9(1), 145-185.

· Polanía, R., Nitsche, M. A., & Ruff, C. C. (2018). Studying and modifying brain function with non-invasive brain stimulation. *Nature neuroscience*, 21(2), 174-187.

· Prieto, M. L., Firouzi, K., Khuri-Yakub, B. T., & Maduke, M. (2018). Activation of Piezo1 but not NaV1. 2 channels by ultrasound at 43 MHz. *Ultrasound in medicine & biology*, 44(6), 1217-1232.

· Qi, X., Lyu, K., Meng, L., Li, C., Zhang, H., Niu, L., ... & Tang, J. (2021). Low-Intensity Ultrasound Causes Direct Excitation of Auditory Cortical Neurons. *Neural Plasticity*, 2021.

· Qiu, Z., Guo, J., Kala, S., Zhu, J., Xian, Q., Qiu, W., ... & Sun, L. (2019). The mechanosensitive ion channel Piezo1 significantly mediates in vitro ultrasonic stimulation of neurons. *Iscience*, *21*, 448-457.

· Qiu, Z., Kala, S., Guo, J., Xian, Q., Zhu, J., Zhu, T., ... & Sun, L. (2020). Targeted neurostimulation in mouse brains with non-invasive ultrasound. *Cell reports*, *32*(7), 108033.

· Retailleau, K., Duprat, F., Arhatte, M., Ranade, S. S., Peyronnet, R., Martins, J. R., ... & Honoré, E. (2015). Piezo1 in smooth muscle cells is involved in hypertension-dependent arterial remodeling. *Cell reports*, 13(6), 1161-1171.

· Rezayat, E., & Toostani, I. G. (2016). A review on brain stimulation using low intensity focused ultrasound.

Basic and clinical neuroscience, 7(3), 187.

· Reznik, S. J., Sanguinetti, J. L., Tyler, W. J., Daft, C., & Allen, J. J. (2020). A double-blind pilot study of transcranial ultrasound (TUS) as a five-day intervention: TUS mitigates worry among depressed participants. *Neurology, Psychiatry and Brain Research*, *37*, 60-66.

· Rinaldi, P. C., Jones, J. P., Reines, F., & Price, L. R. (1991). Modification by focused ultrasound pulses of electrically evoked responses from an in vitro hippocampal preparation. *Brain research*, *558*(1), 36-42.

· Robertson, J. L., Cox, B. T., Jaros, J., & Treeby, B. E. (2017). Accurate simulation of transcranial ultrasound propagation for ultrasonic neuromodulation and stimulation. *The Journal of the Acoustical Society of America*, 141(3), 1726-1738.

· Robinson, S., Todd, T. P., Pasternak, A. R., Luikart, B. W., Skelton, P. D., Urban, D. J., & Bucci, D. J. (2014). Chemogenetic silencing of neurons in retrosplenial cortex disrupts sensory preconditioning. *Journal of Neuroscience*, 34(33), 10982-10988.

· Riccio, A., Medhurst, A. D., Mattei, C., Kelsell, R. E., Calver, A. R., Randall, A. D., ... & Pangalos, M. N. (2002). mRNA distribution analysis of human TRPC family in CNS and peripheral tissues. Molecular brain research, 109(1-2), 95-104.

· Roth, B. L. (2016). DREADDs for neuroscientists. *Neuron*, *89*(4), 683-694.

· Sanguinetti, J. L., Hameroff, S., Smith, E. E., Sato, T., Daft, C. M., Tyler, W. J., & Allen, J. J. (2020). Transcranial focused ultrasound to the right prefrontal cortex improves mood and alters functional connectivity in humans. *Frontiers in human neuroscience*, *14*, 52.

· Saotome, K., Murthy, S. E., Kefauver, J. M., Whitwam, T., Patapoutian, A., & Ward, A. B. (2018). Structure of the mechanically activated ion channel Piezo1. *Nature*, *554*(7693), 481-486.

· Sato, T., Shapiro, M. G., & Tsao, D. Y. (2018). Ultrasonic neuromodulation causes widespread cortical activation via an indirect auditory mechanism. *Neuron*, *98*(5), 1031-1041.

· Shi, J., Hyman, A. J., De Vecchis, D., Chong, J., Lichtenstein, L., Futers, T. S., ... & Beech, D. J. (2020). Sphingomyelinase disables inactivation in endogenous PIEZO1 channels. *Cell reports*, 33(1), 108225.

· Shin, S. M., Moehring, F., Itson-Zoske, B., Fan, F., Stucky, C. L., Hogan, Q. H., & Yu, H. (2021). Piezo2 mechanosensitive ion channel is located to sensory neurons and nonneuronal cells in rat peripheral sensory pathway: implications in pain. *Pain*, 162(11), 2750-2768.

· Sinai, A., Nassar, M., Sprecher, E., Constantinescu, M., Zaaroor, M., & Schlesinger, I. (2021). Focused Ultrasound Thalamotomy in Tremor Dominant Parkinson's Disease: Long-Term Results. Journal of *Parkinson's Disease*, (Preprint), 1-8.

· Singh, P., Doshi, S., Spaethling, J. M., Hockenberry, A. J., Patel, T. P., Geddes-Klein, D. M., ... & Meaney, D. F. (2012). N-methyl-D-aspartate receptor mechanosensitivity is governed by C terminus of NR2B subunit. *Journal of Biological Chemistry*, *287*(6), 4348-4359.

· Smith, S. M., & Vale, W. W. (2022). The role of the hypothalamic-pituitary-adrenal axis in neuroendocrine responses to stress. *Dialogues in clinical neuroscience*.

· Solis, A. G., Bielecki, P., Steach, H. R., Sharma, L., Harman, C. C., Yun, S., ... & Flavell, R. A. (2019).

Mechanosensation of cyclical force by PIEZO1 is essential for innate immunity. *Nature*, 573(7772), 69-74.

· Sorum, B., Rietmeijer, R. A., Gopakumar, K., Adesnik, H., & Brohawn, S. G. (2021). Ultrasound activates mechanosensitive TRAAK K+ channels through the lipid membrane. *Proceedings of the National Academy of Sciences*, 118(6).

· Suchyna, T. M. (2017). Piezo channels and GsMTx4: Two milestones in our understanding of excitatory mechanosensitive channels and their role in pathology. *Progress in biophysics and molecular biology*, 130, 244-253.

· Sukharev, S., & Anishkin, A. (2004). Mechanosensitive channels: what can we learn from 'simple'model systems?. *Trends in neurosciences*, *27*(6), 345-351.

· Sun, J., & Hynynen, K. (1998). Focusing of therapeutic ultrasound through a human skull: a numerical study. *The Journal of the Acoustical Society of America*, 104(3), 1705-1715.

· Suter, D. M., & Miller, K. E. (2011). The emerging role of forces in axonal elongation. *Progress in neurobiology*, 94(2), 91-101.

· Swain, S. M., & Liddle, R. A. (2021). Piezo1 acts upstream of TRPV4 to induce pathological changes in endothelial cells due to shear stress. *Journal of Biological Chemistry*, 296.

· Syeda, R., Florendo, M. N., Cox, C. D., Kefauver, J. M., Santos, J. S., Martinac, B., & Patapoutian, A. (2016). Piezo1 channels are inherently mechanosensitive. *Cell reports*, 17(7), 1739-1746.

· Syeda, R., Xu, J., Dubin, A. E., Coste, B., Mathur, J., Huynh, T., ... & Patapoutian, A. (2015). Chemical activation of the mechanotransduction channel Piezo1. *Elife*, 4, e07369.

· Tabarean, I. V., & Morris, C. E. (2002). Membrane stretch accelerates activation and slow inactivation in Shaker channels with S3–S4 linker deletions. *Biophysical journal*, *82*(6), 2982-2994.

· TAKAGI, S. F., Higashino, S. Y. O. J. I., Shibuya, T. A. T. S. U. A. K. I., & Osawa, N. O. B. U. T. A. K. A. (1960). The actions of ultrasound on the myelinated nerve, the spinal cord and the brain. *The Japanese Journal of Physiology*, 10(2), 183-193.

· Tang, S. C., & Clement, G. T. (2009). Standing-wave suppression for transcranial ultrasound by random modulation. *IEEE transactions on Biomedical Engineering*, 57(1), 203-205.

· Tasaki, I., Kusano, K., & Byrne, P. (1989). Rapid mechanical and thermal changes in the garfish olfactory nerve associated with a propagated impulse. *Biophysical journal*, 55(6), 1033-1040.

· Teissier, A., Chemiakine, A., Inbar, B., Bagchi, S., Ray, R. S., Palmiter, R. D., ... & Ansorge, M. S. (2015). Activity of raphé serotonergic neurons controls emotional behaviors. *Cell reports*, 13(9), 1965-1976.

· Ter Haar, G. (2007). Therapeutic applications of ultrasound. *Progress in biophysics and molecular biology*, 93(1-3), 111-129.

· Tsai, S. J. (2015). Transcranial focused ultrasound as a possible treatment for major depression. *Medical hypotheses*, 84(4), 381-383.

· Tufail, Y., Matyushov, A., Baldwin, N., Tauchmann, M. L., Georges, J., Yoshihiro, A., ... & Tyler, W. J. (2010). Transcranial pulsed ultrasound stimulates intact brain circuits. *Neuron*, *66*(5), 681-694.

· Tufail, Y., Yoshihiro, A., Pati, S., Li, M. M., & Tyler, W. J. (2011). Ultrasonic neuromodulation by brain

stimulation with transcranial ultrasound. *nature protocols*, 6(9), 1453-1470.

· Tyler, W. J. (2012). The mechanobiology of brain function. *Nature Reviews Neuroscience*, 13(12), 867-878.

· Tyler, W. J., Lani, S. W., & Hwang, G. M. (2018). Ultrasonic modulation of neural circuit activity. *Current opinion in neurobiology*, *50*, 222-231.

· Tyler, W. J., Tufail, Y., Finsterwald, M., Tauchmann, M. L., Olson, E. J., & Majestic, C. (2008). Remote excitation of neuronal circuits using low-intensity, low-frequency ultrasound. *PloS one*, 3(10), e3511.

· Ucar, H., Watanabe, S., Noguchi, J., Morimoto, Y., Iino, Y., Yagishita, S., ... & Kasai, H. (2021). Mechanical actions of dendritic-spine enlargement on presynaptic exocytosis. *Nature*, 1-4.

· Ulmer, S., & Jansen, O. (2010). *fMRI*. Berlin Heidelberg: Springer-Verlag.

· Urban, D. J., & Roth, B. L. (2015). DREADDs (designer receptors exclusively activated by designer drugs): chemogenetic tools with therapeutic utility. *Annual review of pharmacology and toxicology*, 55, 399-417.

· Urban, D. J., Zhu, H. U., Marcinkiewcz, C. A., Michaelides, M., Oshibuchi, H., Rhea, D., ... & Roth, B. L. (2016). Elucidation of the behavioral program and neuronal network encoded by dorsal raphe serotonergic neurons. *Neuropsychopharmacology*, 41(5), 1404-1415.

· Velasco-Estevez, M., Gadalla, K. K., Liñan-Barba, N., Cobb, S., Dev, K. K., & Sheridan, G. K. (2020). Inhibition of Piezo1 attenuates demyelination in the central nervous system. *Glia*, 68(2), 356-375.

· Velasco-Estevez, M., Mampay, M., Boutin, H., Chaney, A., Warn, P., Sharp, A., ... & Sheridan, G. K. (2018). Infection augments expression of mechanosensing Piezo1 channels in amyloid plaque-reactive astrocytes. *Frontiers in aging neuroscience*, 332.

· Vennekens, R., Menigoz, A., & Nilius, B. (2012). TRPs in the brain. *Reviews of Physiology, Biochemistry and Pharmacology, Vol. 163*, 27-64.

· Verhagen, L., Gallea, C., Folloni, D., Constans, C., Jensen, D. E., Ahnine, H., ... & Sallet, J. (2019). Offline impact of transcranial focused ultrasound on cortical activation in primates. *Elife*, *8*, e40541.

· Wang, F., Knutson, K., Alcaino, C., Linden, D. R., Gibbons, S. J., Kashyap, P., ... & Beyder, A. (2017). Mechanosensitive ion channel Piezo2 is important for enterochromaffin cell response to mechanical forces. *The Journal of physiology*, 595(1), 79-91.

· Wang, J., & Hamill, O. P. (2021). Piezo2—peripheral baroreceptor channel expressed in select neurons of the mouse brain: a putative mechanism for synchronizing neural networks by transducing intracranial pressure pulses. J. Integr. *Neurosci*, 20(4), 825-837.

· Wang, Y., Chi, S., Guo, H., Li, G., Wang, L., Zhao, Q., ... & Xiao, B. (2018). A lever-like transduction pathway for long-distance chemical-and mechano-gating of the mechanosensitive Piezo1 channel. *Nature communications*, 9(1), 1-12.

· Wang, Z., Yan, J., Wang, X., Yuan, Y., & Li, X. (2020). Transcranial ultrasound stimulation directly influences the cortical excitability of the motor cortex in Parkinsonian mice. *Movement Disorders*, 35(4), 693-698.

· Wattiez, N., Constans, C., Deffieux, T., Daye, P. M., Tanter, M., Aubry, J. F., & Pouget, P. (2017).

Transcranial ultrasonic stimulation modulates single-neuron discharge in macaques performing an antisaccade task. *Brain stimulation*, *10*(6), 1024-1031.

· Wemmie, J. A., Chen, J., Askwith, C. C., Hruska-Hageman, A. M., Price, M. P., Nolan, B. C., ... & Welsh, M. J. (2002). The acid-activated ion channel ASIC contributes to synaptic plasticity, learning, and memory. *Neuron*, *34*(3), 463-477.

· White, P. J., Clement, G. T., & Hynynen, K. (2006). Longitudinal and shear mode ultrasound propagation in human skull bone. *Ultrasound in medicine & biology*, 32(7), 1085-1096.

· Wu, J., Goyal, R., & Grandl, J. (2016). Localized force application reveals mechanically sensitive domains of Piezo1. *Nature communications*, *7*(1), 1-10.

· Wu, J., Young, M., Lewis, A. H., Martfeld, A. N., Kalmeta, B., & Grandl, J. (2017). Inactivation of mechanically activated Piezo1 ion channels is determined by the C-terminal extracellular domain and the inner pore helix. *Cell reports*, 21(9), 2357-2366.

· Xiao, B. (2020). Levering mechanically activated Piezo channels for potential pharmacological intervention. *Annual review of pharmacology and toxicology*, 60, 195-218.

· Yang, F. Y., Lu, W. W., Lin, W. T., Chang, C. W., & Huang, S. L. (2015). Enhancement of neurotrophic factors in astrocyte for neuroprotective effects in brain disorders using low-intensity pulsed ultrasound stimulation. *Brain stimulation*, 8(3), 465-473.

· Yang, P. F., Phipps, M. A., Jonathan, S., Newton, A. T., Byun, N., Gore, J. C., ... & Chen, L. M. (2021). Bidirectional and state-dependent modulation of brain activity by transcranial focused ultrasound in non-human primates. *Brain stimulation*, *14*(2), 261-272.

· Yang, P. F., Phipps, M. A., Newton, A. T., Chaplin, V., Gore, J. C., Caskey, C. F., & Chen, L. M. (2018). Neuromodulation of sensory networks in monkey brain by focused ultrasound with MRI guidance and detection. *Scientific reports*, 8(1), 1-9.

· Yang, Y., Pacia, C. P., Ye, D., Zhu, L., Baek, H., Yue, Y., ... & Chen, H. (2021). Sonothermogenetics for noninvasive and cell-type specific deep brain neuromodulation. *Brain Stimulation*, *14*(4), 790-800.

· Yau, J. O. Y., & McNally, G. P. (2015). Pharmacogenetic excitation of dorsomedial prefrontal cortex restores fear prediction error. *Journal of Neuroscience*, 35(1), 74-83.

· Ye, P. P., Brown, J. R., & Pauly, K. B. (2016). Frequency dependence of ultrasound neurostimulation in the mouse brain. *Ultrasound in medicine & biology*, *42*(7), 1512-1530.

· Yoo, S. S., Bystritsky, A., Lee, J. H., Zhang, Y., Fischer, K., Min, B. K., ... & Jolesz, F. A. (2011a). Focused ultrasound modulates region-specific brain activity. *Neuroimage*, *56*(3), 1267-1275.

· Yoo, S. S., Kim, H., Min, B. K., & Franck, S. P. E. (2011b). Transcranial focused ultrasound to the thalamus alters anesthesia time in rats. *Neuroreport*, 22(15), 783.

· Yoo, S., Mittelstein, D. R., Hurt, R. C., Lacroix, J., & Shapiro, M. G. (2022). Focused ultrasound excites cortical neurons via mechanosensitive calcium accumulation and ion channel amplification. *Nature Communications*, 13(1), 1-13.

· Younan, Y., Deffieux, T., Larrat, B., Fink, M., Tanter, M., & Aubry, J. F. (2013). Influence of the pressure

field distribution in transcranial ultrasonic neurostimulation. *Medical physics*, 40(8), 082902.

· Yu, K., Liu, C., Niu, X., & He, B. (2020). Transcranial focused ultrasound neuromodulation of voluntary movement-related cortical activity in humans. *IEEE Transactions on Biomedical Engineering*, 68(6), 1923-1931.

· Yu, K., Niu, X., Krook-Magnuson, E., & He, B. (2021). Intrinsic functional neuron-type selectivity of transcranial focused ultrasound neuromodulation. *Nature communications*, *12*(1), 1-17.

· Zeng, K., Darmani, G., Fomenko, A., Xia, X., Tran, S., Nankoo, J. F., ... & Chen, R. (2021). Induction of human motor cortex plasticity by theta burst transcranial ultrasound stimulation. Annals of neurology.

· Zhang, J., Zhou, H., Yang, J., Jia, J., Niu, L., Sun, Z., ... & Wang, G. (2021). Low-intensity pulsed ultrasound ameliorates depression-like behaviors in a rat model of chronic unpredictable stress. *CNS neuroscience & therapeutics*, 27(2), 233-243.

· Zhang, W. K., Wang, D., Duan, Y., Loy, M. M., Chan, H. C., & Huang, P. (2010). Mechanosensitive gating of CFTR. *Nature cell biology*, *12*(5), 507-512.

· Zhang, Z., Qiu, W., Gong, H., Li, G., Jiang, Q., Liang, P., ... & Zhang, P. (2019). Low-intensity ultrasound suppresses low-Mg2+-induced epileptiform discharges in juvenile mouse hippocampal slices. *Journal of neural engineering*, 16(3), 036006.

· Zhao, Q., Wu, K., Chi, S., Geng, J., & Xiao, B. (2017). Heterologous expression of the Piezo1-ASIC1 chimera induces mechanosensitive currents with properties distinct from Piezo1. *Neuron*, 94(2), 274-277.

· Zhao, Q., Zhou, H., Chi, S., Wang, Y., Wang, J., Geng, J., ... & Xiao, B. (2018). Structure and mechanogating mechanism of the Piezo1 channel. *Nature*, *554*(7693), 487-492.

· Zheng, W., Gracheva, E. O., & Bagriantsev, S. N. (2019). A hydrophobic gate in the inner pore helix is the major determinant of inactivation in mechanosensitive Piezo channels. *Elife*, 8, e44003.

· Zou, J., Meng, L., Lin, Z., Qiao, Y., Tie, C., Wang, Y., ... & Zheng, H. (2020). Ultrasound neuromodulation inhibits seizures in acute epileptic monkeys. *Iscience*, 23(5), 101066.